

In presenting this dissertation as a partial fulfillment of the requirements for an advanced degree from Emory University, I agree that the Library of the University shall make it available for inspection and circulation in accordance with its regulations governing materials of this type. I agree that permission to copy from, or to publish, this dissertation may be granted by the professor under whose direction it was written when such copying or publication is solely for scholarly purposes and does not involve potential financial gain. In the absence of the professor, the dean of the Graduate School may grant permission. It is understood that any copying from, or publication of, this thesis/dissertation which involves potential financial gain will not be allowed without written permission.

Xingang Fang

Synthesis and Anti-Viral Activity of Novel 3,6-dioxo-[3.2.0]bicyclonucleoside Nucleotide Analogs

By

Xingang Fang
Doctor of Philosophy

Department of Chemistry

Dennis C. Liotta
Advisor

Lanny S. Liebeskind
Committee Member

Stefan Lutz
Committee Member

Accepted:

Lisa A. Tedesco, Ph.D.
Dean of the Graduate School

Date

Synthesis and Anti-Viral Activity of Novel 3,6-dioxo-[3.2.0]bicyclonucleoside Nucleotide Analogs

By

Xingang Fang

M.S. Fudan University, 2001
B.S., Fudan University, 1998

Advisor: Dennis C. Liotta, Ph.D.

An Abstract of
a dissertation submitted to the Faculty of the Graduate
School of Emory University in partial fulfillment
of the requirements of the degree of
Doctor of Philosophy

Department of Chemistry

2007

Abstract

This study involves the design and synthesis of novel 3,6-dioxo-[3,2,0]bicyclonucleoside analogs as potential hepatitis C virus RNA-dependant RNA polymerase inhibitors. Both enantiomers of thymidine, 5-Fluorocytidine, cytidine, 6-Methoxypuridine and adenosine analogs were synthesized respectively. A convergent strategy was employed in the synthesis. The sugar moieties were synthesized from a chiral source, including carbohydrates and amino acid and coupled with various nucleoside bases through Vorbrüggen reactions. An intramolecular S_N2 reaction completed the synthesis. The bicyclic nucleoside analogs were tested in HCV replicon assay in Huh 7 Clone B cells for anti-HCV activity. Triphosphates of some chosen analogs were also synthesized for biological testing in order to exclude overlooking any potent inhibitor because of a poor phosphorylation step. The triphosphate compounds were tested in HCV RdRp enzymatic assay.

Synthesis and Anti-Viral Activity of Novel 3,6-dioxo-[3.2.0]bicyclonucleoside Nucleotide Analogs

By

Xingang Fang

M.S. Fudan University, 2001
B.S., Fudan University, 1998

Advisor: Dennis C. Liotta, Ph.D.

A dissertation submitted to the Faculty of the Graduate
School of Emory University in partial fulfillment
of the requirements of the degree of
Doctor of Philosophy

Department of Chemistry

2007

Acknowledgements

I would like to express my sincere gratitude to my advisor Prof. Dennis C. Liotta for being such an excellent supervisor. His kindness, generosity and endless support made my Ph.D. study smooth and enjoyable. He not only brought me into the fascinating area of medicinal chemistry but also showed me the way to become a good research professional.

I would like to thank Prof. Lanny S. Liebeskind and Prof. Stefan Lutz. As my committee members, they gave me a lot of constructive suggestions and tried to help me to become a better chemist. In addition, I am also grateful to Prof. Blakey for giving me a lot of useful comments for my proposal; Prof. McDonald, Prof. Padwa and Prof. Mohler for teaching me a lot of chemistry through their courses. The help from Prof. Schinazi and his group as valuable collaborators in the nucleoside project was indispensable to my research. I am truly grateful to their endeavor and enthusiasm in the collaboration. I am also grateful to Dr. Snyder, who has always been willing to help me whenever I have any questions or difficulties. I would like to thank Cindy Gaillard for her help.

I also appreciate the generous help from Dr. Michael Hager and Dr. Ustun Sunay. They are great mentors and have spent a lot of time in teaching me and sharing experiences with me. I wouldn't forget those wonderful days that we had together.

It is also a very pleasant experience to work with other members in this group, especially those related with my research field, including Dr. Martin Bouygues, Dr. Shuli Mao, Yongfeng Li, Kimberlynn Becnel-Davis, Gregory R.

Bluemling, Sanna Malick and Annette W. Neuman. We really had a good time together to work as a team and I appreciate each of you for your hard work to push the project further. I would also like to thank my former and current lab mates and office mates Dr. Muriel Joubert, Dr. Marike Herold, Dr. Uston Sunay, Dr. Sarah E. Trotman, Yi Jiang, Jamie Purcell, Ernest E. Murray and Sanna Malick. Life will never be that enjoyable without you guys. I also want to thank all the other past and present Liotta group members, including all the synthetic people (Dr. Larry Wilson, Christopher MacNevin, Cara Mosley, Mark Baillie, etc.) and the computational modeling people.

I also want to thank the chemistry department's facility managers: Dr. Shaoxiong Wu, Dr. Bing Wang, Dr. Fred Strobel and Dr. Kenneth Hardcastle. Their help was indispensable to my research. The help from Ann, Tanya, and Deirdre are also appreciated.

Finally, I will give my thanks to my wife, my parents and all my friends. Without you, I wouldn't have had such a nice and memorable time during these years.

DEDICATED TO MY FAMILY

TABLE OF CONTENT

Table of Content.....	I
1 Synthesis and Anti-Viral Activity of Novel 3,6-dioxo-[3.2.0]bicyclonucleoside Nucleotide Analogs.....	1
1.1 Statement of Purpose.....	1
1.2 Introduction	2
1.2.1 Hepatitis C Virus	2
1.2.2 HIV and HIV/HCV coinfection.....	15
1.2.3 Nucleoside RNA dependant RNA Polymerase Inhibitors and Their Triphosphates.....	16
1.3 Background	20
1.3.1 General Approaches of Nucleoside Synthesis	20
1.3.2 Oxetane Ring Formation	25
1.3.3 Bicyclic Nucleoside Analogs	31
1.3.4 Syntheses of Nucleoside Triphosphates	33
1.4 Design and Syntheses of 3,6-dioxo-[3.2.0]bicyclonucleoside Analogs.....	36
1.4.1 Syntheses of D-3,6-Dioxo-[3.2.0]bicyclonucleoside Analogs	39
1.4.2 Syntheses of L-3,6-Dioxo-[3.2.0]bicyclonucleoside Analogs	45
1.4.3 Syntheses of Nucleoside Triphosphates	59
1.5 Biological Activities.....	59
1.6 Conclusion	65
2 Experimental Section	66
2.1 General Notes	66
2.2 Syntheses of D-3,6-dioxo-[3.2.0]bicyclonucleoside Analogs	67
2.3 Syntheses of L-3,6-dioxo-[3.2.0]bicyclonucleoside Analogs.....	89
2.3.1 Route Starting from L-xylose.....	89
2.3.2 Route Starting from D-glutamic acid	114
2.4 Syntheses of Nucleoside Triphosphates	128
3 Abbreviations and Definitions.....	130
4 References.....	133

List of Figures

Figure 1 D, L-3,6-dioxo[3,2,0] bicyclic nucleoside and nucleotide analogs	2
Figure 2 Ribavirin.....	6
Figure 3 Hepatitis C virus	7
Figure 4 The HCV genome and its translational products	7
Figure 5 HCV replication cycle ¹⁸	9
Figure 6 Attachment to host cell ¹⁸	10
Figure 7 HCV entry and uncoating ¹⁸	11
Figure 8 RNA dependent RNA polymerase and helicase ³⁵	13
Figure 9 Nucleoside reverse transcriptase inhibitors of HIV	17
Figure 10 Structure of representative nucleoside inhibitors for HCV RdRp	18
Figure 11 D, L-3,6-dioxo[3,2,0] bicyclic nucleoside and nucleotide analogs.....	20
Figure 12 Representative natural products with oxetane ring	26
Figure 13 Nielson's synthesis of D-bicyclic nucleosides	32
Figure 14 Comparison of target molecules with other structures	36
Figure 15 Representative L-nucleoside antiviral agents	46
Figure 16 Potential starting materials for synthesizing L-bicyclic nucleosides ...	46

List of Schemes

Scheme 1 Potential outcomes of an HCV infection.....	5
Scheme 2 β selectivity through anchimeric assistance	23
Scheme 3 Titanium Lewis acid in glycosylation reaction of dioxolanyl acetate ..	23
Scheme 4 Regioselectivity and anchimeric assistance	25
Scheme 5 Paternò-Büchi reaction	26
Scheme 6 Total synthesis of oxetanocin by Paternò-Büchi reaction.....	27
Scheme 7 Paternò-Büchi reaction of ascorbic acid derivative.....	28
Scheme 8 Norbeck and Kramer's synthesis of Oxetanocin A.....	28
Scheme 9 Fleet's synthesis of Oxetanocin A.....	29
Scheme 10 Oxetane formation in Taxol synthesis	30
Scheme 11 Iodine catalyzed S _N 2 type cyclization.....	31
Scheme 12 Precedent of 3,6-dioxo[3.2.0]bicyclic nucleosides	31
Scheme 13 Synthesis of 1',2'- and 3',4'- fused bicyclic nucleosides.....	32
Scheme 14 Ludwig one-pot procedure in synthesis of ATP.....	34
Scheme 15 Syntheses involving nucleoside phosphoramidates.....	34
Scheme 16 Syntheses involving nucleoside phosphites.....	35
Scheme 17 Synthesis of 3-oxa[3.2.0]bicycloheptane nucleosides.....	38
Scheme 18 S _N 2 disconnections	39
Scheme 19 Retrosynthetic analysis of D-3,6-dioxo-[3.2.0]bicyclonucleosides...	40
Scheme 20 Synthesis of 92	41
Scheme 21 Nitrogen glycosylation reactions (D-enantiomers)	42
Scheme 22 Final transformations	44
Scheme 23 Synthesis of 118	47
Scheme 24 Nitrogen glycosylation reactions (L-enantiomers)	48

Scheme 25 Final transformations	49
Scheme 26 Retrosynthetic analysis of L-biclonucleosides from D-glutamic acid	52
Scheme 27 Synthesis of intermediate 129	52
Scheme 28 1,3-Dipole cycloaddition of dihydrofuranone 134	53
Scheme 29 Photo Michael addition.....	54
Scheme 30 Stereoselective hydroxylation reactions using MoOPH.....	55
Scheme 31 MoOPH hydroxylation	56
Scheme 32 Reduction-acetylation	57
Scheme 33 Model study on glycosylation reaction of 149	57
Scheme 34 Deprotection of MOM group on 150β	57
Scheme 35 Completion of the synthesis of 2a	58
Scheme 36 Synthesis of nucleoside 5'-O triphosphates	59

List of Tables

Table 1 Glycosylation reactions of pyrimidine and purine bases.....	43
Table 2 Nitrogen glycosylation reaction of 92	43
Table 3 Nitrogen glycosylation reaction of 118	48
Table 4 Oxetane formation conditions.....	51
Table 5 α -Hydroxylation conditions	56
Table 6 Conditions for glycosylation reaction of 149	57
Table 7 MOM deprotection conditions of 150β	58
Table 8 Anti-HCV activities	60
Table 9 Anti-HIV activities	62

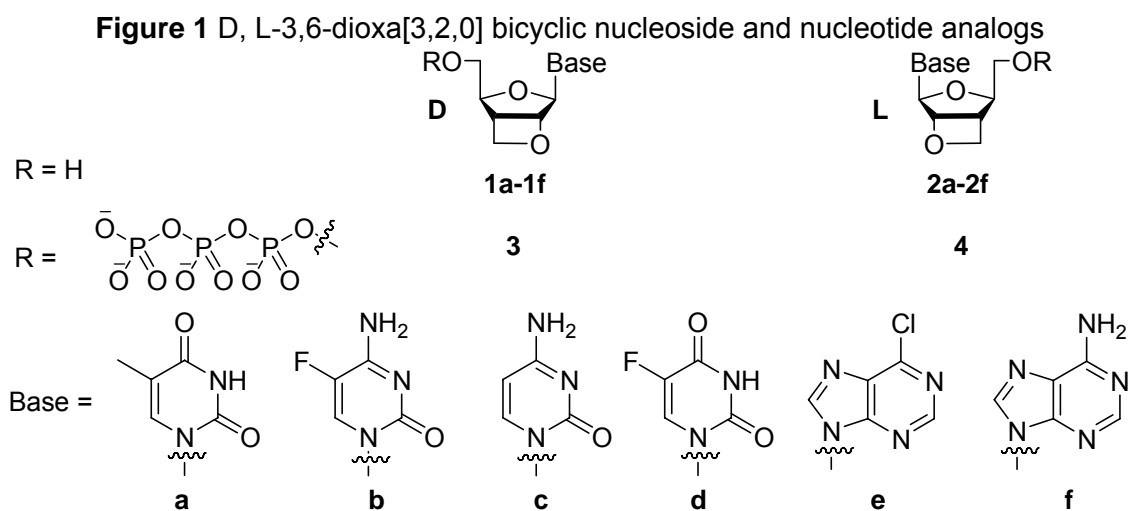
1 SYNTHESIS AND ANTI-VIRAL ACTIVITY OF NOVEL 3,6-DIOXA-[3.2.0]BICYCLONUCLEOSIDE NUCLEOTIDE ANALOGS

1.1 Statement of Purpose

In 1988, decades after the identification of hepatitis A and B, an RNA (ribonucleic acid) virus was identified and was suspected to be the agent causing NANB (non A-non B) hepatitis infections. This virus was named hepatitis C virus (HCV).¹ Researchers at the National Institutes of Health (NIH) discovered that 70% to 90% of NANB hepatitis cases were actually HCV infections from their archived samples. HCV is recognized as a major cause of chronic liver disease as well as the leading cause of liver transplantations in developed countries.² The current standard and only treatment for HCV is a combination of two drugs: pegylated interferon (peg-IFN)³ and ribavirin⁴. The clinical benefit of this combination is limited by its low efficacy, poor tolerability and high expense. Moreover, there is no vaccine for HCV to date. New treatment options that are more potent and less toxic are desperately needed. In the United States, an estimated 16-25% of HIV-positive individuals are coinfecting with HCV; as many as 90% of the people who acquired HIV through injection drug use are coinfecting with HCV. In 1999, hepatitis C was classified as an opportunistic infection of HIV (human immunodeficiency virus) disease.

HCV RNA dependent RNA polymerase (RdRp), which is pivotal in HCV viral replication, constitutes an attractive target for drug discovery. Nucleoside analogs are important potential HCV RdRp inhibitors because they either inhibit

the enzyme, terminate the RNA synthesis or reduce the viability of RNA by incorporation into the growing RNA strand. Given the fact that HCV polymerase uses ribonucleoside triphosphates to make RNA, 3,6-dioxo-[3,2,0]bicyclonucleoside analogs were chosen as targets. These compounds possess an eclipsed 2'-3' orientation, which mimics the 2'-3'-diol functionality in natural ribonucleosides. In addition, comparison of activities with 3-oxa[3,2,0]bicyclonucleosides will also provide insight to whether the 2'-oxygen serves as a recognition site for the polymerase. Triphosphates of the bicyclonucleosides were also synthesized for biological testing in order to exclude overlooking any potent inhibitor because of a poor phosphorylation step.



1.2 Introduction

1.2.1 Hepatitis C Virus

In the mid 1970s, it was proposed that a viral agent other than hepatitis type A or B caused transfusion-associated hepatitis.⁵ In 1988-89 a group of researchers at Chiron identified an RNA virus that they suspected might be the

agent causing NANB (non A-non B) hepatitis infections. This virus was named hepatitis C virus.¹ An antibody test was rapidly developed.⁶ When researchers at the National Institutes of Health (NIH) tested the new antibody on archived blood samples, they discovered that 70% to 90% of NANB hepatitis cases were actually HCV infections.

1.2.1.1 Prevalence and Transmission of HCV

HCV is recognized as a major cause of chronic liver disease as well as the leading cause of liver transplantations in developed countries.² According to Center of Disease Control and Prevention (CDC)'s most recent HCV fact sheet published on 2005, estimated 1.4% of the United States population, or 4.1 million people, have been infected with HCV, of whom 3.2 million are chronically infected.⁷ HCV is a major cause of acute hepatitis and chronic liver disease, including cirrhosis and liver cancer, which cause between 10,000 and 12,000 deaths per year in the United States. The World Health Organization (WHO) estimates that about 170 million people, 3% of the world's population, are infected with HCV and are at risk of developing liver cirrhosis and/or liver cancer.

HCV is a bloodborne infection with three major routes of transmission: injection drug use, unsafe therapeutic injection and blood transfusion. Injection drug use is the primary route of transmission in the developed countries. In developing countries, unsafe therapeutic injection is a major route of HCV transmission. For example, the wide spread of HCV in Egypt is believed to be the consequence of contaminated syringes used in a nationwide schistosomiasis treatment campaign between 1961 and 1986.⁸ The blood transfusion

transmission has been virtually eliminated in developed countries since the development of a screening test for HCV.⁶ However, transfusion-related HCV transmission is still believed to be a major route in developing countries, where donated blood is not well screened for the presence of HCV.² Other possible routes of transmission are: sexual intercourse with an infected partner, perinatal transmission, tattooing, body piercing and acupuncture.

1.2.1.2 HCV Variations

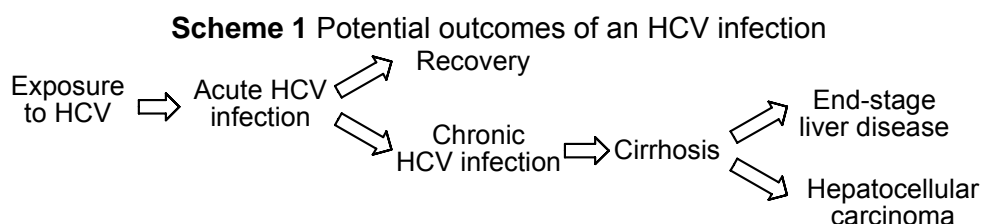
HCV is classified into eleven major genotypes (designated 1-11), many subtypes (designated a, b, c, etc.), and about 100 different strains (numbered 1,2,3, etc.) based on the genomic sequence heterogeneity.⁹ The different genotypes are diversely spread throughout the world, where the genotypes 1-3 are spread globally. The genotypes 1a and 1b are by far the most common throughout the world, accounting for about 60 % of all infections. The genotype 1a is spread predominantly in North America and Northern Europe, and the genotype 1b in Southern and Eastern Europe and Japan. Genotype 2 is also global but less frequent than the genotype 1. Genotype 3 is spread mainly in South-East Asia and quite variably in the rest of the world. Genotype 4 is found mainly in the Middle East, Egypt, and Central Africa. Genotype 5 is almost exclusively found in South Africa, and genotypes 6-11 are distributed throughout Asia.

The determination of the infecting genotype is important for the prediction of response to antiviral treatment: genotype 1 is generally associated with a poor

response to interferon alone, whereas genotypes 2 and 3 are associated with more favorable responses to interferon.

1.2.1.3 Outcome and Symptoms of an HCV Infection

HCV primarily infects human hepatocytes in the liver causing immune-mediated inflammation and other liver problems. The clinical symptoms and outcome are highly individual and there is no single typical course of the disease. A schematic representation of possible outcomes of an HCV infection is presented in **Scheme 1**.



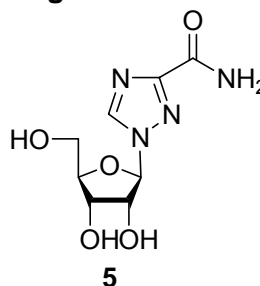
1.2.1.4 Current Treatment for Hepatitis C

In 1986, it was reported that the naturally occurring immune agent interferon- α (IFN- α) could be used to treat patients infected with non-A, non-B hepatitis.¹⁰ Since then, the medical treatment of HCV has relied on this 165-amino-acid peptide via injection. The current standard and only treatment for hepatitis C is a combination of two drugs: pegylated interferon(peg-IFN)³ and ribavirin **5** (**Figure 2**)⁴. In pegylated interferon, α -2a or α -2b interferon is connected to the non-toxic polyethylene glycol (PEG) to provide a better half life and maintain a more constant level of interferon in bloodstream. Of the treated individuals, sustained responders range from 50-80 %, depending on the infecting HCV genotype.¹¹ The clinical benefit of this therapy is limited by its low

efficacy (highly depending on viral genotype, race, weight, etc.), poor tolerability (significant side effects)¹² and high expense (roughly &40,000 per year).

Moreover, there is no vaccine for HCV to date. Given the high prevalence of the disease, there is an urgent need to develop more effective, more efficient, well tolerated and less expensive therapies for chronic hepatitis C.

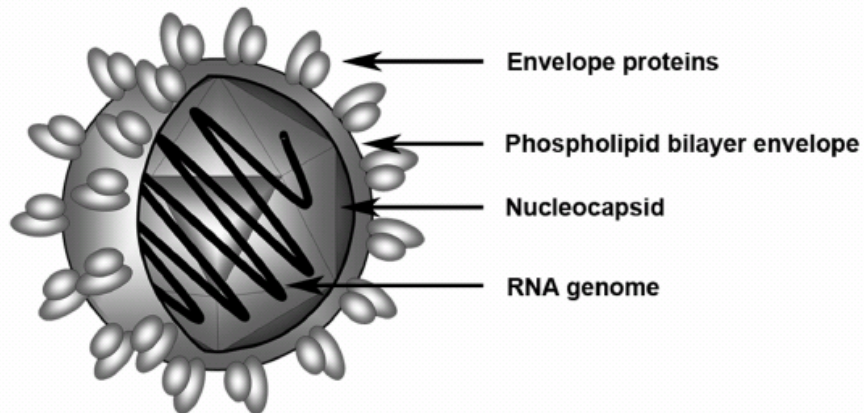
Figure 2 Ribavirin



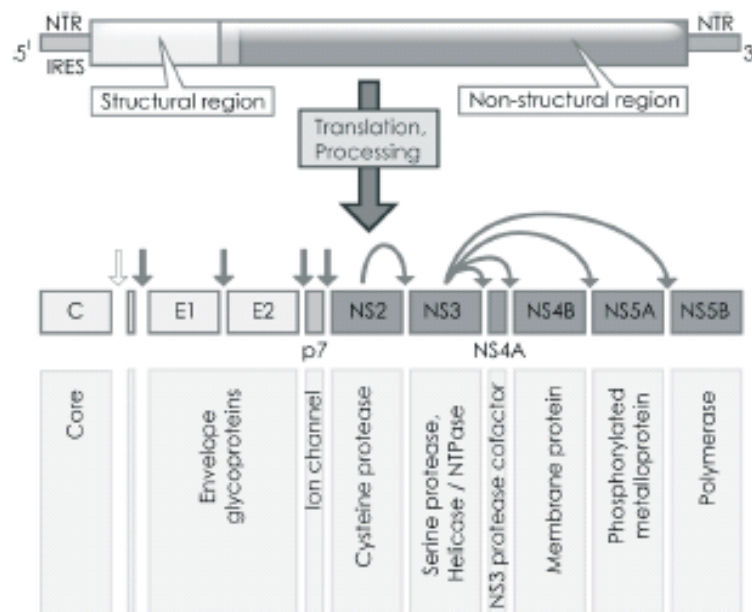
1.2.1.5 Basic Virology

HCV has been classified as the sole member of the genus *Hepacivirus* of the family *Flaviviridae*, which also includes the *Pestivirus* and the *Flavivirus*.^{13, 14}

HCV is a small, enveloped RNA virus, which consists of the viral genome (a single strand of RNA) enclosed in a capsid shell and surrounded by a viral envelope, or membrane. (**Figure 3**)

Figure 3 Hepatitis C virus

The genome of the HCV comprises of ~9600 nucleotides, coding for a single open reading frame (ORF) translated into a polyprotein of ~3000 amino acids,^{15, 16} which is proteolytically cleaved into a set of viral proteins (**Figure 4**).

Figure 4 The HCV genome and its translational products

1.2.1.6 The Hepatitis C Viral Replication Cycle

Replication, to make new copies of them, is the primary goal of all viruses, including HCV. Unlike other organisms, viruses cannot replicate on their own,

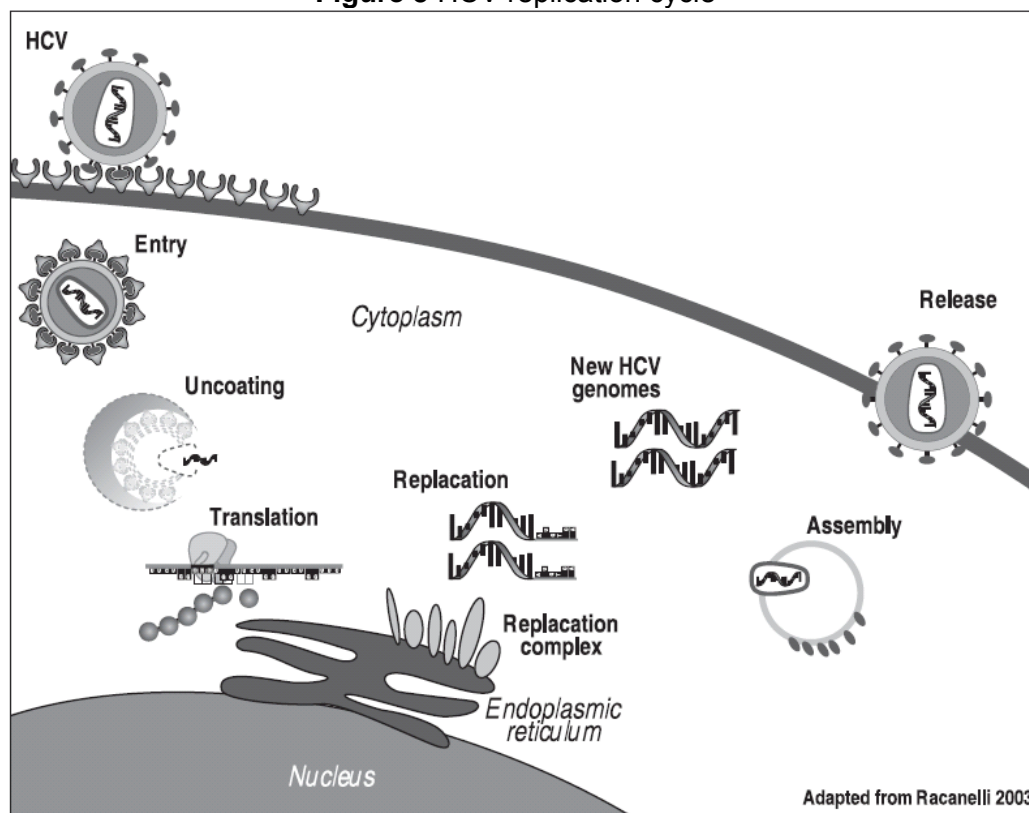
and they can only replicate themselves by infecting a host cell. To replicate, HCV and other viruses must infect other cells and hijack the cell's translational apparatus, including enzymes and other proteins. An infected, or target, cell is called a host cell, which "hosts" the virus. The term "host" is also used to describe the species susceptible to infection by a given virus. The HCV primarily targets human hepatocytes in the liver, the virus is considered hepatotropic.

Once HCV enters the host cell, all subsequent events in the replication cycle occur in the cell's cytoplasm, the main area of the cell between its membrane and nucleus. Both cellular proteins and viral proteins facilitate the progression of HCV throughout its replication cycle. The HCV genome encodes at least ten different viral proteins, including structural proteins and nonstructural proteins. The structural proteins are incorporated into the capsid and envelope of new virions, while the nonstructural proteins are involved in the viral replication process. Research over the last decade has elucidated the functions of many of these proteins, but some proteins' roles in viral replication remain unclear, and many aspects of HCV replication and viral-host cell protein interactions are poorly understood.¹⁷

The HCV replicates through the cycle depicted in **Figure 5**.

1. Attachment to host cell, entry and uncoating;
2. Translation and processing of viral polyprotein within the cell cytoplasm;
3. Viral RNA replication;
4. Assembly and release of new virions from host cell.

Figure 5 HCV replication cycle¹⁸



1.2.1.6.1 Stage 1: Host cell attachment, entry and uncoating

Virions must enter a target cell to replicate. Although the entry of HCV remains unclear, in general, viruses in the *Flaviviridae* family enter cells in three steps: attachment, entry and uncoating.

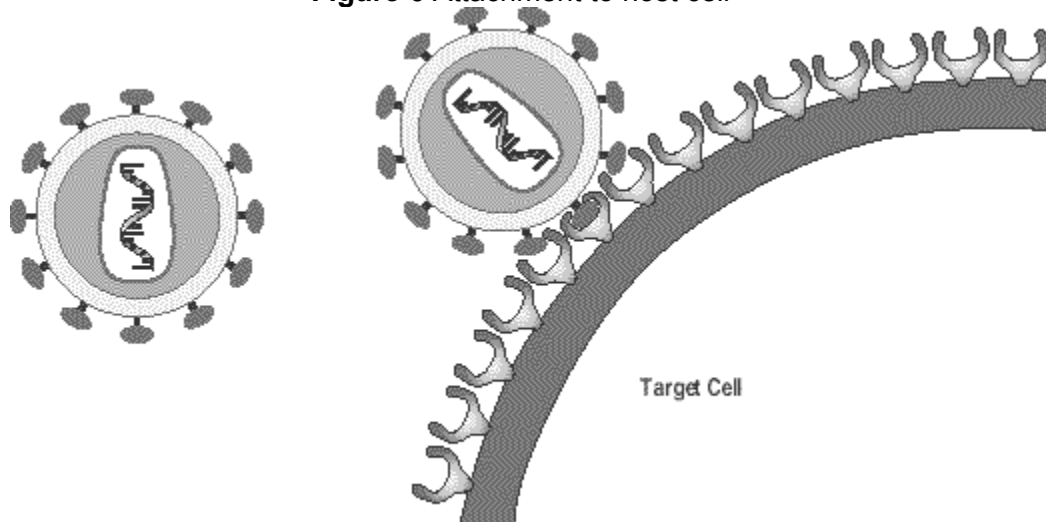
HCV primarily infects hepatocytes, the main cell type in liver tissue; however, HCV has also been found in a range of other cells outside of the liver. These cells include white blood cells, components of the immune system.

Attachment is believed (by analogy to similar viruses) to occur through interactions between HCV's envelope and receptors on the surface of potential host cells. The HCV envelope includes two envelope proteins, E1 and E2, produced by the virus itself. E1 and E2 are bound together on the envelope,

forming heterodimers.¹⁹ HCV uses one or both of these envelope proteins to attach to cell surface receptors on target cells.

While several candidate HCV receptors have been proposed, their roles in viral entry have not been definitively established. HCV may require more than one type of receptor for attachment as with HIV infection.²⁰ Three primary candidates of cell surface receptors are thought to be capable of binding to HCV virions: the CD81 receptor, the low-density lipoprotein (LDL) receptor, and the human scavenger receptor class B type I (SR-BI). HCV also binds to the cell adhesion molecules DC-SIGN (dendritic cell-specific intercellular adhesion molecule 3-grabbing non-integrin) and L-SIGN (liver/lymph node-specific intercellular adhesion molecule-3-grabbing integrin).

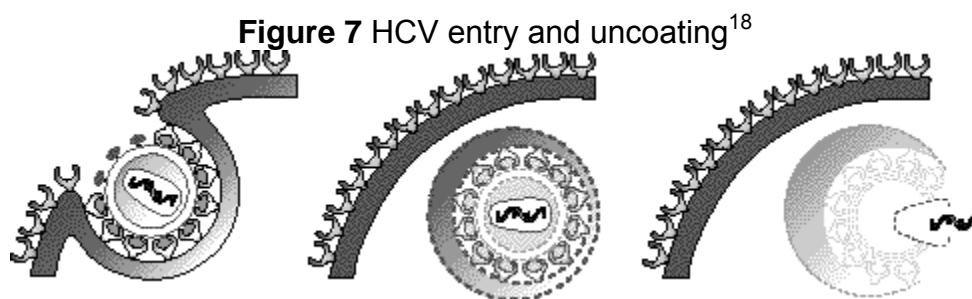
Figure 6 Attachment to host cell¹⁸



The entry of HCV into target cells most likely occurs through receptor-mediated endocytosis, in which a cell internalizes a ligand-bound surface receptor. The receptor-ligand complex enters the cell encapsulated within a

vesicle, a small pocket of fluid surrounded by a thin membrane. Recent evidence indicates that hepatitis C viral entry is dependent on pH, a characteristic of receptor-mediated endocytosis but not of direct fusion.²¹

Uncoating is the process that releases the viral genome into the cell's cytoplasm. Thus, HCV releases its genome from its capsid shell and surrounding viral envelope to begin replication. Though the specific uncoating process for HCV has not been characterized, it likely resembles other enveloped viruses entering through receptor-mediated endocytosis. In this model, the HCV envelope would fuse to the vesicle membrane once inside the cell. Fusion may depend on a change in pH levels within the vesicle. Envelope-vesicle membrane fusion results in the degradation of the viral capsid surrounding the viral genome, releasing the viral RNA into the cell's cytoplasm to be transported to the endoplasmic reticulum (ER).



1.2.1.6.2 Stage 2: Polyprotein translation and processing

Once released inside the cell, HCV RNA is used as a blueprint for the production of viral proteins. Translation of the HCV open reading frame (ORF) is directed via a C340 nucleotide long 5' non-translated region (NTR) functioning as

an internal ribosome entry site (IRES) and permitting the direct binding of ribosomes in close proximity to the start codon of the ORF.^{22, 23}

The HCV polyprotein is cleaved co- and post-translationally by cellular and viral proteases into ten different products, with the structural proteins located in the 5' terminal and the nonstructural replicative proteins in the remainder.²⁴ Cellular signal peptidases, localized in the lumen of the endoplasmic reticulum (ER), catalyze the cleavage of the structural region.²⁵⁻²⁷ The cleavage of NS2 (nonstructural protein 2) and NS3 is accomplished through the action of a protease comprised of the NS2 and NS3 proteins themselves, a process described as auto cleavage.^{28, 29} The cleavages of the other downstream nonstructural (NS) proteins including NS5B RNA dependant RNA polymerase (RdRp) are mediated by the separate NS3 serine protease.^{24, 30} The activity of the NS3 serine protease involves the HCV protein NS4A serving as a cofactor to facilitate cleavage and stabilize NS3.³¹⁻³⁴

After cleavage, further post-translational modifications of E1, E2 and some other proteins occur before these proteins really function.

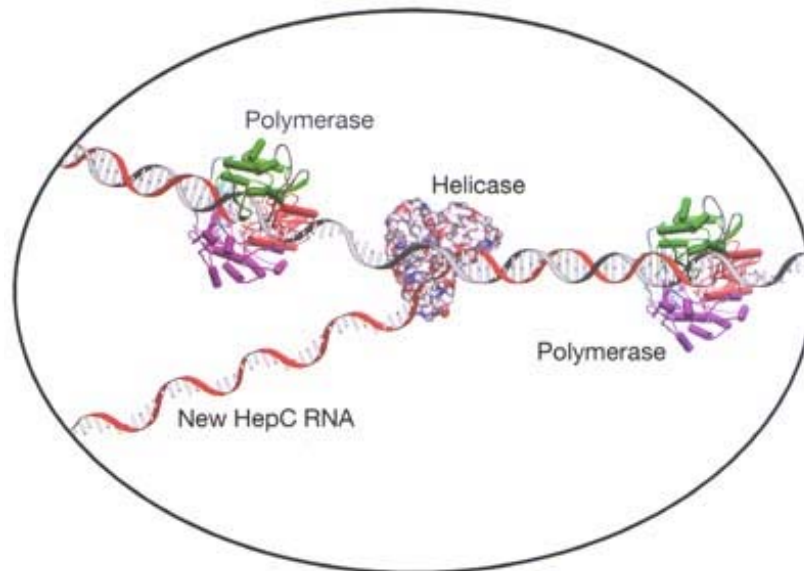
1.2.1.6.3 Stage 3: Viral RNA replication

Replication of the HCV genome is the pivotal event in the viral life cycle. Each new virion requires its own viral genome. These new HCV genomes are RNA strands that have been copied, or transcribed, from the original HCV RNA. There is no direct way to copy a positive-sense RNA from the original positive-sense RNA strand. The replication is achieved in two steps: 1) the original positive-sense RNA serves as a template for the synthesis of the complementary

negative-sense RNA strand, and 2) the resulting negative-sense then direct the synthesis of new, genomic, positive-sense viral RNA.

This process virtually involved all nonstructural viral proteins as well as some cellular proteins. They form the viral replication complex where RNA strand synthesis occurs. Among those proteins, viral NS5B RdRp and NS3 helicase/NTPase play the most important role in the RNA replication process. RdRp uses nucleoside triphosphates to assemble a chain of nucleotides complementary to the original RNA strand to synthesize new negative and positive RNA. Helicase/NTPase, with NS4A acting as a cofactor, moves along the template RNA strand to prevent the formation of double helix of original and newly synthesized RNA strands. (**Figure 8**)

Figure 8 RNA dependent RNA polymerase and helicase³⁵



1.2.1.6.4 Stage 4: Virion assembly and release

A new HCV virion consists of three components: single-strand genomic HCV RNA, a capsid shell, and the viral envelope. Those components come from

the translation (core protein and envelope protein) and viral RNA replication (genomic HCV RNA), respectively. The genomic RNA is packed within the capsid from core protein to form the nucleocapsid. It is then enveloped in a section of cellular membrane. The viral envelope proteins are then incorporated into the nucleocapsid to complete the new virion assembly. These new viruses are transported to the cellular membrane and release to infect new cells. The viral protein, p7, may also be involved in viral release by forming ion channels, potentially increasing the permeability of the cell's plasma membrane.³⁶

1.2.1.7 HCV Drug design

The standard treatment for HCV, combination therapy with pegylated interferon α and ribavirin, has limited efficacy, poor tolerability, and significant expense. New treatment options that are more potent and less toxic are desperately needed. Neither interferon- α nor ribavirin was developed specifically to treat HCV infection. Both of them were developed and approved for the treatment of other infections before the actual discovery of HCV. The mechanisms of interferon- α and ribavirin as treatment for HCV are not fully understood, but most likely involve multiple immunomodulatory and antiviral effects.^{37, 38} New HCV treatment are unlikely to supplant pegylated interferon α and ribavirin as the backbone of therapy, therefore many of them are developed for use in combination with these existing drugs.

Similar to human immunodeficiency virus (HIV) and Hepatitis B virus (HBV) reverse transcriptase, the HCV RdRp has no proofreading mechanism to correct errors during RNA synthesis. The resulting high mutation rate brings a high risk

of developing resistance. Similar to the highly active anti retroviral therapy (HAART) for HIV, the treatment of HCV with combination of different kind of anti-HCV agents will minimize the possibility for the emergence of viral resistance. Thus, the development of new drugs targeting diverse aspects of HCV infection is highly desirable.

Several drugs currently in development target aspects of the HCV replication cycle, including translation initiation (antisense oligonucleotides and synthetic ribozymes), cleavage and processing (NS3 serine protease inhibitors), and RNA synthesis (nucleoside and non-nucleoside NS5B RdRp inhibitors, helicase inhibitors). Other drugs with broad antiviral and immunomodulatory properties are also under investigation.³⁹ Most of these drugs are in very early stages of preclinical or clinical development.⁴⁰ The development of vaccines to prevent HCV infection is challenging due to lack of small animal model and HCV's genetic diversity. A few therapeutic vaccine candidates have entered small clinical trials.

1.2.2 HIV and HIV/HCV coinfection

In 1981, documentation began on the disease that became known as AIDS (Acquired Immune Deficiency Syndrome). Up till now, AIDS has become a major world health problem being the first cause of death in Africa and the fourth leading cause of death worldwide.⁴¹ The affected individuals displayed a specific immune deficiency resulting from the depletion of CD4+ lymphocytes. In 1983, the etiological cause of AIDS was determined to be the human immunodeficiency virus (HIV).^{42, 43}

In the United States, an estimated 16-25% of HIV-positive individuals are coinfecting with HCV,⁴⁴⁻⁴⁶ as many as 90% of the people who acquired HIV through injection drug use are coinfecting with HCV. In 1999, hepatitis C was classified as an opportunistic infection of HIV disease.

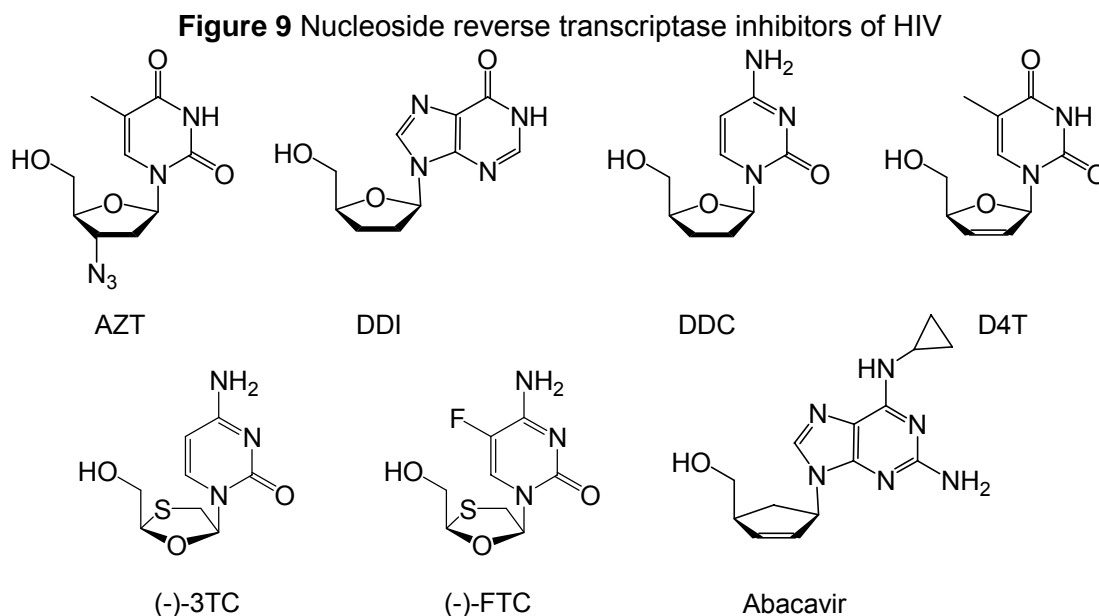
Since the AIDS-related mortality has decreased dramatically by the advent of highly active antiretroviral therapy (HAART), end-stage liver disease (ESLD) has become a leading cause of death for HIV-infected individuals.⁴⁷⁻⁵⁰

1.2.3 Nucleoside RNA dependant RNA Polymerase Inhibitors and Their Triphosphates

Nucleoside triphosphates (NTP) are substrates of DNA (deoxyribonucleic acid) polymerase, reverse transcriptase and RNA polymerase. Historically, nucleoside analogs have been developed as inhibitors against DNA viruses and retroviruses, while they have not been fully explored against viral RNA polymerases. A number of nucleoside analogs have been proven to be active against HCV RdRp, but all of them are still in early stage of preclinical or clinical development.

Nucleoside analogs were most extensively used in treatment of Acquired Immune Deficiency Syndrome (AIDS) caused by Human Immunodeficiency Virus (HIV) as nucleoside reverse transcriptase inhibitors (NRTI). All FDA (Food and Drug Administration) approved NRTIs for HIV (**Figure 9**) share the 2',3'-dideoxy sugar moiety. They disrupt the viral replication process by either direct competitive inhibition of the HIV reverse transcriptase or chain termination when incorporated into the growing DNA strand. The absence of 3'-hydroxyl group is

believed to be essential for the chain termination because it is used to form a 3'-5' phosphodiester bond with the next nucleoside substrate in the elongating DNA strand.⁵¹

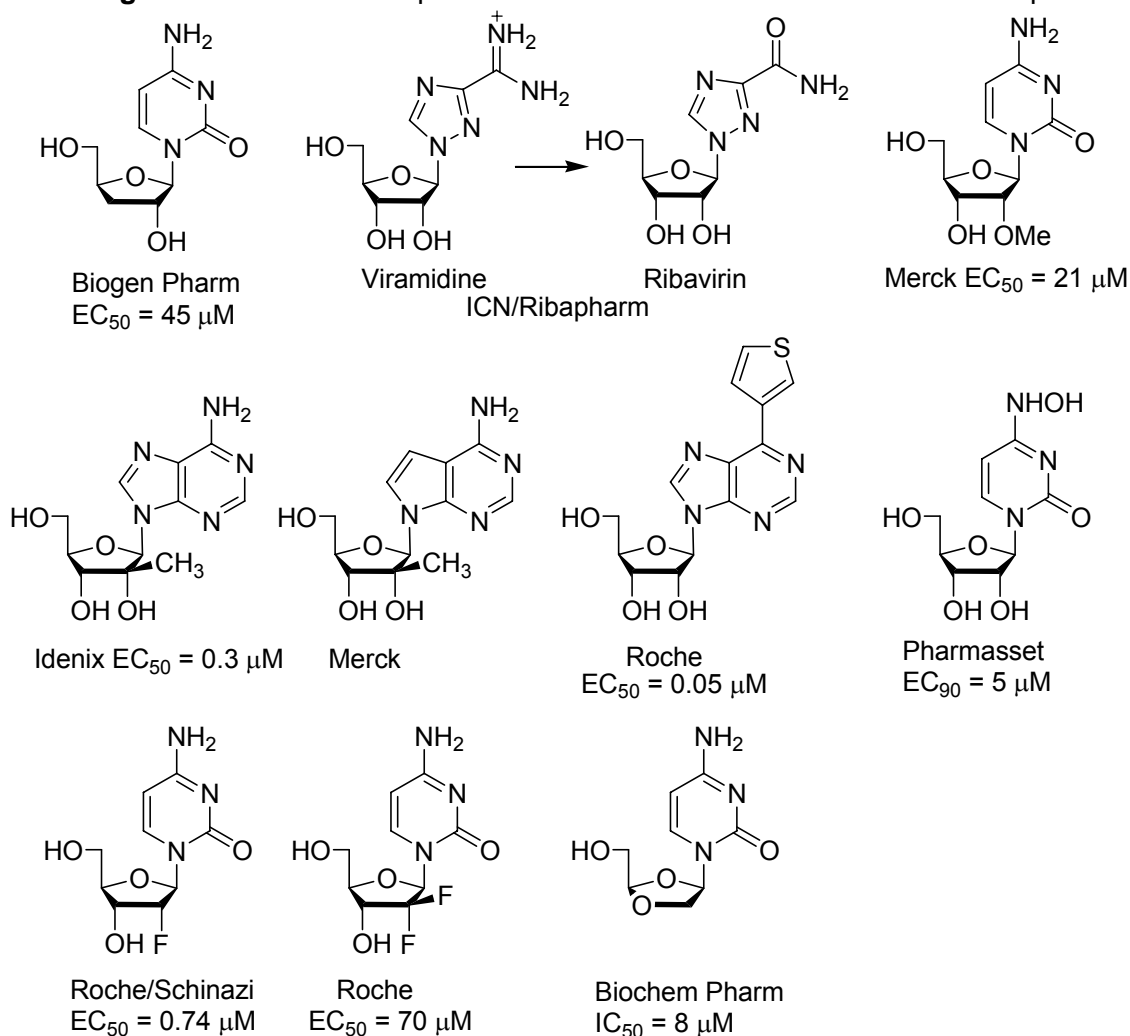


In the case of HCV RdRp inhibitors, in addition to the two inhibition mechanisms mentioned above, the study of antiviral effects of ribavirin (a nucleoside analog) revealed the “error catastrophe” mechanism in HCV RNA replication. In this mechanism, the nucleoside triphosphate may act as a substrate and be incorporated into viral genome, functioning as a mutagen to reduce the viability of progeny viruses and thereby cause the so-called “error catastrophe”.⁵²

The structures of representative nucleoside HCV RdRp inhibitors are listed in **Figure 10**.⁵³⁻⁶² Since HCV RdRp uses ribonucleoside triphosphates (rNTP) as substrate to make RNA, it is not surprising that most of the active

structures feature 3'-substitutions, particularly hydroxyl group or fluorine group. Some structures are reported to act as chain terminator with the presence of 2'-hydroxyl group.⁶³

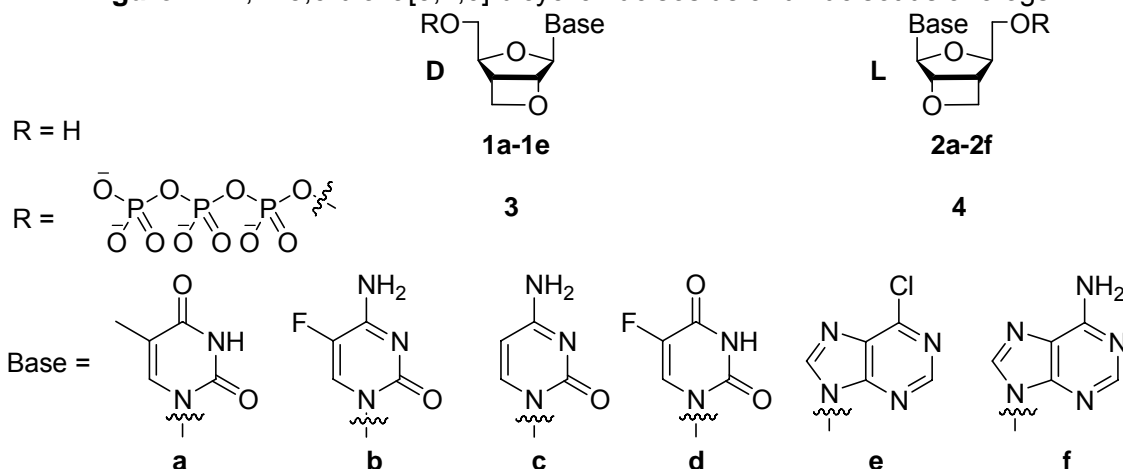
Figure 10 Structure of representative nucleoside inhibitors for HCV RdRp



Given the factor that NTPs are natural substrates of HCV RdRp to make RNA, we think that a 2'-hydroxyl or -fluorine substituent will contribute to the potency and selectivity toward the HCV polymerase. Moreover, according to some early results showing that some α-2'-F-3'-deoxynucleosides were inactive

against HCV RdRp, we hypothesize that the presence of an α -2'-F- substituent alone is insufficient to produce potent HCV inhibition, probably as a consequence of conformational factors. Such conformation of ribonucleoside exist predominantly in gauche or near-eclipsed 2'-3'- orientations because of hydrogen bonding and/or dipole-dipole interactions. They are very different from the conformations observed in nucleosides that lack a 2'-substituent. For that reason, we choose 3,6-dioxa-[3,2,0]bicyclonucleosides as targets. These compounds possess an eclipsed 2'-3' orientation, which mimics the 2'-3'-diol functionality in natural ribonucleosides. In addition, comparison of activities with 3-oxa-[3,2,0] bicyclonucleosides will also provide insight to whether the 2'-oxygen serves as a recognition site for the polymerase.

In the biological evaluation of nucleoside HCV RdRp inhibitors, HCV RNA replicon assays in human Huh-7 cells are employed for the *in vivo* screening. In the cellular setting, nucleoside inhibitor mostly rely on viral or kinase-mediated (i.e., thymidine kinase) activation steps to produce the nucleoside triphosphate (NTP), which is necessary to display biological activity. The nucleosides are themselves prodrugs. The phosphorylation steps, especially the first step, of a nucleoside are known to be structurally dependent. Therefore, a poor kinase mediated phosphorylation cascade can lead to the overlooking of potent nucleoside inhibitors in the biological screening. The *in vitro* HCV RdRp enzymatic assay test of the nucleoside 5'- triphosphates are necessary to exclude the overlooking of any potent inhibitor.

Figure 11 D, L-3,6-dioxo[3,2,0] bicyclic nucleoside and nucleotide analogs

1.3 Background

1.3.1 General Approaches of Nucleoside Synthesis

In general, there are two approaches in synthesizing nucleoside analogs: divergent approach and convergent approach. The divergent approach usually modifies natural occurring nucleosides to afford the desired nucleoside analogs, which is obviously limited by the availability of the natural nucleosides. The convergent approach involves a nitrogen glycosylation reaction, which combines various ribose portions with various pyrimidine or purine bases. The latter method is generally preferred in our group for the convenience of combinatorially generating a variety of nucleoside analogs from various ribose rings and nucleoside bases.

The key step of the convergent approach is the nitrogen glycosylation reaction. A typical nitrogen glycosylation reaction involves the nucleophilic attack of a nitrogen center on a heterocycle onto an oxonium ion. This type of reaction was first reported in Fischer and Helferich's synthesis of purine nucleosides⁶⁴

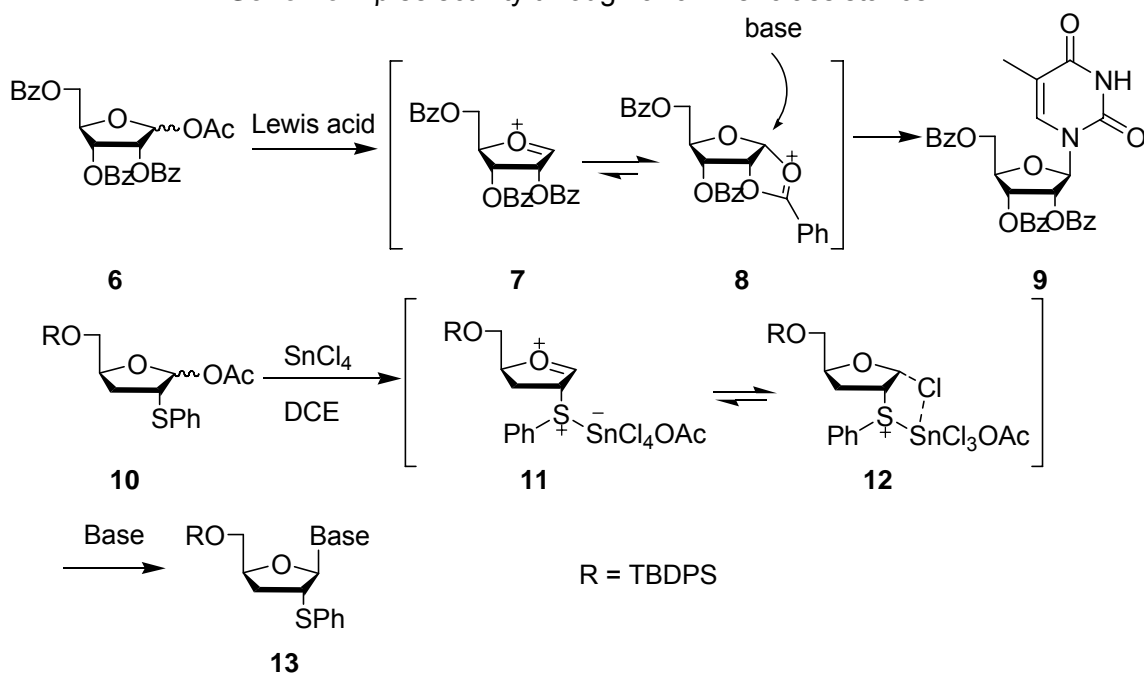
and then further developed by Hilbert and Johnson for the synthesis of pyrimidine nucleosides.⁶⁵ Since then, researchers have developed several more efficient variations of this reaction. The silyl variant of the Hilbert-Johnson approach developed by Vorbrüggen has proven to be a very efficient method in the synthesis of nucleoside analogs.⁶⁶⁻⁷¹

In Vorbrüggen reactions, silylated bases and Lewis acids are important components. The introduction of silyl groups (typically TMS group) onto bases not only increases the nucleophilicity of the nitrogen center in the bases, but also improves the solubility of the poorly soluble bases in common solvents. Lewis acids, originally referred to as Friedel-Crafts catalysts by Vorbrüggen and coworkers, play an important role in Vorbrüggen reactions. They react with the ribofuranosyl acetate to provide the reactive oxonium ion. The properties of Lewis acids can be easily modulated by changing either the center atoms or ligands. A good example is the successful use of a titanium Lewis acid in the synthesis of FDOC (2',3'-dideoxy-5-fluoro-oxacytidine),⁷² where various combinations of ligands on titanium center were screened to provide the most efficient titanium trichloroisopropoxide as the catalyst. In addition, the choice of proper solvent is also important in order to obtain optimized yield, reaction rate and selectivity.

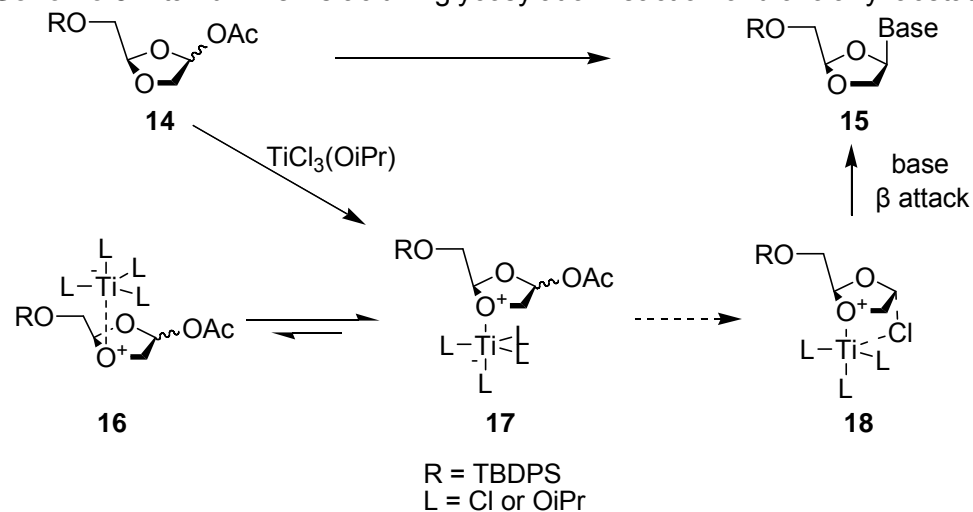
The mechanism of Vorbrüggen reactions is believed to involve three reversible processes: 1) reaction of the acetylated sugar with a Lewis acid to give rather stable electrophilic sugar cations; 2) reversible formation of σ complexes

between the silylated bases and Lewis acids; 3) reaction of the sugar cation with silylated bases to form the glycosyl bond.

A major obstacle in the convergent approach is determining how to control the anomeric stereochemistry during the nitrogen glycosylation step. The Lewis acid condition generates a planar oxonium ion intermediate (for example: **7**, **11**), which can be attacked by silylated nucleoside base from either the top face (β -face) or the bottom face (α -face). One strategy to obtain high β selectivity is through anchimeric assistance. As shown in **Scheme 2**, Vorbrüggen and coworkers have reported that in the presence of a 2- α -O- acetyl (benzoyl) group, only the desired β product was obtained.⁷³ The oxonium ion is stabilized by interacting with the neighboring benzoyl group to form intermediate **6**, which is consequently attacked by the nucleoside base in an S_N2 fashion from the less hindered β -face to afford β product **7**. The 2- α -phenylselenenyl and 2- α -phenylsulfenyl groups have also been reported capable of directing nucleoside base to the β -face through anchimeric assistance.⁷⁴ Wilson and Liotta proposed the ligated intermediate **10**, which is consequently displaced in an S_N2 fashion by the nucleoside base to yield β nucleoside **13** (**Scheme 2**).

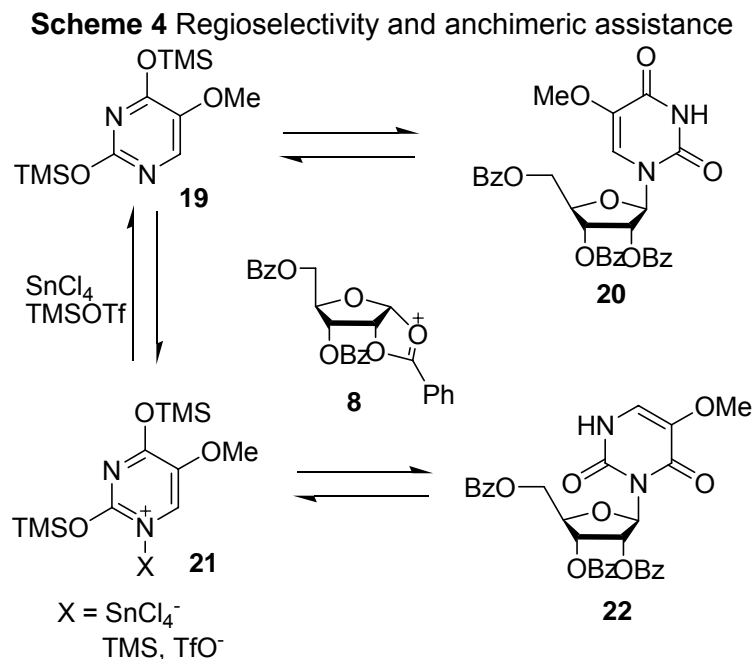
Scheme 2 β selectivity through anchimeric assistance

In the syntheses of dioxolanyl nucleoside analogs, Choi and Liotta has reported the use of titanium Lewis acids in the glycosylation reaction to provide high β -facial selectivity.⁷² The mechanism is proposed as shown in **Scheme 3**, in which an intermediate **18** was proposed.

Scheme 3 Titanium Lewis acid in glycosylation reaction of dioxolanyl acetate

In addition to anchimeric assistance, bulky 2- α -substituents have also been reported to induce β selectivity by blocking α face, but it is generally less selective than anchimeric assistance.

Another issue of the nitrogen glycosylation reaction is regioselectivity. Though oxygen attack is minimized in the silylated condition, attack from multiple nucleophilic nitrogen centers on nucleoside base (N^1 , N^3 for pyrimidines; N^9 , N^7 for purines) generates two regioisomers. The selectivity comes from the competition between the reversible σ complexation and the reversible nucleoside bond formation process (exemplified in **Scheme 4**). The reversible σ complexation depends highly on the basicity of silylated bases, the property of Lewis acid and solvent. Lewis acids such as SnCl_4 and TiCl_4 form strong σ complexes while the milder TMSOTf and TMSClO_4 form weaker complexes. The employment of the more polar acetonitrile, which competes with silylated bases for σ complexation, provides better result when σ complexation is an issue.⁷³

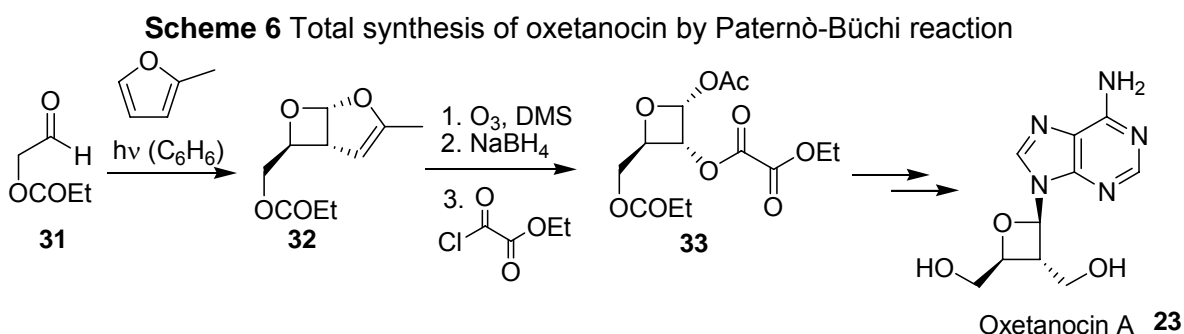


1.3.2 Oxetane Ring Formation

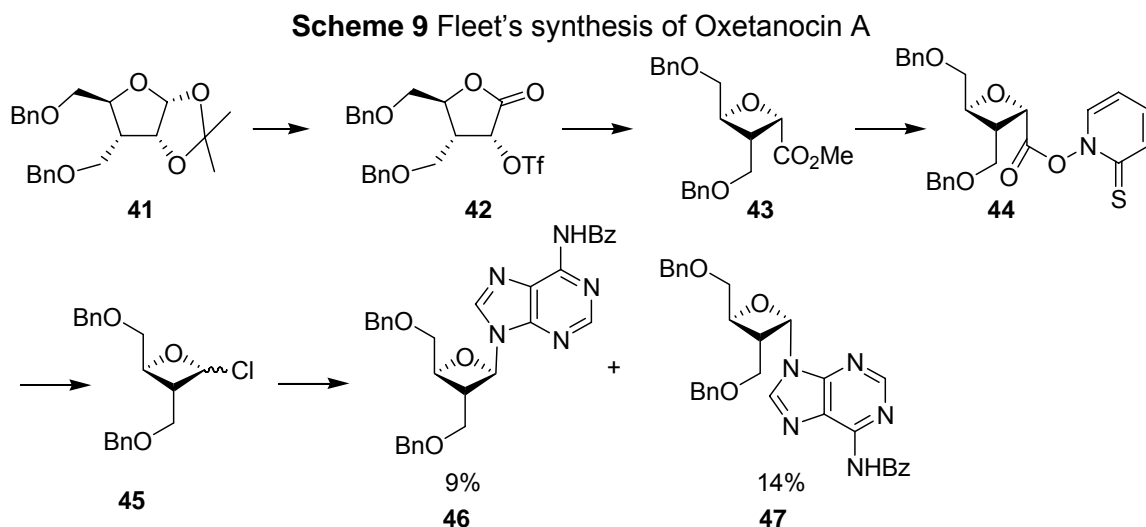
Though less common than its three-membered and five and six-membered counterparts, oxetane is still a common substructure in many important molecules (**Figure 12**) such as antiviral agent Oxetanocin A **23**, and FDA approved anti-cancer agent Taxol **24**. The preparation of the oxetane ring can be categorized into three major classes: [2+2] photocycloaddition of alkenes with carbonyl compounds, ring contraction reactions and intramolecular cyclization in an $\text{S}_{\text{N}}2$ fashion.

compounds that react from their singlet states lead to high stereo- but moderate regiocontrol. Saturated aldehydes are representative of this class. Ketones, particularly conjugated one, react from the triplet state giving rise to high regioselectivity but moderate stereoselectivity. High HOMO (Highest Occupied Molecular Orbital) energy of the alkene that is ensured by electron donating substituents promotes this selectivity pattern.

The Paternò–Büchi reaction has been employed in the synthesis of antiviral nucleoside Oxetanocin A **23** as shown in **Scheme 6**. The exo-selective cycloaddition of 2-methylfuran to a 2-acetoxy substituted aldehyde **29** was used to set up the relative configuration at C(3) and C(4).⁷⁹ The low yield was due to regioselectivity problems in the Paternò–Büchi reaction. Ozonolysis of the photocycloadduct **30** gave the desired acetal **31** which could be further transformed to Oxetanocin A according to a published procedure.⁸⁰



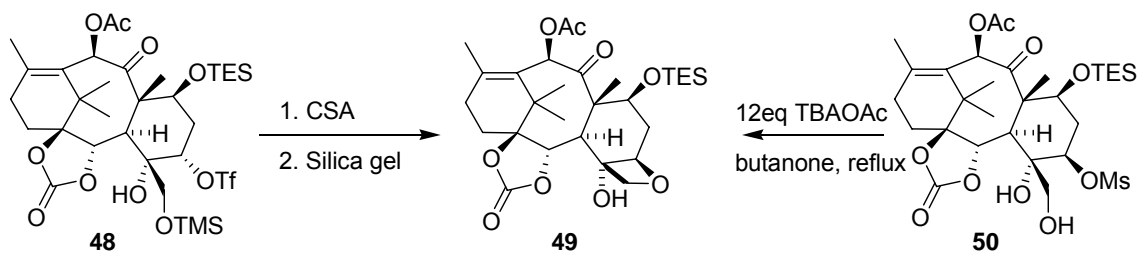
Two bicyclic oxetane containing compounds **36**, **37** were synthesized through the Paternò–Büchi reaction between the protected electron rich L-



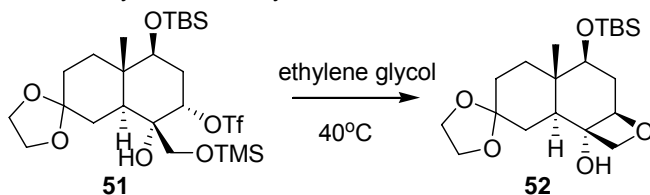
The last approach of oxetane formation, intramolecular cyclization in an S_N2 fashion is most extensively explored in the Taxol related study. It is generally achieved by an intramolecular S_N2 displacement of a leaving group under appropriate basic or acidic conditions. In Nicolaou's total synthesis of Taxol,⁸⁴ the installation of the oxetane ring is achieved in two approaches as shown in **Scheme 10**. In the first approach, the triflate (trifluoromethanesulfonate) **48** was intramolecularly displaced under mildly acidic condition (silica gel), while in the second approach, the mesylate (methanesulphonate) **50** was displaced in the presence of excess TBAOAc (N-tetrabutylammonium acetate) under refluxing butanone conditions. In the model study from the Danishefsky group,⁸⁵ ethylene glycol was used to catalyze the sequential deprotection and S_N2 displacement of **51**. In Potier's study,⁸⁶ TBAOAc (tetra-n-butylammonium acetate) was employed in the oxetane formation step. The use of TBAF (tetra-n-butylammonium fluoride) afforded **53** through sequential deprotection/substitution reactions. DBU (1,8-diazabicyclo[5.4.0]undec-7-ene) was reported to catalyze similar reactions.⁸⁷

Scheme 10 Oxetane formation in Taxol synthesis

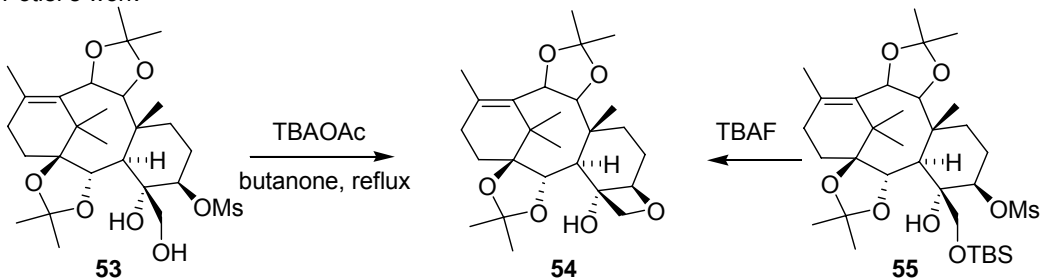
Nicolaou's total synthesis of taxol



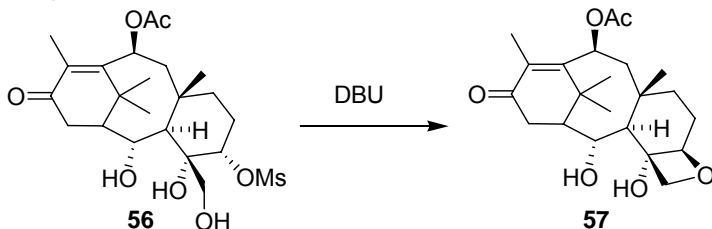
Denishefsky's model study



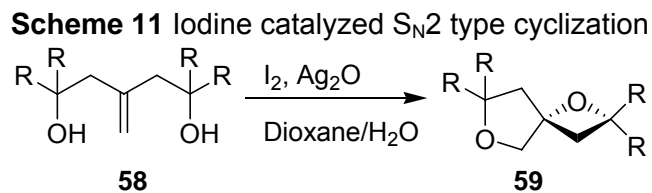
Potier's work



Yin, D. L.'s work



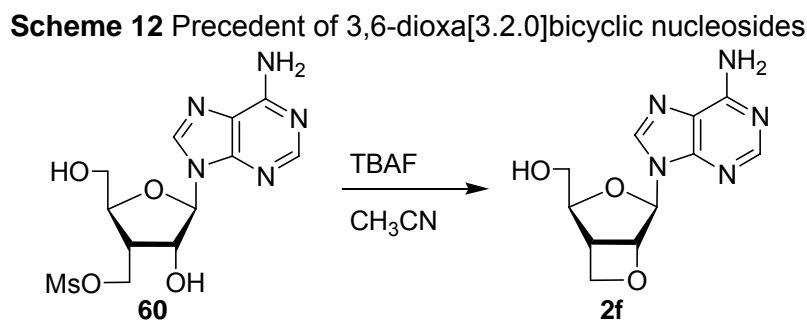
It has been reported that the homoallylic alcohol **58** was employed to form to a spiro oxetane containing compound **59** through an iodine catalyzed S_N2 type reaction as shown in **Scheme 11**.



1.3.3 Bicyclic Nucleoside Analogs

Recently, conformationally constrained nucleosides have drawn considerable attention since these nucleosides adopt certain desired, restricted, geometrical shapes and are potentially useful as small molecule inhibitors of certain enzymes or as building blocks for oligonucleotides (ON's) with potential therapeutic and diagnostic applications.^{88, 89}

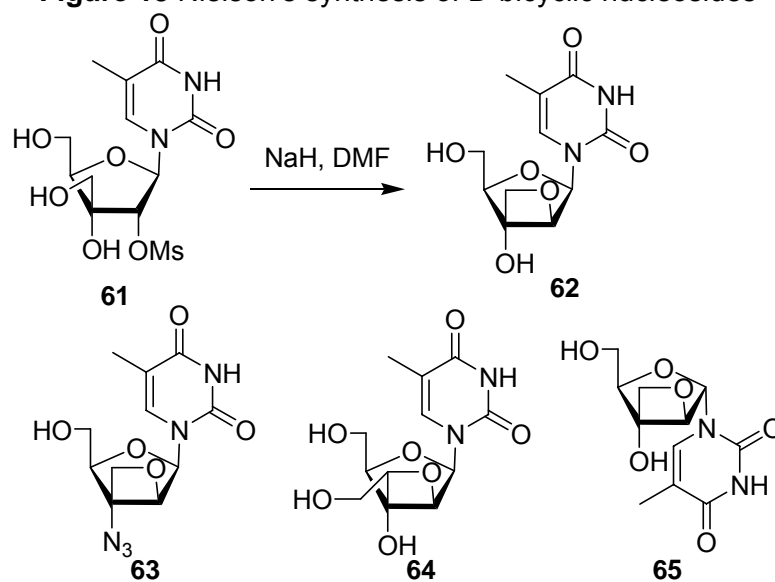
Among them, several bicyclic nucleoside analogs containing oxetane ring have been reported. As the only known synthesis of the proposed structures, the β -D- bicyclic adenosine derivative **2f** has been reported by the Mikhailopulo group. It was observed as an undesired product after treating the mesylate **60** was treated with TBAF as the fluorine source to displace the mesyloxy group. (Scheme 12)⁹⁰



The Nielsen group has reported a series of D- bicyclic thymidine derivatives as shown in **Figure 13**.⁹¹⁻⁹⁴ Upon treatment with NaH as base in DMF,

3'-O-methanesulfonates (or TsO-) in **61** were intramolecularly substituted to afford the oxetane containing product **62**.

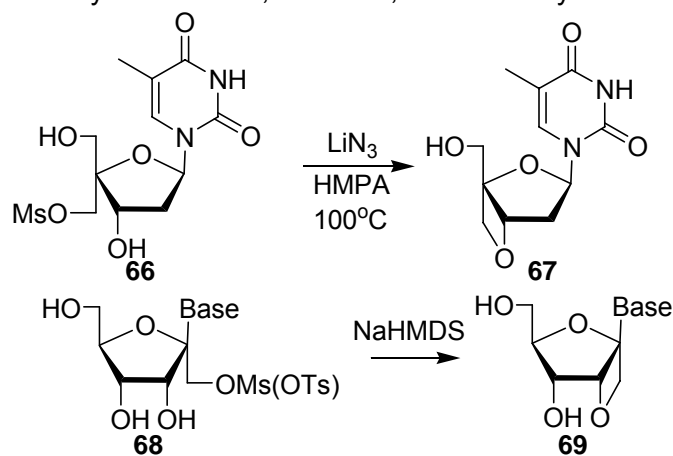
Figure 13 Nielson's synthesis of D-bicyclic nucleosides



In addition to the 2',3' fused bicyclic nucleosides, 1',2'- and 3',4'- fused bicyclic nucleoside analogs (**67**, **69**) were synthesized as shown in **Scheme 13**.⁹⁵

96

Scheme 13 Synthesis of 1',2'- and 3',4'- fused bicyclic nucleosides



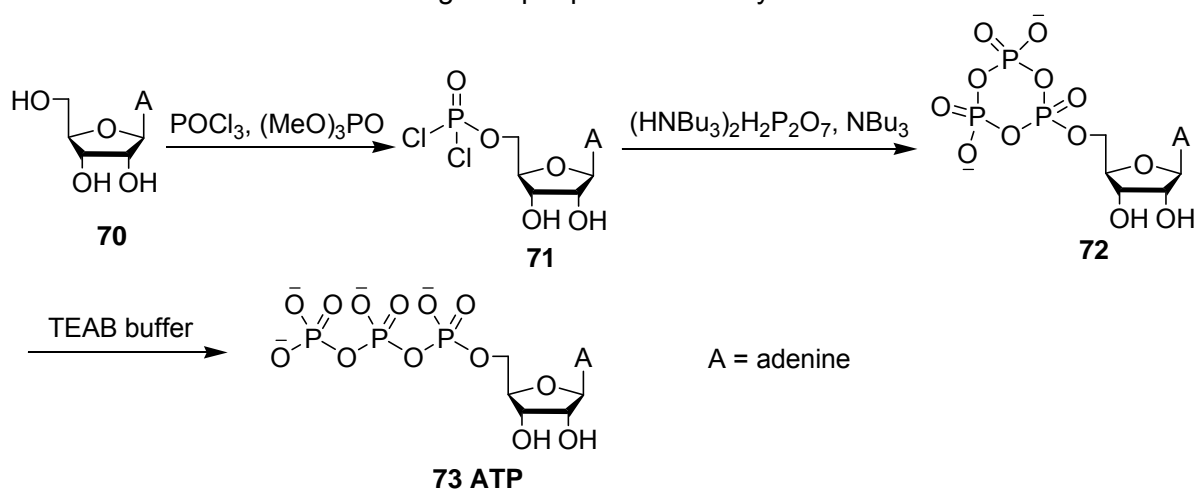
1.3.4 Syntheses of Nucleoside Triphosphates

The need for a general and efficient route to nucleoside triphosphates is an unsolved problem. Some methods work very well for certain substrates, but none of the protocols is universally satisfactory. The synthesis can be achieved chemically or biochemically. Several most frequently used chemical strategies are listed below:

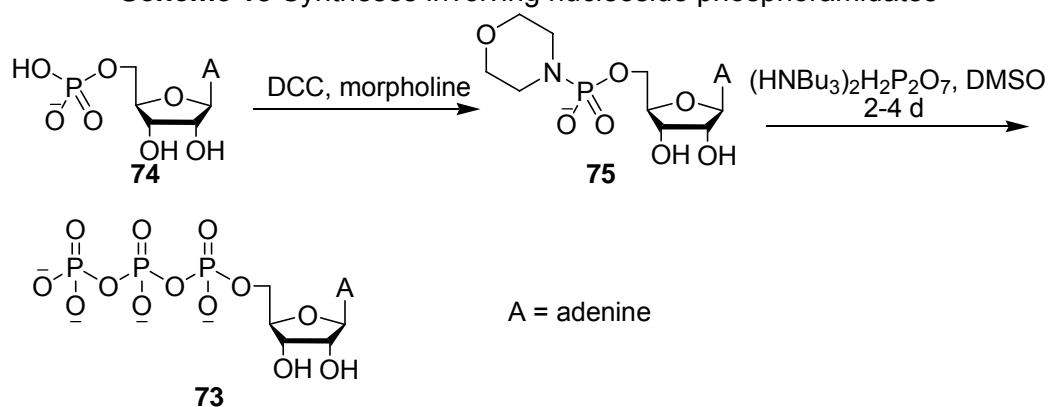
1.3.4.1 Syntheses Involving Activated Nucleoside Monophosphates

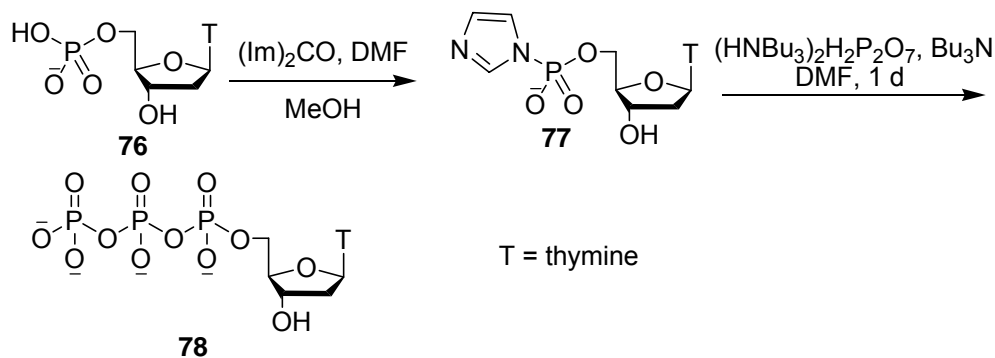
In this strategy, the activated NMP (nucleoside monophosphate) derivative is nucleophilically attacked by a pyrophosphate to afford nucleoside triphosphate.

Ludwig developed a one-pot procedure using nucleoside dichlorophosphates as the activated NMP species to react with tri-*n*-butylammonium pyrophosphate and afford the NTPs.⁹⁷ The Ludwig one-pot procedure employed in chemical synthesis of ATP **73** was shown in **Scheme 14**. The nucleoside dichlorophosphate **71** was generated by Yoshikawa's monophosphorylation procedure by reacting adenosine **70** with phosphorus oxychloride in the reaction media of trimethyl- or triethyl- phosphate. The nucleophilic attack of tri-*n*-butylammonium pyrophosphate in the presence of tri-*n*-butylamine afforded the cyclic triphosphate **72**, which was transformed to the ATP **73** upon quenching with TEAB (triethylammonium bicarbonate) buffer. The yield decreased when an amine base was not present.

Scheme 14 Ludwig one-pot procedure in synthesis of ATP

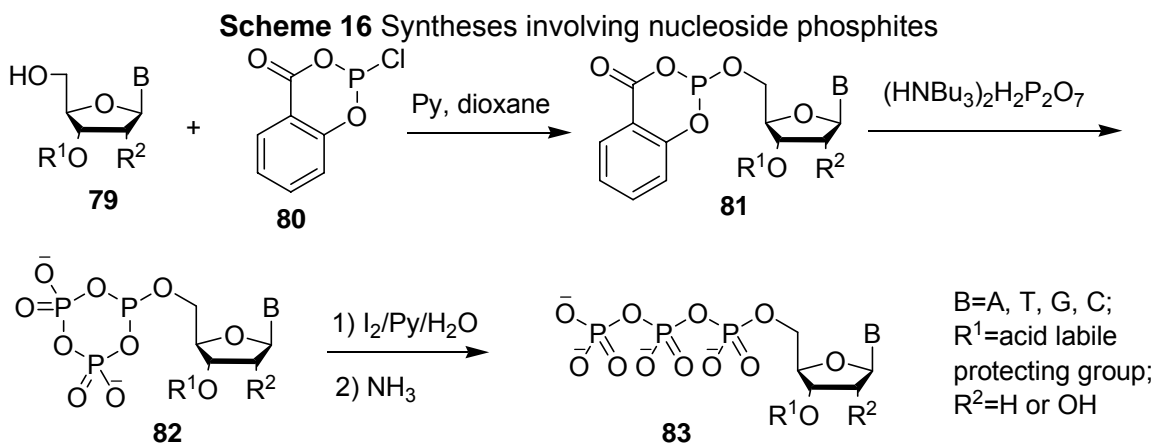
The syntheses of NTPs using nucleoside phosphoramidates as activate NMP species were conducted stepwise. A NMP was synthesized and isolated first, and then reacted with an amine (i.e. morpholine⁹⁸, imidazole **Scheme 15**) to form the activated nucleoside phosphoramidate. The resulting phosphoramidate was nucleophilically attacked by pyrophosphate to afford the NTP.

Scheme 15 Syntheses involving nucleoside phosphoramidates



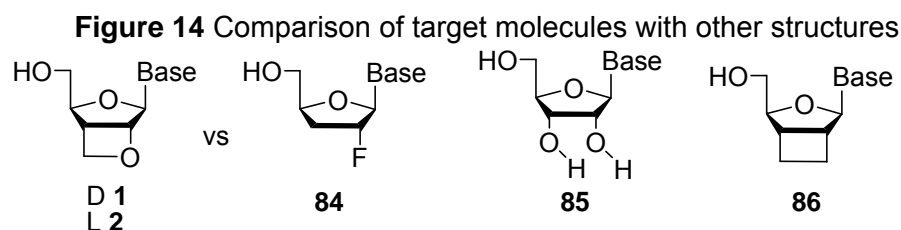
1.3.4.2 Syntheses Involving Activated Phosphites

Ludwig and Eckstein developed an alternate methodology involving the activated nucleoside phosphite intermediates.⁹⁹ The nucleoside analog **79** was treated with 2-chloro-4*H*-1, 3, 2-benzodioxaphosphorin-4-one **80** to afford an activated nucleoside phosphite **81** (Scheme 16). The resulting phosphite **81** was attacked by pyrophosphate to form a cyclic intermediate **82**, which was then hydrolyzed and oxidized to give the corresponding NTP **83**.



1.4 Design and Syntheses of 3,6-dioxa-[3.2.0]bicyclonucleoside Analogs

Nucleoside HCV RdRp inhibitors interrupt viral replication through either directly inhibiting the enzyme or terminating the RNA elongation by incorporation of the analog into the growing RNA strand.



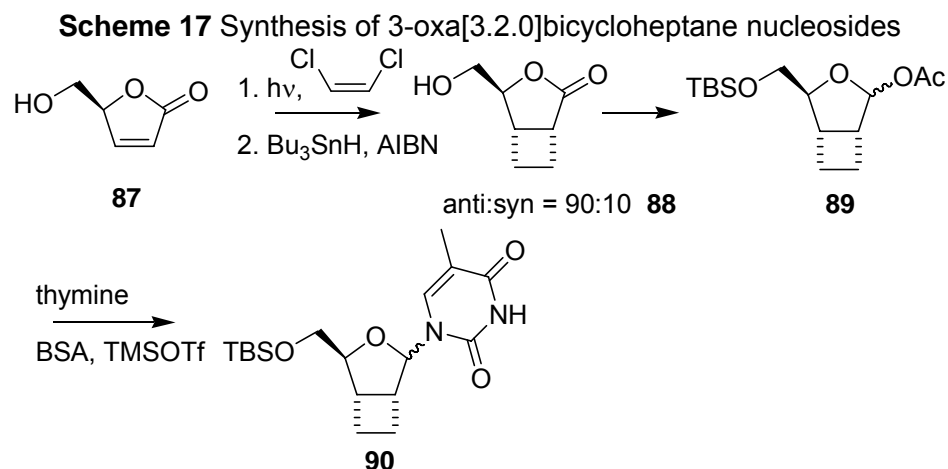
Given the fact that HCV RdRp utilizes ribonucleoside triphosphates (rNTP) to synthesize RNA, a 2'-hydroxyl or -fluoro substituent should contribute to the potency and selectivity toward HCV polymerase. Moreover, according to the early results that show D and L- α -2'-F-3'-deoxynucleosides **84** were inactive in HCV replicon assay, we hypothesize that the presence of an α -2'-F- substituent alone is insufficient to produce potent HCV inhibition, probably as a consequence of conformational factors. The conformations of natural ribonucleosides exist predominantly in gauche or near-eclipsed 2'-3'- orientations because of hydrogen bonding and/or dipole-dipole interactions, which are very different from those observed in nucleosides that lack a 2'-substituent.^{100, 101} We chose 3,6-dioxa[3,2,0] bicyclonucleoside analogs (**1**, **2**) as the targets because they possess a near-eclipsed 2'-3' orientation, locked by the oxetane ring, which mimics the 2'-3'-diol functionality in natural ribonucleosides **85**. (**Figure 14**) In addition, the comparison of activities with 3-oxa[3,2,0]bicyclonucleosides **86** will

also provide us insight as to whether the 2'-oxygen atom serves as a recognition site for HCV RdRp.

The only known compound in this family, a D-3,6-dioxo[3,2,0]bicyclic adenosine derivative, has been reported as an unexpected product in the synthesis of the 3'-C-fluoromethyl-3'-deoxy adenosine analog. Since the synthetic route was not specifically designed for the synthesis of our desired structure, a variety of potential routes were considered.

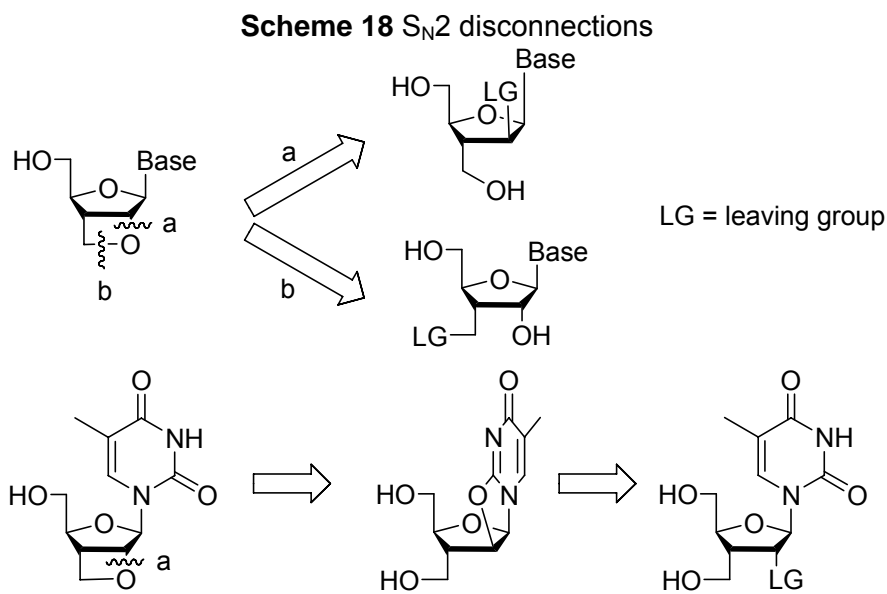
As mentioned in section 1.3.2, three strategies are commonly employed in the construction of oxetane rings: The Paternò-Büchi reaction, the ring contraction reaction and the intramolecular S_N2 substitution.

The Paternò-Büchi reaction seems to be the most direct method provided that the same strategy in the synthesis of 3-oxa[3.2.0]bicycloheptane nucleoside analogues **90** (**Scheme 17**)¹⁰² can be applied. However, literature research suggests that the use of Paternò-Büchi reaction in the synthesis of 3,6-dioxo [3.2.0] bicyclic nucleosides would be impractical for the following reasons: 1) It is very difficult to introduce an electron rich alkene as required by the electronic demand in any stage of the synthesis; 2) substitutions on the carbonyl component are generally required in order to stabilize its triplet state, but the undesired substitutions need extra effort to remove; 3) despite good stereoselectivities Paternò-Büchi reactions may have, they usually suffer poor regioselectivity.



The ring contraction strategy has been used in the syntheses of single ring oxetane nucleoside analogs (i.e. Oxetanocin A^{82, 83}), because their precursors with five-membered sugar ring can be easily obtained from modification of natural carbohydrates or nucleosides. In the case of 3,6-dioxa-[3.2.0]bicyclic nucleosides, the possible precursors for ring contraction reactions were examined, none of which could be easily obtained from available carbohydrates or nucleosides. The removal of undesired substituents was another issue which made the ring contraction strategy unsuitable in this synthesis.

Thus, intramolecular $\text{S}_{\text{N}}2$ strategy was determined as the best way to synthesize our target molecules. There are two possible disconnections (**Scheme 18**) for the intramolecular $\text{S}_{\text{N}}2$ type strategy. Pyrimidine analogs could react through a neighboring group participation mechanism shown in **Scheme 18**.



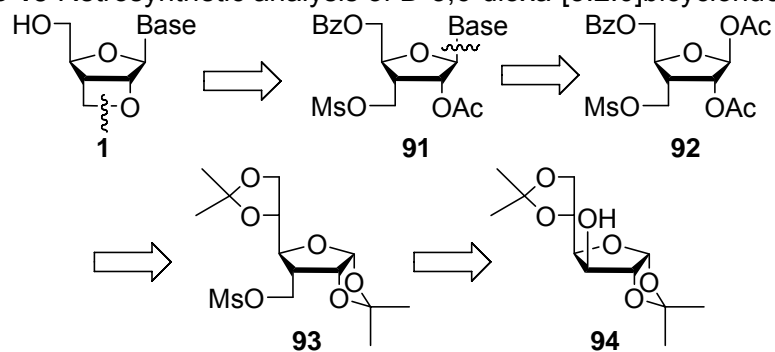
Disconnection **a** involves an intramolecular S_N2 attack of a primary alcohol onto a secondary leaving group, which is well precovered as shown in many syntheses of Taxol (**Scheme 10**) and Neilson's synthesis of 2',3'-fused bicyclic nucleoside analogs (**Scheme 13**). Considering that the 2'-β leaving group could not be directly obtained from 2'-α-acyloxy group which is required in the nitrogen glycosylation reaction, extra effort has to be added to manipulate the 2' functional group. Though pyrimidine nucleosides can be obtained from precursors with an α leaving group, disconnection **b** is employed in the synthesis of target molecules, as a general method to synthesize both pyrimidine and purine nucleosides is desired.

1.4.1 Syntheses of D-3,6-Dioxa-[3.2.0]bicyclonucleoside Analogs

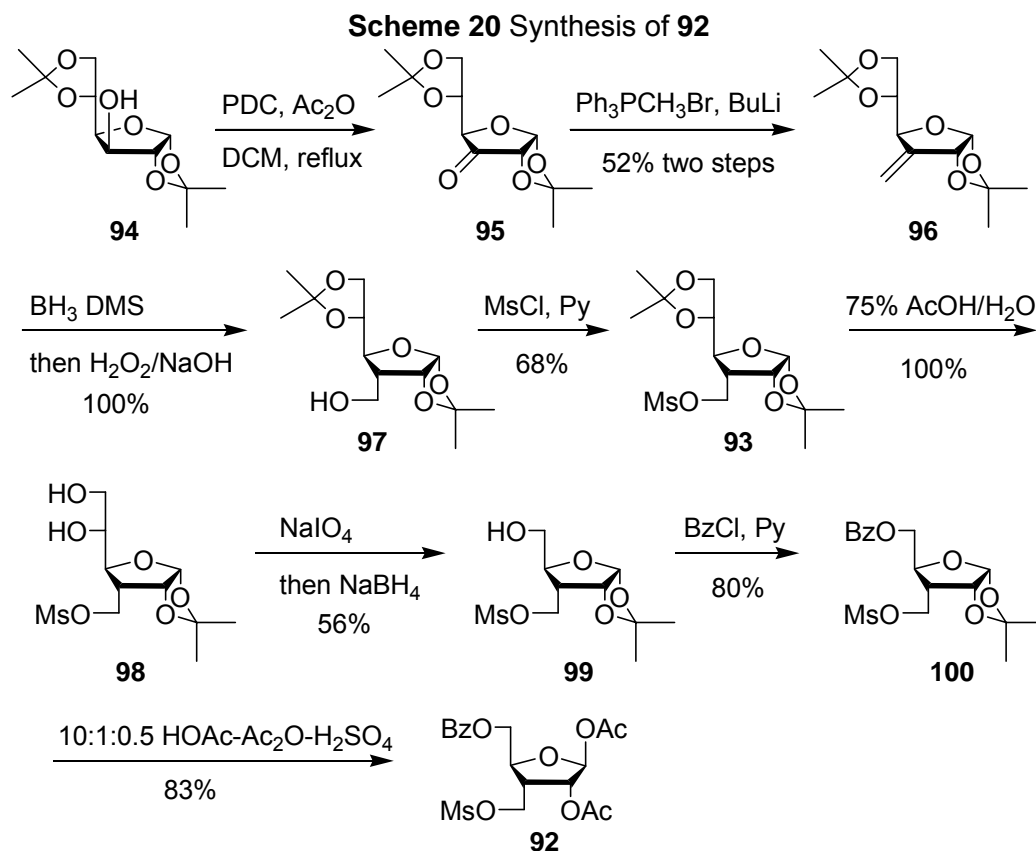
The literature approach that was used in the synthesis of D-[3.2.0]bicyclic adenosine derivative was slightly modified to accommodate the syntheses of analogs with thymine, 5-F-cytosine, 5-F-uracil, cytosine, and 6-chloropurine

bases. The retrosynthetic analysis of D-[3.2.0]bicyclic nucleoside analogs is shown in **Scheme 19**.

Scheme 19 Retrosynthetic analysis of D-3,6-dioxa-[3.2.0]bicyclonucleosides

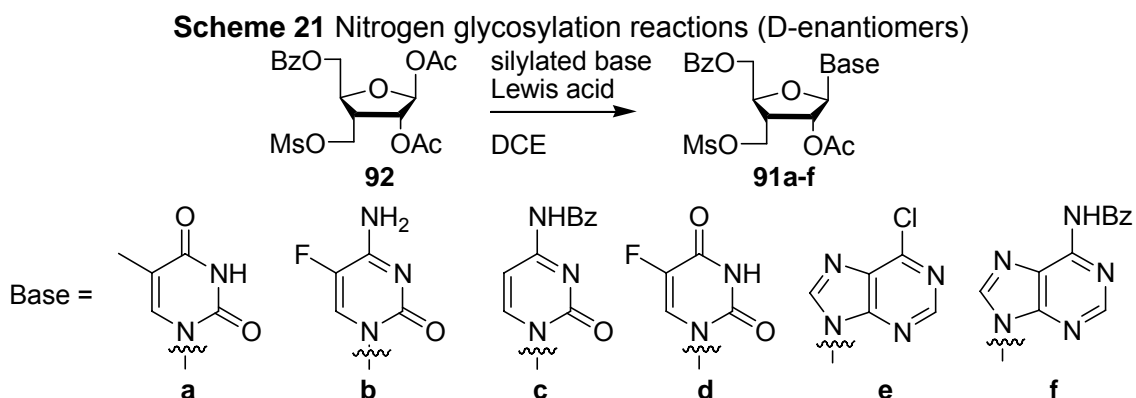


The oxetane ring in the target compounds **1** was constructed by the intramolecular S_N2 substitution. Intermediate **91** was obtained from the nitrogen glycosylation reaction of ribofuranosyl acetate **92**, which is modified from diacetoneid protected D-glucose **94**.



The synthesis of the key intermediate **92** is illustrated in **Scheme 20**. The commercially available 1,2:5,6-di-O-isopropylidene- α -D-glucopyranose **94** was oxidized by pyridinium dichromate (PDC)-acetic anhydride, which is milder than the common chromium (VI) oxide as well as the ruthenium (IV) oxide/ sodium periodate condition¹⁰³. It is also better than the Swern oxidation when applied to a large scale. The following Wittig reaction transformed the ketone **95** to alkene **96**. In the boration-oxidation step, the borane dimethyl sulfide (DMS) complex attacked the double bond from the less hindered terminal position and the top face to give the 3-hydroxymethyl functionality. The resulting primary alcohol was protected as a mesylate. The less hindered 1,2-O-isopropylidene protection was selectively removed with 75% acetic acid solution. Cleavage of the resulting diol

98 by sodium periodate followed by sodium borohydride reduction furnished intermediate **99**. Benzoylation in pyridine afforded a crystalline **100**. Acetylation of **100** in 10:1 glacial acetic acid-acetic anhydride in the presence of a catalytic amount of concentrated sulfuric acid afforded the β ribofuranosyl acetate **92**, which is the starting material for the key Vorbrüggen reaction.



The nitrogen glycosylation reactions are shown in **Scheme 21**. As mentioned in section 1.3.1, nucleoside bases were silylated to improve their lipophilicity as well as nucleophilicity, which was achieved by refluxing in hexamethyldisilazane (HMDS) in the presence of a catalytic amount of ammonium sulfate. TMSOTf and tin (IV) chloride were the preferred Lewis acids. Due to the different reactivity between pyrimidine and purine bases in the glycosylation step, model studies on glycosylation conditions for thymine and 6-Cl-purine were performed. As listed in **Table 1**, the milder TMSOTf gave better yield for the more reactive pyrimidine bases; however, it was not reactive enough to complete the reaction of the less reactive purine bases. At the same time, tin

(IV) chloride, which gave lower yields for the thymine coupling, provided higher reaction rates, better yields and higher regioselectivity for 6-Cl-purine.

Table 1 Glycosylation reactions of pyrimidine and purine bases

Base	1.1eq TMSOTf, DCE	1.1eq SnCl ₄ , DCE
Thymine	r.t. 6 h 94%	r.t. 1h 77%
6-Cl-purine	r.t. 16h, 70°C 12h 28% N ⁹ product, 11% N ⁷ product, 28% recovered SM	r.t. 6h 57% N ⁹ product, trace N ⁷ product

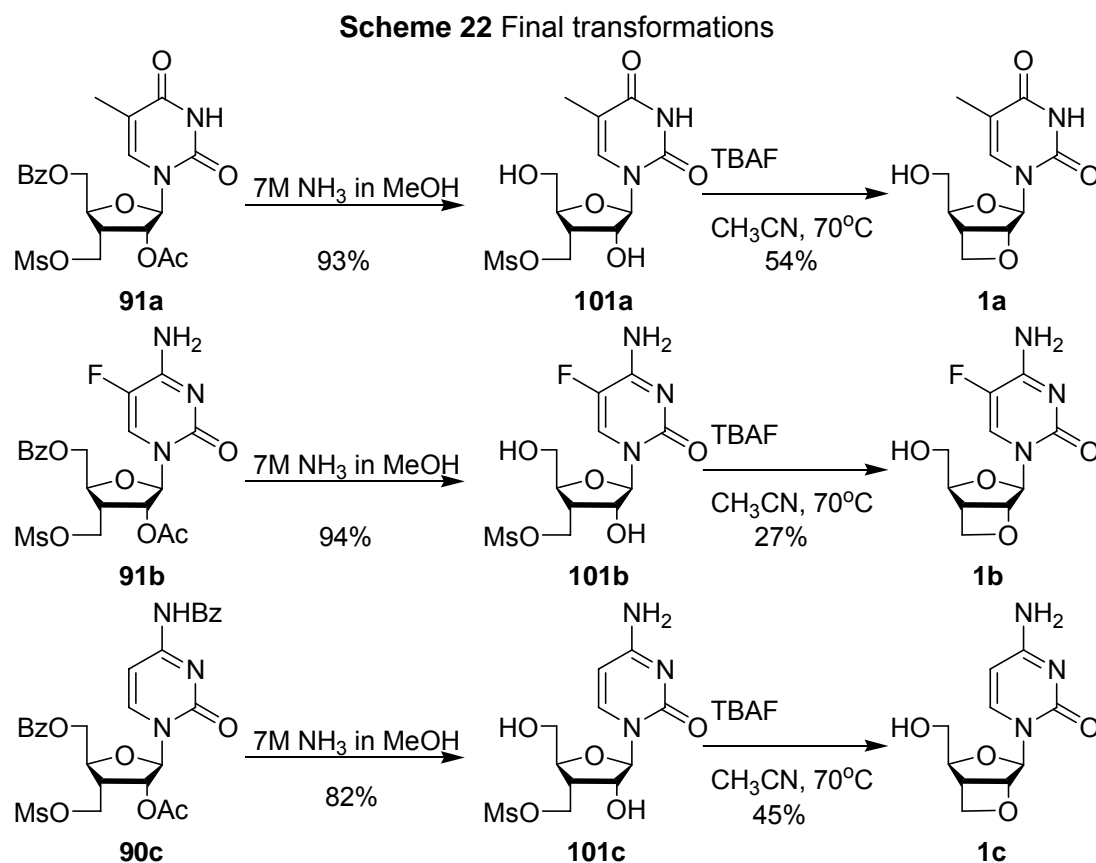
For all pyrimidine bases, the premixed DCE solution of 1.1 eq of TMSOTf with 1.2 eq of silylated bases was added to the solution of acetate **92** in DCE to afford only the β product. Due to the basicity of the free amino group, the direct glycosylation of the silylated cytosine was not successful. The introduction of electron withdrawing Bz group on the free amino group provided acceptable yields. The stereoselectivity was determined by 1D NOE differential spectroscopy.

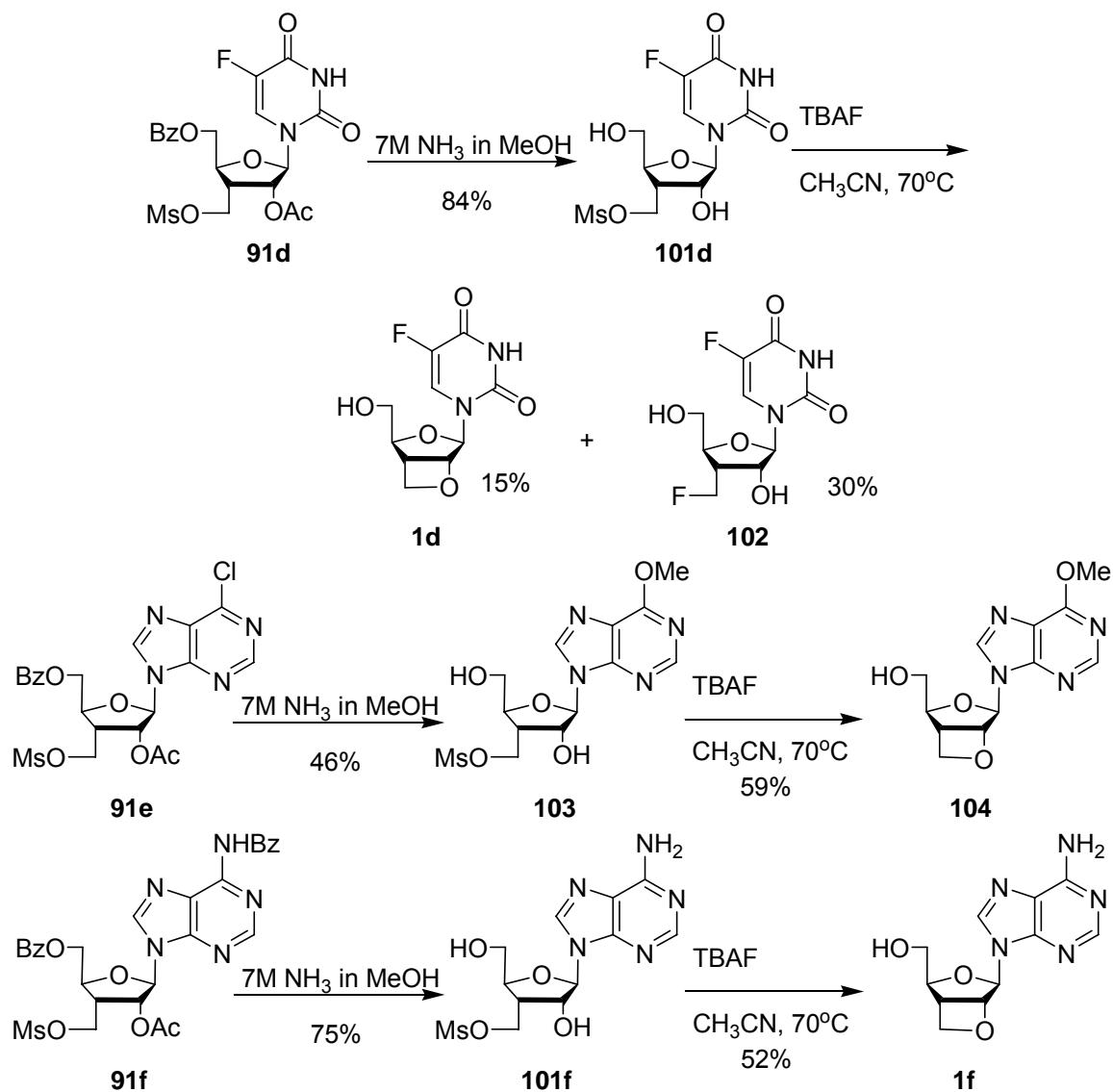
For 6-Cl-purine, 1.1 eq of SnCl₄ solution was added to a solution of acetate **92** and 1.2 eq of silylated base to afford β N⁹ product at a 57% yield with trace amounts of the N⁷ regioisomer. The regioselectivity was determined by ¹H and ¹³C NMR as reported in the literature.¹⁰⁴ 1D NOE spectrum was taken to confirm the stereoselectivity as well.

Table 2 Nitrogen glycosylation reaction of **92**

Silylated Base	Reaction condition	Results
thymine	TMSOTf, 6h	94%
5-F-cytosine	TMSOTf, 6h	92%
N ⁴ -benzoyl cytosine	TMSOTf, 6h	38%
5-F-uracil	TMSOTf, 6h	99%
6-Cl-purine	SnCl ₄ , 6h	57% N ⁹ product
N ⁶ -benzoyl cytosine	2.5eq SnCl ₄ , CH ₃ CN, 6h	60%

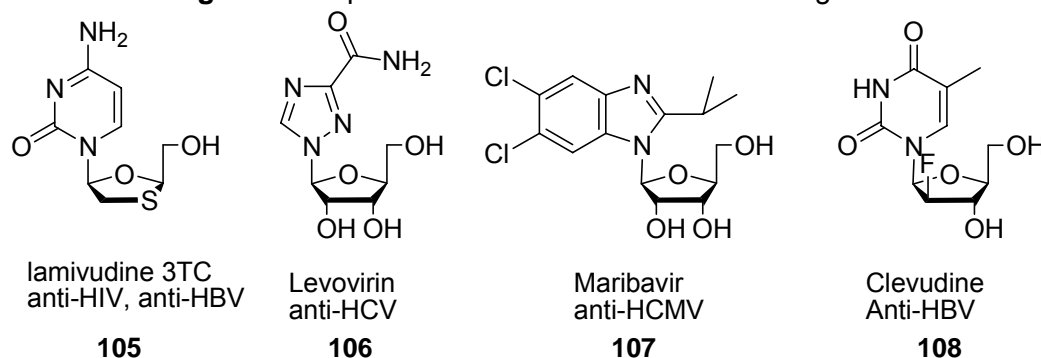
The following transformations are similar for all bases as demonstrated in **Scheme 22**. The coupling product **91a-e** was dissolved in 7 M ammonia in methanol and kept for 2 days to completely remove the Bz group. The chloro group on 6-Cl-purine product was displaced by methoxy group to afford **103** in this process. The resulting 6-methoxypurine derivative **104** was submitted for testing. TBAF in acetonitrile at 70°C afforded acceptable yields and least 3'-C substitution products. Excess TBAF in the final compound was difficult to remove by column chromatography. Thus, preparative RP-HPLC was used to purify the final compounds. The fluoro substituted product **102** under TBAF conditions was only observed on the 5-F-uracil analog, which is also submitted for biological testing.



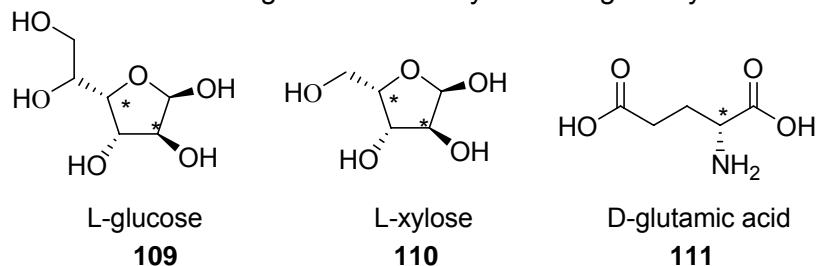


1.4.2 Syntheses of L-3,6-Dioxa-[3.2.0]bicyclonucleoside Analogs

Although L-ribonucleoside triphosphates are not the natural substrates of RNA polymerase, reverse transcriptase or DNA polymerase, there are still some L-nucleoside analogs showing antiviral activity. Since the discovery of lamivudine (3TC) **105**, the first FDA approved anti-HIV/HBV agent with L-configuration, several other L-nucleosides are currently under development as antiviral agents.¹⁰⁵ Three representatives are listed in **Figure 15**.

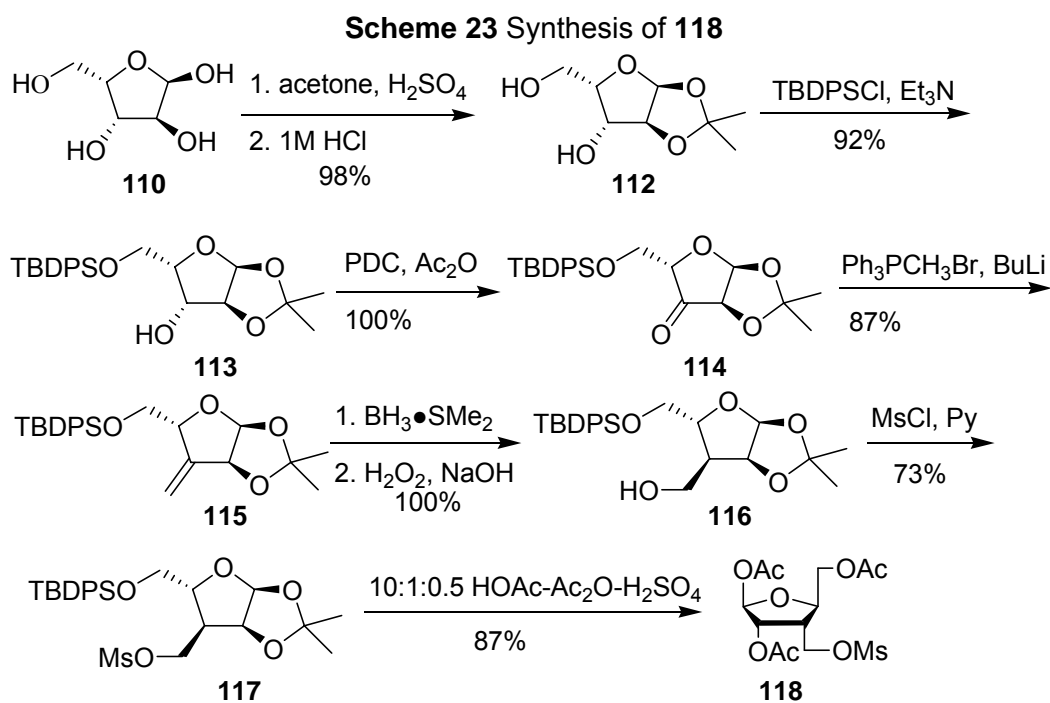
Figure 15 Representative L-nucleoside antiviral agents

The synthesis of L-3,6-dioxo[3.2.0]bicyclic nucleoside analogs is obviously limited by the starting materials because most natural nucleosides and carbohydrates exist in the D form. The configuration of the 2- and 4- carbon centers on the sugar moiety are essential to induce all correct stereo configurations in the target molecules. L-glucose **109** and L-xylose **110** both satisfy this requirement, but L-xylose is much less expensive than L-glucose. Another approach was also designed for the syntheses of L-bicyclic nucleosides starting from D-glutamic acid **111**, which will be discussed in section 1.4.2.2. Although L-xylose is more expensive than D-glutamic acid, the L-xylose approach proven to be more efficient (less steps and higher overall yields).

Figure 16 Potential starting materials for synthesizing L-bicyclic nucleosides

1.4.2.1 Approach starting from L-xylose

The strategy resembled the syntheses of D-bicyclic nucleosides from D-glucose except for changes of protecting groups. The key intermediate **118** is synthesized as shown in **Scheme 23**.



Commercially available L-xylose was protected with two acetonoids and one acetonoid was selectively deprotected to provide the mono protected intermediate **112**. The selective protection of the primary alcohol on **112** with TBDPS ether afforded mono silylated intermediate **113**. Mild PDC-acetic anhydride conditions oxidized the secondary alcohol on **113** to the ketone **114** with the chiral center on 5- position preserved. The Wittig reaction followed by a boration/oxidation step stereoselectively introduced the hydroxymethyl group onto the 3- position. After protection of the free hydroxyl group as a mesylate, the acetonoid protected diol was deprotected and acetylated in acetic acid-acetic

anhydride-sulfuric acid to give the intermediate **118**. The 5-O-TBDPS group was cleaved in these acidic conditions and the hydroxyl group was also acetylated. The configuration of **118** was confirmed by 1D NOE spectrum.

The ribofuranosyl acetate **118** was obtained as a colorless oil and was found likely to lose the anomeric acetyl group even when stored under argon at 0 °C. This stability issue was overcome by the crystallization of **118** to provide needle like crystals, which can be stored under argon at -20 °C with no decomposition observed.

Scheme 24 Nitrogen glycosylation reactions (L-enantiomers)

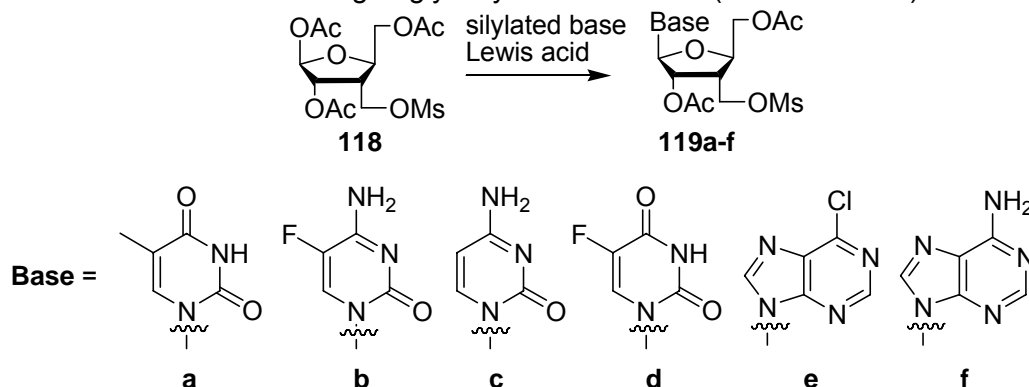


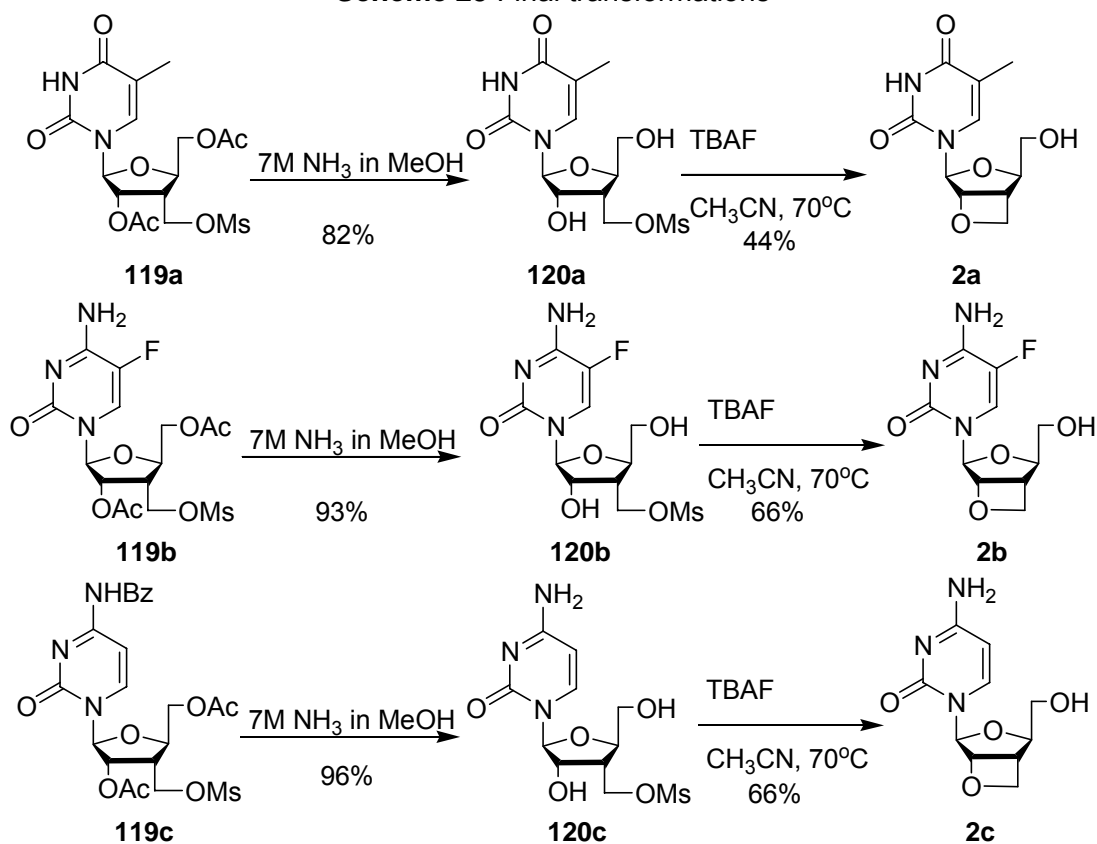
Table 3 Nitrogen glycosylation reaction of **118**

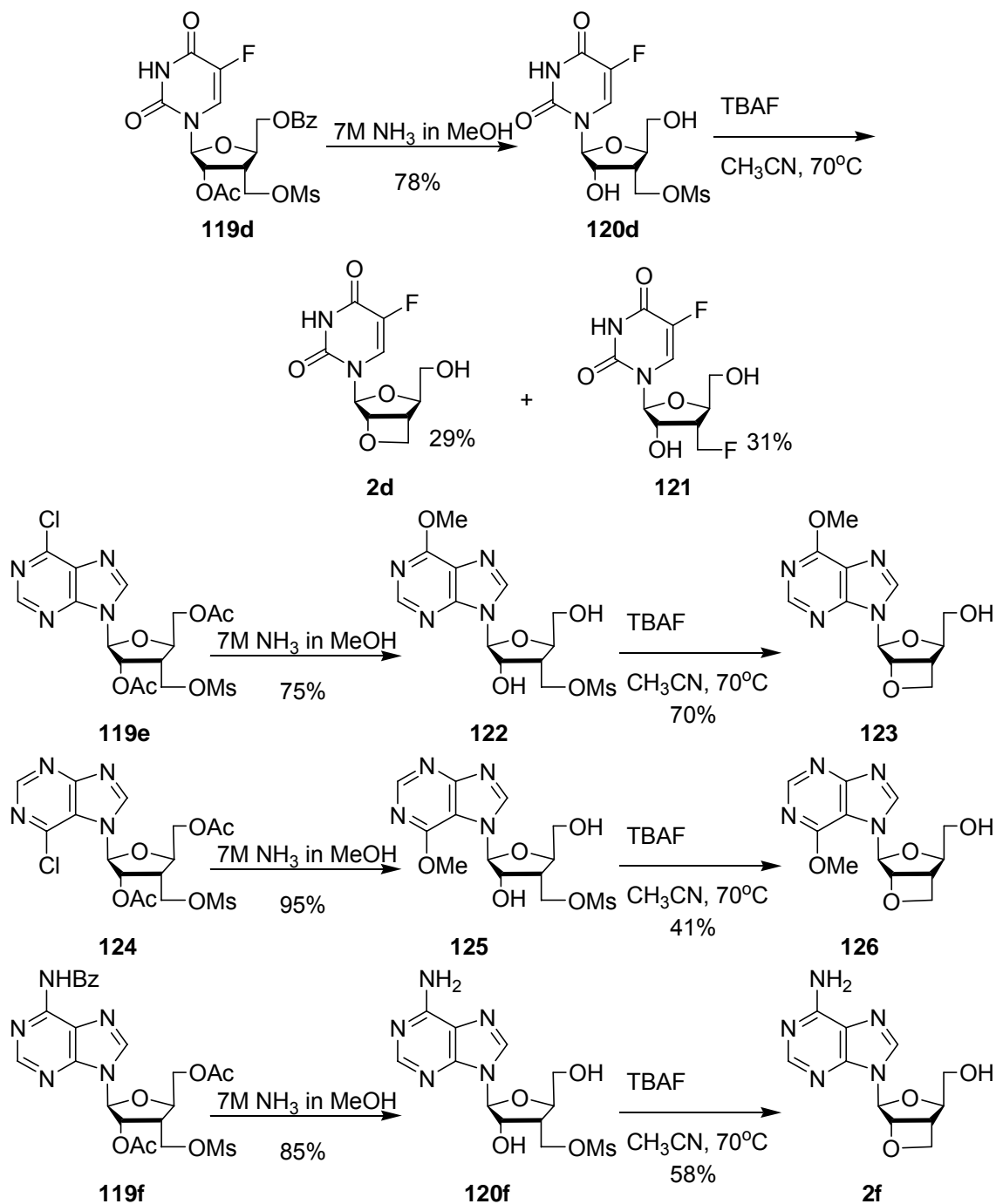
Silylated Base	Reaction condition	Results
thymine	1.1eq TMSOTf, DCE, 6h	93%
5-F-cytosine	1.1eq TMSOTf, DCE, 6h	84%
4-N-benzoyl cytosine	1.1eq TMSOTf, DCE, 6h	84%
5-F-uracil	1.1eq TMSOTf, DCE, 6h	89%
6-Cl-purine	2.5eq SnCl ₄ , CH ₃ CN, 6h	61% N ⁹ product, 28% N ⁷ product
6-N-benzoyl adenine	2.5eq SnCl ₄ , CH ₃ CN, 6h	64%

Silylated thymine, benzoyl cytosine, 5-F-cytosine, 5-F-uracil, 6-Cl-purine and benzoyl adenine coupled with **118** respectively (**Scheme 24**, **Table 3**) to provide **119a-f**. The benzoyl adenine was coupled with **118** with low yields under

the Vorbrüggen conditions developed for synthesizing D purine analogs (1.1 eq SnCl_4 , 1.2 eq silylated base in DCE). More conditions were screened and 2.5 eq SnCl_4 , 1.2 eq silylated base in acetonitrile was found more effective (64%). In the case of 6-Cl-purine under the same conditions, the N⁷ 6-Cl-purine product **124** was obtained as the minor product.

Scheme 25 Final transformations





The further transformations for various analogs are shown in **Scheme 25**.

The duration of the following aminolysis steps were reduced when the Bz group was absent. The fluorine substitution was only observed in 5-F-uracil analog **121**.

For the last cyclization step, more cyclization conditions were studied. Various

bases and conditions (**Table 4**) were studied on the thymine analog **120a**. Of these, TBAF in acetonitrile at 70°C afforded the best yields and the least fluorine substitution. The TBAF catalyzed reaction could be purified by very careful repeat column chromatography, but the employment of cationic ion exchange resin for the preliminary removal of tetrabutylammonium salt greatly improved the isolated yield and reduced the contamination of the final bicyclic product.

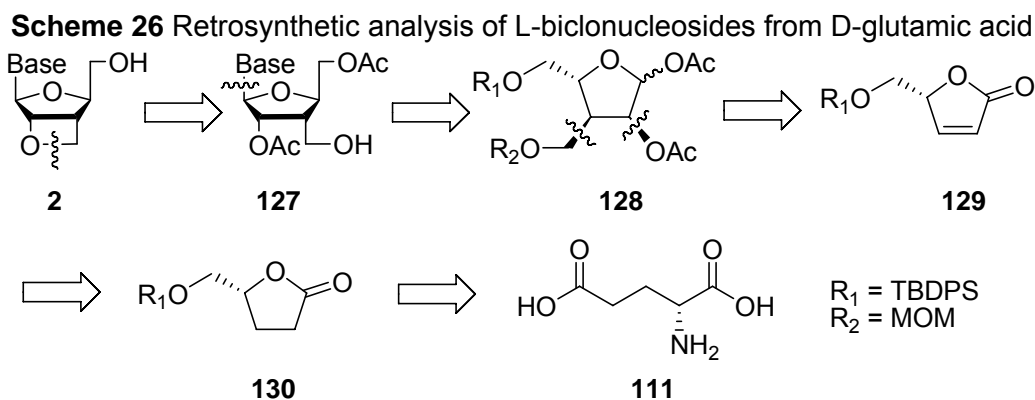
Table 4 Oxetane formation conditions

Conditions	Results
TBAF	Modest yields, salt contamination, improved by ion exchange resin
NaHMDS	decomposed
aq. NaOH/dioxane	-OH substitution
Cs ₂ CO ₃	decomposed
DBU	decomposed
TBAOAc	-OAc substitution

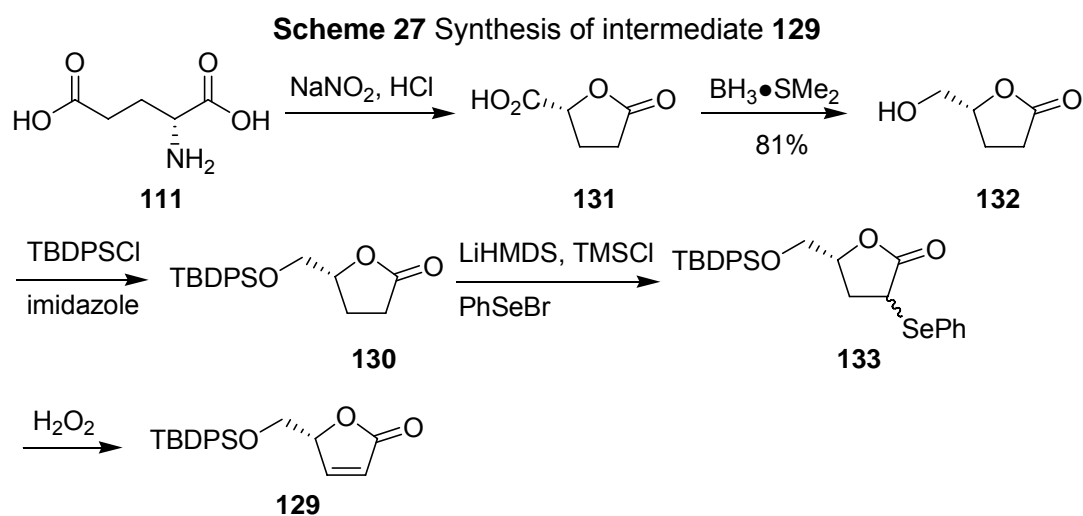
In addition to the bicyclic nucleoside analogs, the OAc substituted thymidine and 5-F-cytidine derivatives as well as the fluorine substituted 5-F-uridine derivative **121** were submitted for biological evaluation. The N⁷ bicyclic nucleoside **126** was also synthesized and submitted.

1.4.2.2 Approach starting from D-glutamic acid

As a less expensive starting material, D-glutamic acid was initially chosen as the starting material before the employment of L-xylose. The retrosynthetic analysis is described in **Scheme 26**.

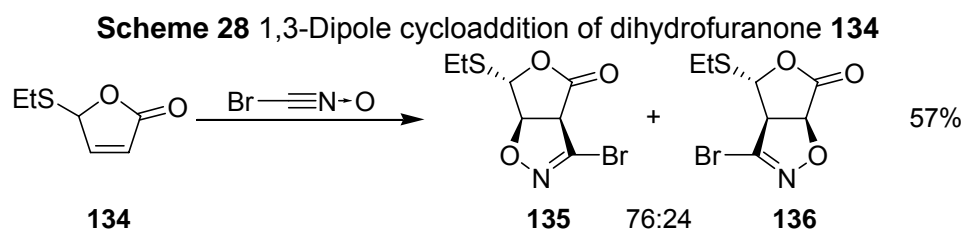


A similar intramolecular $\text{S}_{\text{N}}2$ substitution strategy was designed for the formation of the oxetane ring. The leaving group would be introduced after the nitrogen glycosylation reaction because of the early reduction step of the lactone. The cis α - and β - substitution would be installed onto the double bond of the α,β -unsaturated γ -lactone **129**, in which the stereoselectivity would be induced by the 4- chiral center. The conjugated double bond could be obtained by selenation-oxidative elimination sequence starting from the γ -lactone **130**, which would be synthesized following the known procedure from D-glutamic acid **111**.



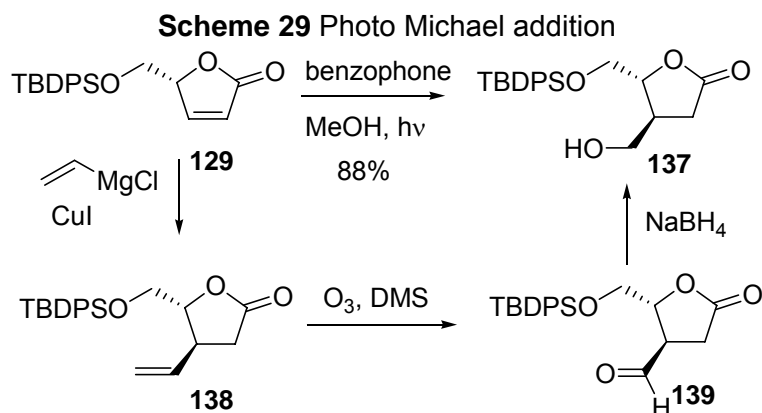
The unprotected precursor of intermediate **129** or its S- enantiomer has been synthesized starting from glutamic acid¹⁰⁶, D-mannitol¹⁰⁷, ribolactone¹⁰⁸ and ascorbic acid. Considering the efficiency and availability of starting material for the desired R-enantiomer **129**, the procedure followed the literature synthesis of its D counterpart starting from L-glutamic acid.¹⁰⁶ The D-glutamic acid **111** was treated with sodium nitrite under acidic conditions to afford the carboxylic acid **131** with retention (double inversion) of the chiral center. The resulting carboxylic acid was reduced to the primary alcohol in **132** by a borane dimethylsulfide complex. The resulting free alcohol was then protected to form TBDPS protected **130**. The α,β -unsaturated lactone **129** were obtained through an α -selenation-oxidative elimination sequence.

One potential way of synthesizing 2,3-cis disubstituted compound is a concerted cycloaddition reaction. The 1,3-dipole cycloaddition reaction of nitrile oxides provides oxazoline which can be further transformed into cis 2-hydroxyl 3-hydroxymethyl disubstituted product. However, the desired regioisomer is not preferred product in this reaction as illustrated in **Scheme 28**.¹⁰⁹



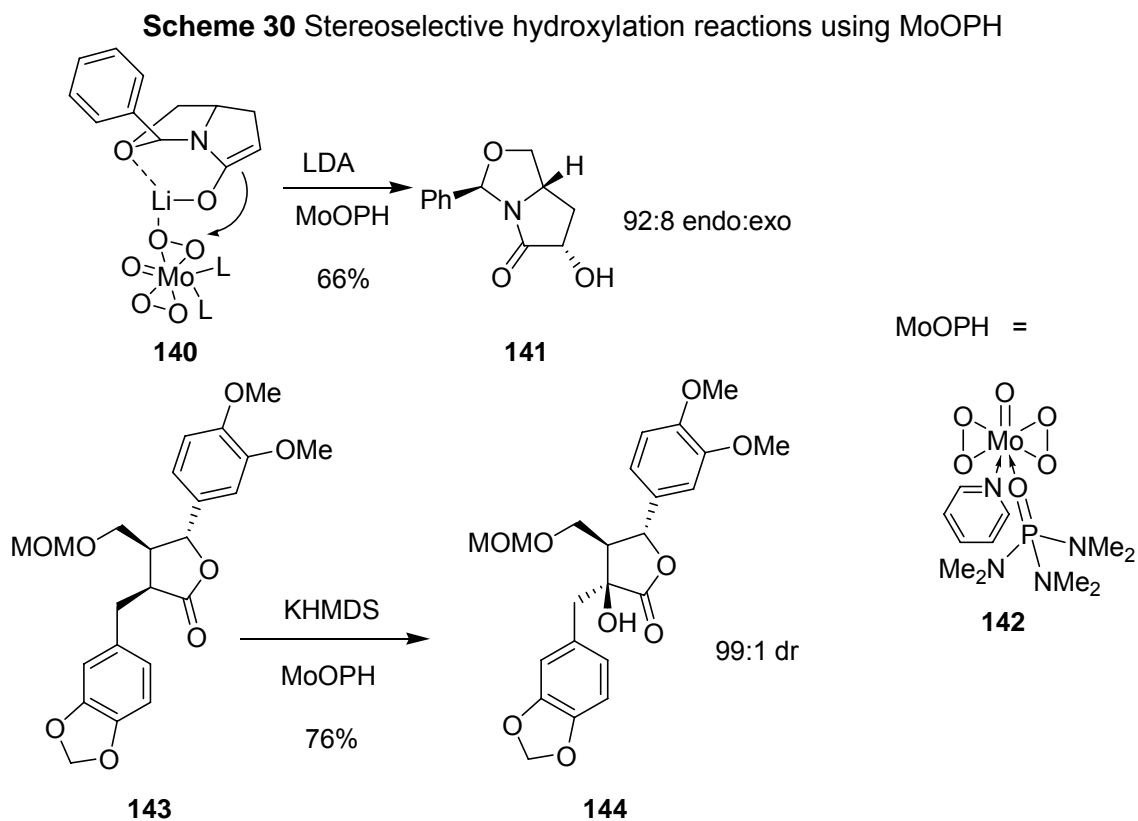
With no efficient concerted method, a stepwise approach was designed to introduce the 2,3- cis substituents. Although the stereoselective installation of the 3- hydroxymethyl substituent could be achieved by a three-step sequence of

Michael addition of lithium divinylcuprate, ozonolysis, and then reduction, a one-step photoaddition of methanol to the unsaturated lactone **129** seemed more efficient to provide **137**.¹¹⁰



The approaches of α -hydroxylation of carbonyl compounds were reviewed¹¹¹ and various conditions were discussed. Since the introduction of α -hydroxyl group was achieved by epoxidation/dihydroxylation of an enolate or enol ether followed by a rearrangement, many common epoxidation and dihydroxylation reagents also worked in the α -hydroxylation reaction. Among them, m-CPBA (3-Chloroperoxybenzoic acid), 3,3-dimethyl dioxirane, Davis reagent (trans-2-phenylsulfonyl-3-aryloxaziridine)¹¹² and MoOPH **142** [oxodiperoxymolybdenum (pyridine) (hexamethylphosphoric triamide)] were frequently used. In most conditions, the oxidative reagents attack from the less hindered face to afford exo product. However, an unusual endo selectivity has been observed in the α -hydroxylation with MoOPH through an intramolecular delivery mechanism.¹¹³ In the hydroxylation reaction of the MOM protected

intermediate **143** with MoOPH, the cis product was obtained selectively (**Scheme 30**).¹¹⁴



Therefore, the MoOPH/KHMDS conditions were used to oxidize the MOM protected lactone **145** as shown in **Scheme 31**. However, these conditions did not show facial selectivity as expected and gave a nearly 1:1 ratio of cis and trans diastereomers as well as recovered starting materials. More conditions were studied (**Table 5**). None of them show satisfactory result.

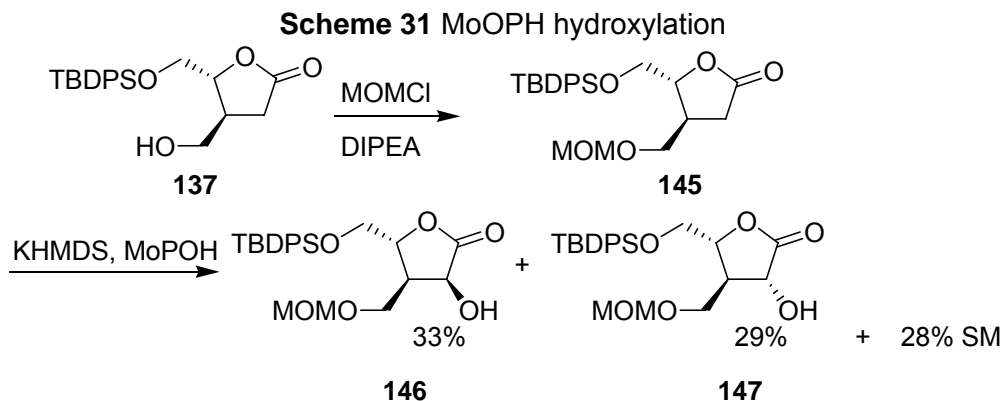
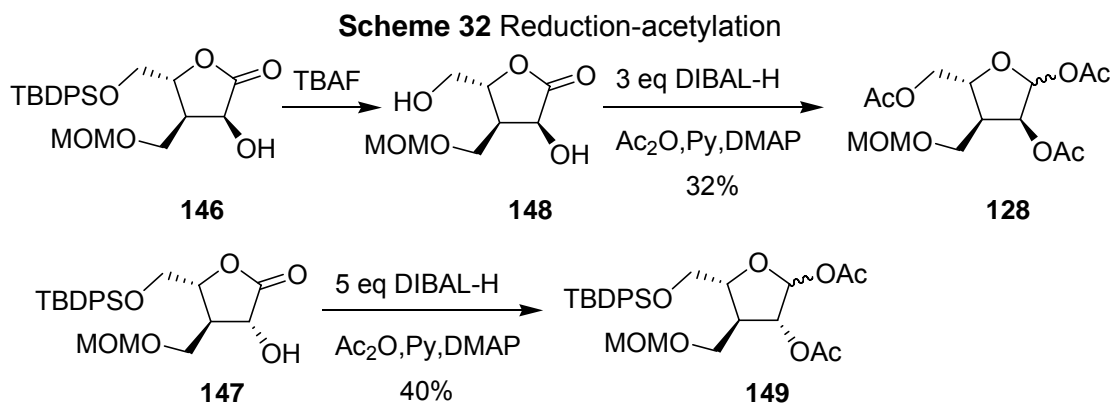


Table 5 α -Hydroxylation conditions

Substrate	Condition	Result
 145	KHMDS, TMSCl, MoOPH	No reaction
 137	2.2eq KHMDS, MoOPH	No reaction
 137	KHMDS, VO(acac) ₂ , tBuOOH	No reaction

The reduction-acetylation step of both 2,3-cis and trans lactone (**146**, **147**) is listed in **Scheme 32**. To reduce the 2,3-cis lactone **146**, the conditions with 2 equivalents of DIBAL-H at low temperature were initially used but was not successful. More conditions were studied, but conditions with up to 5 equivalents of DIBAL-H at high temperature failed to reduce the lactone according to IR spectra. Since the shielding effect of the TBDPS group was suspected to cause the problem, it was deprotected before DIBAL-H reduction. Therefore, after the deprotection of TBDPS group, 3 eq of DIBAL-H was able to reduce the lactone, and the addition of acetic anhydride, pyridine and DMAP yielded the desired **128**.

Conditions with 5 equivalents of DIBAL-H was able to reduce the 2,3-trans lactone **147** and provide the trans ribofuranosyl acetate **149**.



For the key Vorbrüggen step, the standard TMSOTf conditions gave a mixture of two products with the MOM group deprotected or intact. These two products were difficult to separate. A model study was performed on the glycosylation reaction of the 2,3- trans acetate **149**.

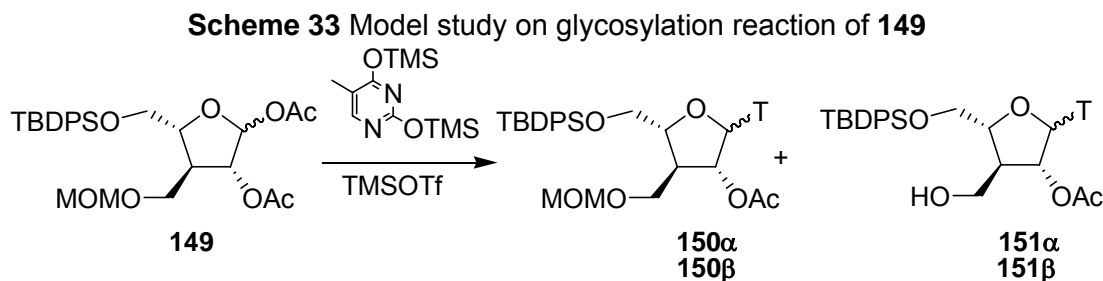


Table 6 Conditions for glycosylation reaction of **149**

Conditions	Results
2eq silylated base, 2eq TMSOTf	Mixture of 151β and 151α
1eq silylated base, 2eq TMSOTf	Mixture of 150β and 151β
1eq silylated base, 1eq TMSOTf	Mixture of 150β and 151β

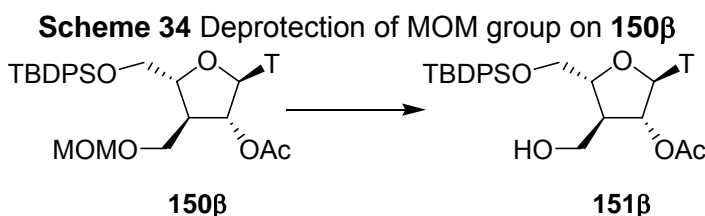
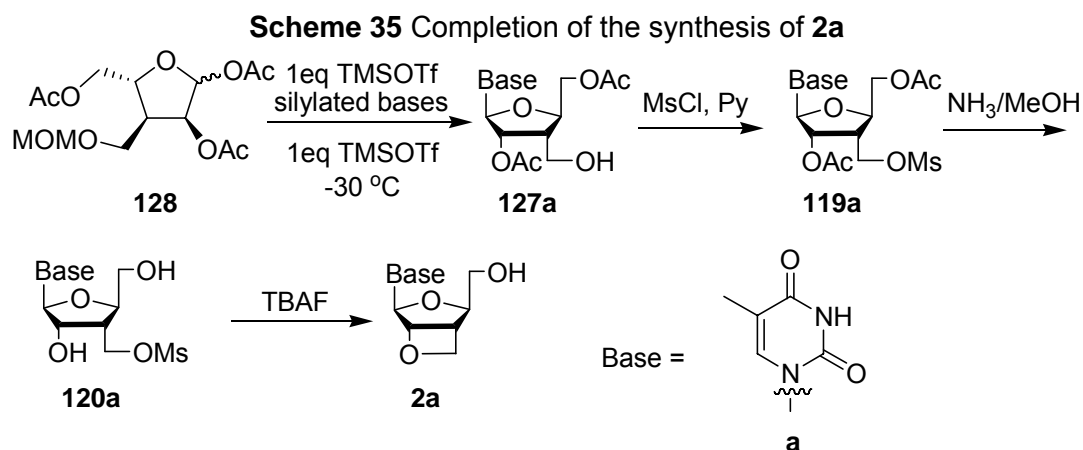


Table 7 MOM deprotection conditions of **150 β**

Conditions	Results
1eq TMSOTf, r.t.	α and β products
PPTS, DCE, Δ	No reaction
PPTS, tBuOH, Δ	No reaction
Ethylene glycol, 100 °C	decomposed
1eq TMSBr, -30 °C	desired β product
1eq TMSOTf, -30°C	desired β product

According to the results listed in **Table 6** and **Table 7**, after the standard glycosylation condition, the reaction mixture was cooled to about -30 °C and one equivalent of TMSOTf was added to completely deprotect the MOM ether. These conditions worked for the cis acetate **128** and afforded desired products.

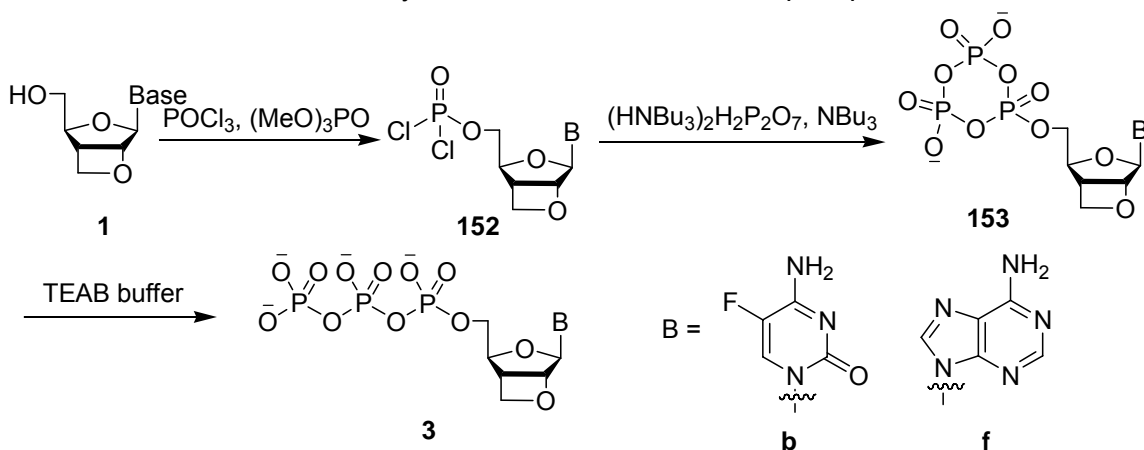


The primary alcohol on **127a** was then protected as a mesylate **119a**. Acetyl groups were removed in methanolic ammonia solution. The deprotection product **120a** was cyclized using TBAF in acetonitrile at 70 °C to afford desired bicyclic nucleoside **2a**.

1.4.3 Syntheses of Nucleoside Triphosphates

Ludwig one-pot procedure, stepwise phosphoramidate method and Ludwig-Eckstein nucleoside phosphite method were tried in synthesizing nucleoside triphosphates. The Ludwig one-pot procedure provided best results and was employed in the synthesis of nucleoside triphosphate **3b** and **3f**. Bicyclic nucleoside analog was treated with phosphorus oxychloride in trimethyl phosphate to afford the dichloro intermediate **152**. The nucleophilic attack of bis-(*tri-n*-butylammonium)pyrophosphate to **152** provide cyclic triphosphate **153**, which was then quenched by TEAB buffer to give nucleoside triphosphate **3**.

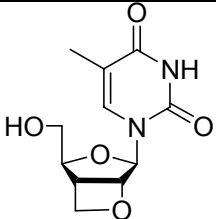
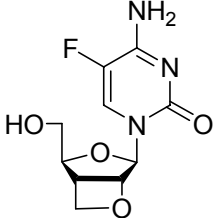
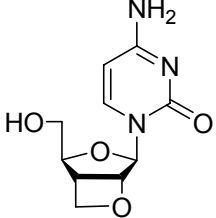
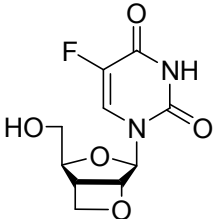
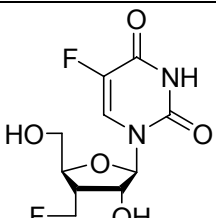
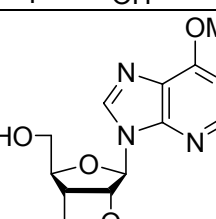
Scheme 36 Synthesis of nucleoside 5'-O triphosphates

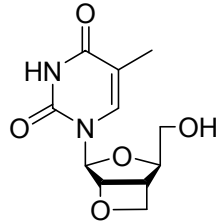
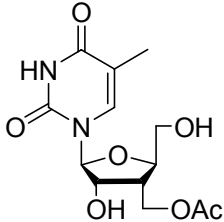
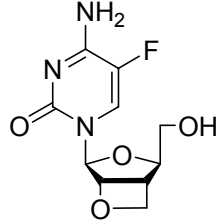
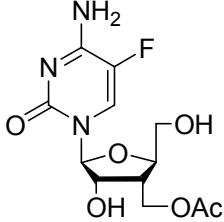
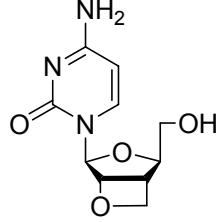
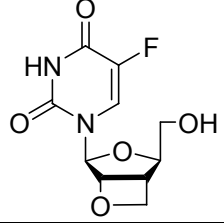
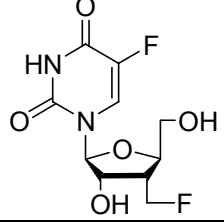


1.5 Biological Activities

Anti-HCV activities and cytotoxicities were tested in HCV replicon assay in Huh-7 cells.⁶² Anti-HIV activities were tested in human PMB cells. Cytotoxicities were tested in PMB, CEM, and Vero cells respectively. Anti-HCV data were listed in **Table 8** and anti-HIV data were listed in and **Table 9**.

Table 8 Anti-HCV activities

#	Structure	Tag	Anti-HCV in Huh-7 cells	
			Activity EC ₉₀ μM	Cytotoxicity IC ₅₀ μM
2'-MeC		Control	<10	>10
1a		F1-031-1	>10	>10
1b		F1-032-1	>10	>10
1c		F1-046-1	>10	>10
1d		F2-026-2	>10	>10
88		F2-026-1	>10	>10
90		F1-038-1	>10	>10

2a		F1-305-1	>10	>10
		F1-262-1	>10	>10
2b		F2-018-2	>10	>10
		F1-263-1	>10	>10
2c		F1-258-1	>10	>10
2d		F2-015-1	>10	>10
107		F2-015-2	>10	>10

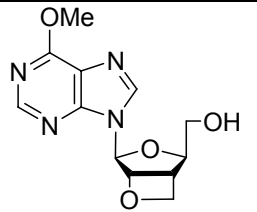
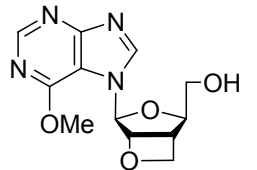
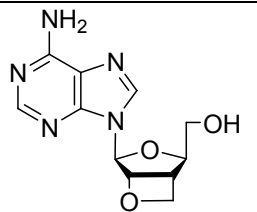
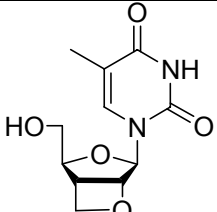
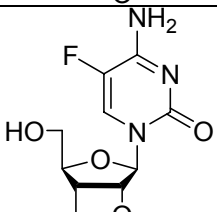
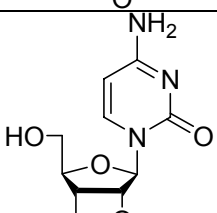
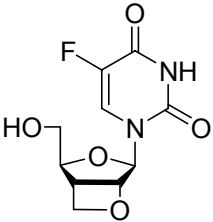
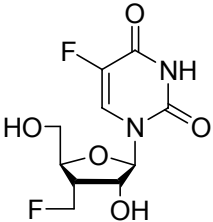
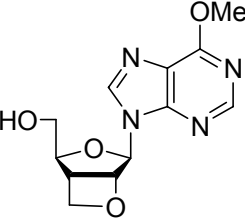
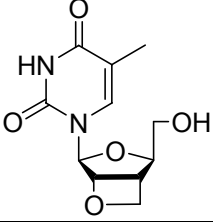
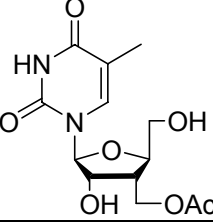
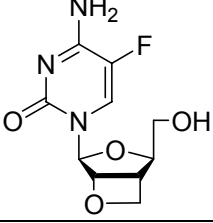
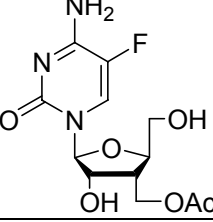
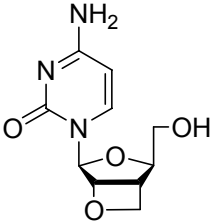
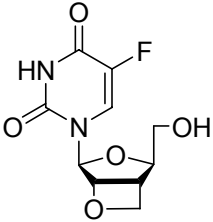
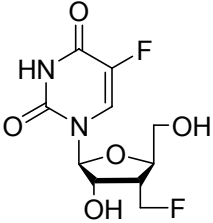
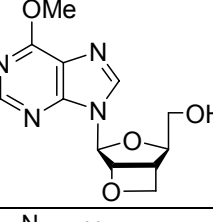
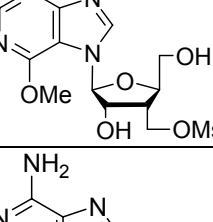
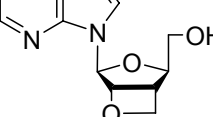
109		F2-027-1	>10	>10
112		F2-028-1	>10	>10
2f		F2-036-1	>10	>10

Table 9 Anti-HIV activities

#	Structure	Tag	Anti-HIV-1 activity in PMB cells		Cytotoxicity (IC50, μM)		
			EC50, μM	EC90, μM	PMB	CEM	Vero
AZT		Control	0.0009	0.013	>100	14.3	50.6
1a		F1-031-1	>100	>100	>100	>100	>100
1b		F1-032-1	>100	>100	>100	>100	>100
1c		F1-046-1	>100	>100	>100	>100	>100

1d		F2-026-2	>100	>100	>100	>100	>100
88		F2-026-1	>100	>100	>100	>100	>100
90		F1-038-1	>100	>100	>100	>100	>100
2a		F1-305-1	>100	>100	>100	>100	>100
		F1-262-1	>100	>100	>100	>100	>100
2b		F2-018-2	>100	>100	>100	>100	>100
		F1-263-1	41.8	>100	>100	>100	>100

2c		F1-258-1	>100	>100	>100	>100	>100
2d		F2-015-1	>100	>100	>100	>100	>100
107		F2-015-2	17.0	86.7	>100	>100	>100
2e		F2-027-1	>100	>100	>100	>100	>100
112		F2-028-1	>100	>100	>100	>100	>100
2f		F2-036-1	>100	>100	>100	>100	>100

Most compounds did not exhibit anti-HCV or anti-HIV activities. Several -OAc or -F substituted product exhibited moderate anti-HIV activities.

1.6 Conclusion

In conclusion, 3,6-dioxo[3.2.0]bicyclonucleoside analogs were synthesized as potential HCV RdRp inhibitors. D and L- enantiomers were synthesized respectively by different strategies according to the availability of the starting materials. All nucleoside analogs were tested in HCV replicon assay in human Huh-7 cells for *in vivo* anti-HCV activities. Anti-HIV activities in human PMB cells were tested as well. All 3,6-dioxo[3.2.0]bicyclonucleoside analogs did not show significant anti-HCV or anti-HIV activities. In addition to the low activities of the nucleoside triphosphates against HCV RdRp, poor phosphorylation steps of nucleoside analogs *in vivo* consist another reason which led to the poor *in vivo* activities. Thus, 5'-O-triphosphates of several nucleoside analogs were synthesized and submitted for HCV enzymatic assay in order to exclude these possibilities. Several -OAc or -F substituted products shown moderate anti-HIV activities.

2 EXPERIMENTAL SECTION

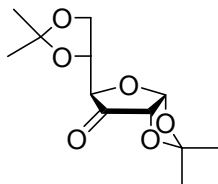
2.1 General Notes

Unless otherwise noted, all reagents were obtained from commercial suppliers and used without further purification. Specific reactions were performed in oven-dried glassware under an atmosphere of argon gas. All solvents used were anhydrous or kept dry over activated 4Å molecular sieves. Reaction progress was monitored through thin layer chromatography (TLC) on pre-coated glass purchased from EM Science. Flash chromatography was carried out with silica gel 60 (230-400 mesh) from EM Science or Silicycle according to the supply. Unless otherwise stated, all organic extracts were dried over commercially available anhydrous sodium sulfate and the solvents removed with a rotary evaporator. Brine refers to saturated sodium chloride solution. Combustion analysis was performed by Atlantic Microlab Inc. Infrared spectra were recorded on Nicolet Avatar 370 DTGS FT-IR spectrometer with the smart orbit diamond accessory. ^1H NMR and ^{13}C NMR spectra were recorded on Mercury 300, Varian 400 or Varian 600 spectrometers. ^{19}F NMR and ^{31}P NMR spectra were recorded on Varian 400 spectrometer. Unless otherwise stated, all NMR spectra were recorded in deuterated chloroform (CDCl_3), methyl alcohol (CD_3OD), acetonitrile (CD_3CN), methyl sulfoxide ($(\text{CD}_3)_2\text{SO}$), deuterium oxide (D_2O) and referenced to the residual peak; chemical shifts (δ) are reported in parts per million, and the coupling constants (J) are reported in Hertz. Mass spectra were obtained on either a VG 70-S Nier Johnson or JEOL Mass

Spectrometer. HPLC analyses were conducted on a Varian ProStar system with PDA detector.

2.2 Syntheses of D-3,6-dioxa-[3.2.0]bicyclonucleoside Analogs

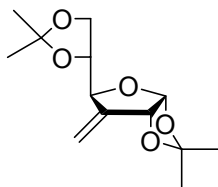
1,2;5,6-Di-O-isopropylidene- α -D-ribo-hexofuranos-3-ulose (**95**)



A solution of 1,2-5,6-di-O-isopropylidene- α -D-glucose **94** (50 g, 188 mmol) in minimal amount of DCM was added to a mixture of PDC (42.5 g, 0.6 eq) and Ac₂O (53.6 ml, 57.9 g, 3eq) in DCM with stirring. The mixture was then refluxed under argon for 12 h. After being cooled down to room temperature, it was concentrated. Three portion of toluene was added and evacuated to carry out high boiling point acetic anhydride, acetic acid, etc. The temperature of rotary evaporator bath was kept under 40 °C. The solid residue was then suspended in EtOAc and was filter through silica gel. Organic layers were combined and dried over anhydrous Na₂SO₄. It was concentrated on the rotary evaporator. If necessary, several portions of toluene was added and then evaporated to remove the high boiling point species. The resulting **95** as pale yellow oil was obtained, which was directly used in next step.

¹H NMR (400 MHz, CDCl₃) δ ppm 6.13 (d, J = 4.5 Hz, 1H), 4.40-4.33 (m, 2H), 4.15-4.07 (m, 1H), 4.05-4.01 (m, 2H), 1.45 (s, 3H), 1.43 (s, 3H), 1.33 (s, 6H)

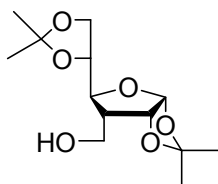
3-Deoxy -1,2;5,6-di-O-isopropylidene-3-methylene - α -D-ribo-hexofuranose (96)



Methyl triphenylphosphonium bromide (68.6 g, 188 mmol) was exposed to vacuum with slightly heating for 5 h to remove moisture and then suspended in anhydrous THF. A portion of 2.5M BuLi hexane solution (75.3 ml, 1.0 eq) was added dropwise at 0 °C and the mixture was stirred for 30 min. A solution of crude 1,2:5,6-diisopropylidene-D-glucose-one **95** (48.6 g, 188 mmol) in dry THF was added slowly. Ice bath was replaced by heating mantle and the reaction mixture was refluxed for 16 h. After TLC indicated that the all starting material was consumed, the reaction mixture was cooled down and filtered through silica gel to remove most of the triphenyl phosphine oxide and LiBr salt. All solvent was evaporated and the residue was dissolved in ether. The precipitate was filtered and the filtrate was dried over anhydrous Na₂SO₄. The solvent was evacuated and the residue was subjected to a column (3:1 to 1:1 hexane/EtOAc) to afford compound **96** (22.1 g, 46% for two steps) as colorless oil.

¹H NMR (400 MHz, CDCl₃) δ ppm 5.80 (d, J = 4.0 Hz, 1H), 5.51-5.49 (m, 1H), 5.45-5.43 (m, 1H), 4.90-4.87 (m, 1H), 4.67-4.63 (m, 2H), 4.09-4.02 (m, 2H), 3.97-3.90 (m, 1H), 1.51 (s, 3H), 1.43 (s, 3H), 1.37 (s, 3H), 1.35 (s, 3H)

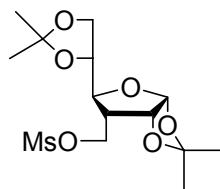
3-Deoxy-3-C-(hydroxymethyl)-1,2;5,6-di-O-isopropylidene- α -D-allofuranose (97)



To a solution of **96** (4.96 g, 19 mmol) in THF was added 2 M borane methyl sulfide complex solution (3.2 ml, 6.4 mmol, 0.33 eq) dropwise via syringe at 0 °C. After the reaction mixture was stirred for 3 h under room temperature, it was cooled down to 0 °C and oxidized with the pre-prepared mixture of 30% hydrogen peroxide (4.4 g, 2 eq) and 3M NaOH solution (7 ml). After stirring for 7 h, potassium carbonate (13 g) was saturated in the reaction mixture and layers were separated. Aqueous layer was extracted four times with ether, and the combined organic layer was washed with distilled water. After dried over anhydrous Na₂SO₄, the solvent was evaporated to give crude **97** as colorless oil, which was directly used in next step.

¹H NMR (400 MHz, CDCl₃) δ ppm 5.77 (d, J = 3.66 Hz, 1H), 4.75 (dd, J = 4.0, 4.5 Hz, 1H), 4.18-4.12 (m, 1H), 4.08-3.96 (m, 3H), 3.95-3.82 (m, 3H), 2.15-2.08 (m, 1H), 1.51 (s, 3H), 1.45 (s, 3H), 1.36 (s, 3H), 1.31 (s, 3H)

3-Deoxy-1,2;5,6-di-O-isopropylidene-3-C-(mesyloxymethyl)- α -D-allofuranose (93)

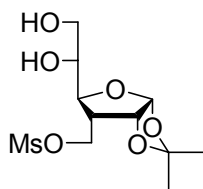


To a solution of **97** (5.4g, 19mmol) in pyridine (100 ml), methanesulfonyl chloride (2.7 g, 2.4 eq) was added via syringe under 0 °C with stirring. After 20 h of reaction, the reaction mixture was poured into ice/water mixture. The aqueous layer was extracted 5 times with ether. The combined organic layer was filter through silica gel and dried over Na₂SO₄. After removal of the solvent, the solid residue was recrystallized using MeOH/water to give **93** (4.5 g, 68% for two steps) as white crystal.

M.P.: 101-103 °C

¹H NMR (300 MHz, CDCl₃) δ ppm 5.83-5.80 (m, 1H), 4.77 (t, J = 4.1 Hz, 1H), 4.64 (dd, J = 9.7, 4.8 Hz, 1H), 4.37 (dd, J = 10.5, 9.9 Hz, 1H), 4.11 (dd, J = 8.3, 5.9 Hz, 1H), 4.03-3.89 (m, 1H), 3.69 (dd, J = 9.8, 7.9 Hz, 1H), 3.05 (s, 3H), 2.46-2.35 (m, 1H), 1.53 (s, 3H), 1.40 (s, 3H), 1.34 (s, 6H)

3-Deoxy-1,2-O-isopropylidene-3-C-(mesyloxymethyl)-α-D-allofuranose (**98**)



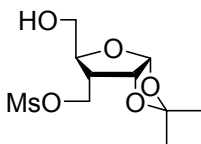
The mesylate **93** (2.96 g, 8.80 mmol) from last step was dissolved in 75% HOAc and was stirred at room temperature for 24 h. The solvent was evaporated and several portions of toluene was added and evaporated to carry out the remaining

HOAc. The crude diol **98** (2.63 g, 100%) was directly used in next step. Product could be purified by recrystallization from MeOH/water.

M.P.: 105-106 °C

^1H NMR (300 MHz, CDCl_3) δ ppm 5.83 (d, $J = 3.6$ Hz, 1H), 4.80-4.76 (m, 1H), 4.67 (dd, $J = 9.9, 4.9$ Hz, 1H), 4.43 (t, $J = 10.0$ Hz, 1H), 3.88-3.65 (m, 1H), 3.05 (s, 1H), 2.55-2.33 (m, 1H), 2.17-2.04 (m, 1H), 1.52 (s, 3H), 1.34 (s, 3H)

3-Deoxy-1,2-O-isopropylidene-3-C-(mesyloxymethyl)- α -D-ribofuranose (**99**)

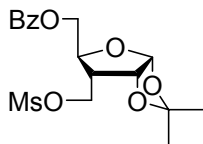


To a solution of **98** (22 g, 74 mmol) in (10:1) EtOH/saturated aq. NaHCO_3 (330 ml) was added an aqueous solution of NaIO_4 (19 g, 1.2 eq in 300 ml water) at room temperature. After stirring for 4 h, NaBH_4 (8.4g, 223mmol, 3eq) was added in several portions of about 2 g per portion every 0.5 h and the reaction mixture was then stirred for 10 h. After being cooled down to 0 °C, it was neutralized by HOAc to pH 7. A portion of ether was added and the layers were separated. The aqueous layer was extracted three times with ether. The combined organic layer was washed with one portion of NaS_2O_3 solution and two portions of water and then dried over Na_2SO_4 . The solvent was evaporated and the residue was subjected to a column (pure EtOAc) to give **99** (10.5 g, 53%) as colorless oil.

^1H NMR (400 MHz, CDCl_3) δ ppm 5.81 (d, $J = 3.6$ Hz, 1H), 4.79-4.75 (m, 1H), 4.64 (dd, $J = 9.7, 4.7$ Hz, 1H), 4.36 (dd, $J = 10.7, 9.8$ Hz, 1H), 4.11 (dd, $J = 8.6,$

6.1 Hz, 1H), 4.02-3.96 (m, 1H), 3.92 (dd, $J = 8.6, 5.0$ Hz, 1H), 3.69 (dd, $J = 9.9, 8.0$ Hz, 1H), 3.05 (s, 3H), 2.44-2.36 (m, 1H), 1.53 (s, 3H), 1.40 (s, 3H)

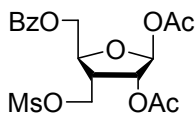
5-O-Benzoyl-3-deoxy-1,2-O-isopropylidene-3-C-(mesyloxymethyl)- α -D-ribofuranose (100)



To a solution of **99** (10.5 g, 37 mmol) in pyridine, benzoyl chloride (6.8 g, 48 mmol, 1.3 eq) was added dropwise at 0 °C. The reaction was stirred for 18 h and was poured into ice water. The mixture was extracted four times with ether. The combined organic layer was washed with water and dried over anhydrous Na_2SO_4 . The solvent was evaporated and the residue was subjected to a column to give the **100** (11.4 g, 79.3%) as white solid.

^1H NMR (600 MHz, CDCl_3) δ ppm 8.18-7.96 (m, 2H), 7.63-7.39 (m, 3H), 5.91 (d, $J = 3.7$ Hz, 1H), 4.78 (t, $J = 4.2$ Hz, 1H), 4.62 (dd, $J = 12.3, 2.7$ Hz, 1H), 4.56 (dd, $J = 10.2, 7.9$ Hz, 1H), 4.44 (dd, $J = 12.3, 5.0$ Hz, 1H), 4.40 (dd, $J = 10.2, 6.7$ Hz, 1H), 4.28-4.23 (m, 1H), 3.05 (s, 3H), 2.51-2.45 (m, 1H), 1.54 (s, 3H), 1.34 (s, 3H)

1,2-Di-O-acetyl-5-O-benzoyl-3-deoxy-3-C-(mesyloxymethyl)- β -D-ribofuranose (92)

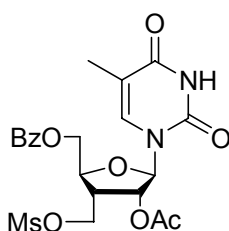


To a solution of **100** (11.4 g, 30 mmol) in 150ml of 10:1 AcOH/Ac₂O, 8ml concentrated sulfuric acid was added slowly at 0 °C. The reaction mixture was then warmed to room temperature and stirred for 2 days. The reaction was quenched by pouring into a mixture of about 300g of ice and 1000 ml saturated NaHCO₃ solution. It was extracted 5 times with dichloromethane and the combined organic layer was filter through silica gel and then dried over anhydrous Na₂SO₄. The solvent was evaporated to give **92** (10.5g, 82%) as white solid, which can be recrystallized from MeOH/water.

M.P.: 123-124 °C

¹H NMR (400 MHz, CDCl₃) δ ppm 8.12-8.02 (m, 2H), 7.64-7.55 (m, 1H), 7.51-7.41 (m, 2H), 6.15 (s, 1H), 5.36 (d, J = 4.8 Hz, 1H), 4.66-4.30 (m, 1H), 3.05 (s, 3H), 3.04-2.91 (m, 1H), 2.15 (s, 3H), 1.96 (s, 3H)

1-[2-O-Acetyl-5-O-benzoyl-3-deoxy-3-C-(mesyloxymethyl)-β-D-ribofuranosyl]thymine (91a)



General procedure for nitrogen glycosylation reaction of pyrimidine bases

Thymine base (0.10g, 0.84mmol, 1.2eq) was refluxed in 10ml 1,1,1,3,3,3-hexamethyldisilazane (HMDS) in presence of trace amount of (NH₄)₂SO₄ for 6 hours. The HMDS was evacuated under reduced pressure to afford bis(trimethylsilyl) thymine.

To a solution of bis(trimethylsilyl) thymine in 7 ml of DCM, TMSOTf (0.151 ml, 0.19g, 1.2eq) was added slowly to give a clear solution, which was then added to a solution of the ribofuranosyl acetate **92** (0.300 g, 0.70 mmol) in 10 ml of dichloroethane. The reaction mixture was stirred overnight. It was quenched by addition of saturated sodium dicarbonate solution. Layers were separated and the aqueous layer was extracted four times with dichloromethane. The combined organic solution was dried over anhydrous Na₂SO₄. All solvent was evaporated and the residue was subjected to a column (1:1 Hexane/EtOAc) to give **91a** (0.33 g, 95%) as white solid.

M.P.: 131-132 °C

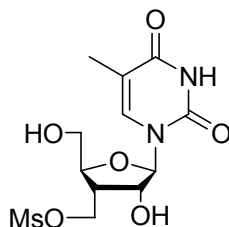
¹H NMR (400 MHz, CDCl₃) δ ppm 8.09-8.03 (m, 2H), 7.63-7.57 (m, 1H), 7.50-7.44 (m, 2H), 7.09 (s, 1H), 5.67 (d, J = 2.7 Hz, 1H), 5.59 (dd, J = 7.0, 2.7 Hz, 1H), 4.74 (dd, J = 12.6, 2.3 Hz, 1H), 4.55 (dd, J = 12.6, 4.3 Hz, 1H), 4.49 (dd, J = 10.3, 6.8 Hz, 1H), 4.45-4.40 (m, 1H), 4.34 (dd, J = 10.3, 6.5 Hz, 1H), 3.18-3.10 (m, 1H), 3.06 (s, 3H), 2.16 (s, 3H), 1.71 (s, 3H)

¹³C NMR (150 MHz, CDCl₃) δ ppm 170.1, 166.3, 150.2, 136.4, 133.8, 129.9, 129.4, 128.9, 111.6, 92.1, 80.0, 76.4, 64.2, 60.6, 41.3, 37.9, 20.9, 12.5

IR (neat) V_{max} 3386, 3191, 1630, 1576, 1417 cm⁻¹

Anal. Calcd. for C₂₁H₂₄N₂O₁₀S C, 50.80; H, 4.87; N, 5.64. Found: C, 50.46; H, 4.98; N, 5.45.

1-[3-Deoxy-3-C-(mesyloxymethyl)-β-D-ribofuranosyl]thymine (101a)



General procedure for deprotection

The compound **91a** (0.593 g 1.23 mmol) was dissolved in 20 ml of 7M methanolic ammonia solution and the reaction mixture was stirred for 48 h at room temperature. The solvent was evaporated and the residue was subjected to a column (9:1 DCM/MeOH) to yield pure **101a** (0.38 g, 93%) as foam.

M.P.: 120-121 °C

^1H NMR (600 MHz, CD_3CN_3) δ ppm 8.98 (s, 1H), 7.80 (s, 1H), 5.70 (d, $J = 2.2$ Hz, 1H), 4.47-4.43 (m, 1H), 4.41-4.36 (m, 1H), 4.31-4.27 (m, 1H), 4.13-4.09 (m, 1H), 3.96-3.88 (m, 1H), 3.71-3.65 (m, 1H), 3.31 (t, $J = 5.3$ Hz, 1H), 3.06 (s, 3H), 2.68-2.62 (m, 1H), 1.82 (s, 3H)

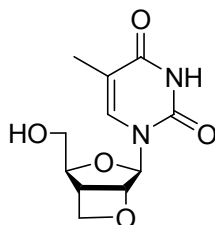
^{13}C NMR (100 MHz, CDCl_3) δ ppm 166.6, 152.5, 138.3, 110.8, 93.2, 84.3, 76.9, 68.0, 62.3, 41.9, 37.1, 12.5

HRMS (ESI): expected $\text{C}_{12}\text{H}_{19}\text{N}_2\text{O}_8\text{S}$ ($\text{M}+1$)⁺ 351.08585 found 351.08566

IR (neat) ν_{max} 3366, 1690, 1347, 1173 cm^{-1}

Anal. Calcd. for $\text{C}_{12}\text{H}_{18}\text{N}_2\text{O}_8\text{S}$ C, 41.14; H, 5.18; N, 8.00. Found: C, 40.86; H, 5.07; N, 8.03.

1-[3-Deoxy-2-O,3-C-(methylene)-β-D-ribofuranosyl]thymine (1a)



General procedure for intramolecular S_N2 reaction

To a solution of **101a** (0.383 g, 1.15 mmol) in CH_3CN , a portion of 1M TBAF solution was added. The reaction mixture was stirred 16 h at 70 °C. The solvent was removed and the residue was subjected to a column (9:1 DCM/MeOH) to give **1a** (0.157 g, 54%) as white solid.

M.P.: 154-156 °C

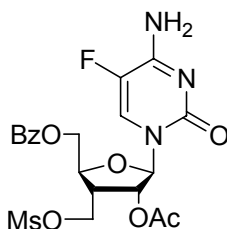
^1H NMR (600 MHz, CD_3CN) δ ppm 8.26 (s, 1H), 5.79 (s, 1H), 4.71 (d, $J = 3.0$ Hz, 1H), 4.13-4.00 (m, 4H), 3.93-3.89 (m, 2H), 3.83 (dd, $J = 13.8, 10.2$ Hz, 1H), 1.82 (s, 3H)

^{13}C NMR (150 MHz, CD_3OD) δ ppm 164.3, 153.1, 135.8, 109.8, 92.7, 83.9, 77.5, 60.9, 42.2, 36.3, 13.6

HRMS (ESI): expected $\text{C}_{11}\text{H}_{15}\text{N}_2\text{O}_5$ ($M+1$)⁺ 255.09746 found 255.09755

Anal. Calcd. for $\text{C}_{11}\text{H}_{14}\text{N}_2\text{O}_5$ C, 51.97; H, 5.55; N, 11.02. Found: C, 51.83; H, 5.53; N, 11.30.

1-[2-O-Acetyl-5-O-benzoyl-3-deoxy-3-C-(mesyloxymethyl)- β -D-ribofuranosyl]-5-fluorocytosine (**91b**)



The intermediate **92** (0.300 g, 0.70mmol) was coupled with silylated 5-F-cytosine to yield **91b** (0.322 g, 92%) as white solid.

M.P.: 152-154 °C

¹H NMR (400 MHz, CDCl₃) δ ppm 8.52 (s, 1H), 8.03 (d, J = 8.0 Hz, 1H), 7.65 (d, J = 6.1 Hz, 1H), 7.61-7.56 (m, 1H), 7.45 (t, J = 7.7 Hz, 1H), 5.69 (d, J = 4.8 Hz, 1H), 5.76 (s, 1H), 4.75-4.65 (m, 2H), 4.50-4.2 (m, 3H), 4.28 (dd, J = 10.2, 6.6 Hz, 1H), 3.01 (s, 3H), 2.97-2.88 (m, 1H), 2.13 (s, 3H)

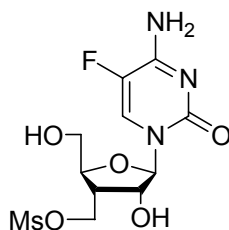
¹³C NMR (100 MHz, CD₃CN) δ ppm 169.7, 166.4, 158.7, 158.5, 138.0, 135.6, 133.8, 129.9, 129.4, 128.9, 125.5, 125.2, 92.2, 80.7, 77.5, 64.0, 63.9, 53.7, 41.0, 37.8, 20.9

HRMS (ESI): expected C₂₀H₂₃FN₃O₉S (M+1)⁺ 500.11316 found 500.11390

IR (neat) V_{max} 3343, 3097, 1718, 1683, 1615, 1507, 1270, 1222, 1173 cm⁻¹

Anal. Calcd. for C₂₀H₂₂FN₃O₉S C, 48.09; H, 4.44; N, 8.41. Found: C, 47.95; H, 4.51; N, 8.45.

1-[3-Deoxy-3-C-(mesyloxymethyl)-β-D-ribofuranosyl]-5-fluorocytosine (**101b**)



The intermediate **91b** (0.527 g, 1.06 mmol) was deprotected with 7 M methanolic ammonia to provide **101b** (0.351 g, 94%) as foam.

^1H NMR (400 MHz, CDCl_3) δ ppm 8.41 (d, $J = 7.6$ Hz, 1H), 7.35 (s, 1H), 7.11 (s, 1H), 5.91 (s, 1H), 5.59 (s, 1H), 5.19 (t, $J = 4.2$ Hz, 1H), 4.39 (dd, $J = 9.6, 6.6$ Hz, 2H), 4.05 (td, $J = 2.4, 9.6$ Hz, 1H), 3.88-3.85 (m, 1H), 3.62-3.59 (m, 1H), 3.08 (s, 3H), 2.53-2.46 (m, 1H)

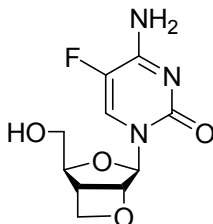
^{13}C NMR (100 MHz, CD_3CN) δ ppm 158.2, 154.2, 136.0, 126.2, 126.0, 92.6, 83.2, 75.8, 67.3, 60.6, 39.6, 36.8

HRMS (ESI): expected $\text{C}_{11}\text{H}_{17}\text{FN}_3\text{O}_7\text{S}$ ($\text{M}+1$) $^+$ 354.07651 found 354.07660

IR (neat) ν_{max} 3338, 1677, 1600, 1509 cm^{-1}

Anal. Calcd. for $\text{C}_{11}\text{H}_{16}\text{FN}_3\text{O}_7\text{S}$ C, 37.39; H, 4.56; N, 11.89. Found: C, 37.55; H, 4.63; N, 11.85.

1-[3-Deoxy-2-O,3-C-(methylene)- β -D-ribofuranosyl]-5-fluorocytosine (**1b**)



The intermediate **101b** (0.351 g, 0.99 mmol) was cyclized to yield **1b** (0.069 g, 27%) as white solid.

M.P.: 183-184 $^{\circ}\text{C}$

^1H NMR (400 MHz, CD_3OD) δ ppm 8.00 (d, $J = 6.73$ Hz, 1H), 5.78 (s, 1H), 5.42 (d, $J = 5.94$ Hz, 1H), 4.83 (t, $J = 6.25, 6.25$ Hz, 1H), 4.69-4.64 (m, 1H), 4.35 (dd, $J = 5.90, 4.02$ Hz, 1H), 3.71 (dd, $J = 11.87, 3.65$ Hz, 1H), 3.58 (dd, $J = 11.82, 5.70$ Hz, 1H), 3.41-3.34 (m, 1H)

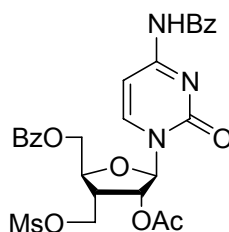
^{13}C NMR (150 MHz, CD_3OD) δ ppm 160.0, 156.7, 139.1, 137.5, 128.8, 128.6, 97.0, 92.6, 92.0, 76.1, 64.5, 42.3

HRMS (ESI): expected $\text{C}_{10}\text{H}_{13}\text{N}_3\text{O}_4$ ($\text{M}+1$)⁺ 258.08826 found 258.08846

IR (neat) ν_{max} 3324, 1672, 1616, 1506 cm^{-1}

Anal. Calcd. for $\text{C}_{10}\text{H}_{12}\text{FN}_3\text{O}_4$ C, 46.69; H, 4.70; N, 16.34. Found: C, 46.89; H, 4.84; N, 16.23.

1-[2-O-Acetyl-5-O-benzoyl-3-deoxy-3-C-(mesyloxymethyl)- β -D-ribofuranosyl]-4-N-benzoylcytosine (91c)



The intermediate **92** (0.300 g, 0.70 mmol) was coupled with silylated benzoylcytosine to yield **91c** (0.154 g, 38%) as white solid.

M.P.: 178-179 °C

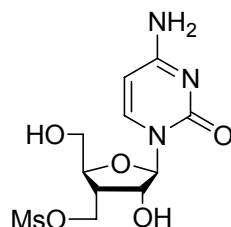
^1H NMR (400 MHz, CDCl_3) δ ppm 8.79 (b, 1H), 8.08-8.06 (m, 3H), 7.90 (d, J = 7.6 Hz, 2H), 7.66-7.60 (m, 3H), 7.54-7.50 (m, 4H), 5.82 (s, 1H), 5.77 (d, J = 5.6 Hz, 1H), 4.77-4.74 (m, 1H), 4.58-4.54 (m, 1H), 4.48 (dd, J = 10.4, 6.8 Hz, 1H), 4.31 (dd, J = 10.8, 6.8 Hz, 1H), 3.02 (s, 3H), 2.17 (s, 3H)

^{13}C NMR (150 MHz, CDCl_3) δ ppm 166.7, 166.4, 145.0, 134.0, 133.5, 129.9, 129.3, 129.0, 127.8, 93.2, 81.1, 77.4, 63.8, 63.7, 41.0, 37.8, 21.0

HRMS (ESI): expected $\text{C}_{27}\text{H}_{28}\text{N}_3\text{O}_{10}\text{S}$ ($\text{M}+1$)⁺ 586.14899 found 586.14777

Anal. Calcd. for $C_{27}H_{27}N_3O_{10}S$ C, 55.38; H, 4.65; N, 7.18. Found: C, 55.39; H, 4.63; N, 7.16.

1-[3-Deoxy-3-C-(mesyloxymethyl)- β -D-ribofuranosyl]cytosine (101c)

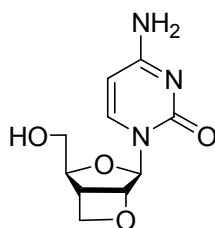


The intermediate **91c** (0.527 g, 1.06 mmol) was deprotected with 7 M methanolic ammonia to provide **101c** (0.351 g, 94%) as foam.

^1H NMR (400 MHz, CD_3CN) δ ppm 8.51 (d, $J = 7.1$ Hz, 1H), 5.64 (s, 1H), 4.48 (dd, $J = 10.0, 7.5$ Hz, 1H), 4.30-4.24 (m, 1H), 4.19-4.13 (m, 1H), 4.03-3.97 (m, 1H), 3.75-3.69 (m, 1H), 3.30 (s, 1H), 3.06 (s, 3H), 2.62-2.53 (m, 1H)

Anal. Calcd. for $C_{11}H_{17}N_3O_7S$ C, 39.40; H, 5.11; N, 12.53. Found: C, 39.64; H, 5.15; N, 12.62.

1-[3-Deoxy-2-O,3-C-(methylene)- β -D-ribofuranosyl]cytosine (1c)



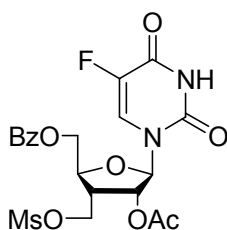
The intermediate **101c** (0.154 g, 0.26 mmol) was cyclized to yield **1c** (0.088 g, 82%) as white solid.

M.P.: 200-201 °C

^1H NMR (400 MHz, CD_3CN) δ ppm 8.51 (d, $J = 7.1$ Hz, 1H), 5.86-5.85 (m, 1H), 5.70 (s, 1H), 5.41 (d, $J = 5.9$ Hz, 1H), 4.81-4.78 (m, 1H), 4.64-4.62 (m, 1H), 4.33-4.29 (m, 1H), 3.66-3.61 (m, 1H), 3.52-3.48 (m, 1H), 3.41-3.35 (m, 1H), 3.26-3.19 (m, 1H)

Anal. Calcd. for $\text{C}_{11}\text{H}_{17}\text{N}_3\text{O}_7\text{S}$ C, 39.40; H, 5.11; N, 12.53. Found: C, 39.64; H, 5.15; N, 12.62.

1-[2-O-Acetyl-5-O-benzoyl-3-deoxy-3-C-(mesyloxymethyl)- β -D-ribofuranosyl]-5-fluorouracil (91d)



The intermediate **92** (0.300 g, 0.70 mmol) was coupled to yield **91d** (0.349 g, 100%) as white solid.

M.P.: 177-178 °C

^1H NMR (400 MHz, CDCl_3) δ ppm 9.54 (b, 1H), 8.08-8.03 (m, 1H), 7.72-7.63 (m, 1H), 7.55-7.48 (m, 1H), 5.76-5.74 (m, 1H), 5.58 (dd, $J = 6.5, 2.2$ Hz, 1H), 4.67 (dd, $J = 12.7, 2.3$ Hz, 1H), 4.57 (dd, $J = 12.8, 4.0$ Hz, 1H), 4.51-4.45 (m, 1H), 4.42 (dd, $J = 10.3, 6.9$ Hz, 1H), 4.33 (dd, $J = 10.3, 6.0$ Hz, 1H), 3.04 (s, 1H), 2.12 (s, 1H)

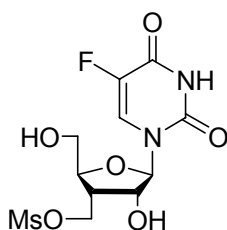
^{13}C NMR (100 MHz, CD_3OD) δ ppm 170.9, 167.3, 158.3, 158.1, 149.9, 143.0, 140.7, 134.8, 130.9, 130.7, 130.0, 125.9, 125.6, 91.8, 81.1, 77.2, 66.7, 65.0, 41.8, 37.7, 21.2

HRMS (ESI): expected $C_{20}H_{22}FN_2O_{10}S$ (M+1)⁺ 501.09706 found 501.09737

IR (neat) V_{max} 3207, 30.89, 1709, 1356, 1272, 1226, 1175 cm^{-1}

Anal. Calcd. for $C_{20}H_{21}FN_2O_{10}S$ C, 48.00; H, 4.23; N, 5.60. Found: C, 48.10; H, 4.33; N, 5.57.

1-[3-Deoxy-3-C-(mesyloxymethyl)-β-D-ribofuranosyl]-5-fluorouracil (**101d**)



The intermediate **91d** (0.349 g, 0.70 mmol) was deprotected with 7M methanolic ammonia to provide **101d** (0.208 g, 84%) as foam.

1H NMR (600 MHz, CD_3OD) δ ppm 8.54 (d, $J = 7.2$ Hz, 1H), 5.72 (s, 1H), 4.51 (dd, $J = 9.9, 7.1$ Hz, 1H), 4.39-4.36 (m, 1H), 4.32 (dd, $J = 9.9, 6.4$ Hz, 1H), ^{13}C NMR (100 MHz, CD_3OD) δ ppm 4.20-4.16 (m, 1H), 4.02-3.98 (m, 1H), 3.74 (dd, $J = 12.46, 2.14$ Hz, 1H), 3.10 (s, 3H), 2.69-2.63 (m, 1H)

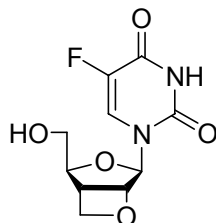
^{13}C NMR (100 MHz, CD_3OD) δ ppm 160.0, 151.0, 142.9, 140.6, 126.7, 126.4, 93.5, 84.7, 77.1, 68.0, 61.9, 41.5, 37.2, 37.2, 22.3, 22.2

HRMS (ESI): expected $C_{11}H_{16}FN_2O_8S$ (M+1)⁺ 355.06045 found 355.06059

IR (neat) V_{max} 3305, 3015, 1679, 1654, 1344 cm^{-1}

Anal. Calcd. for $C_{11}H_{15}FN_2O_8S$ C, 37.29; H, 4.27; N, 7.91. Found: C, 37.20; H, 4.27; N, 7.88.

1-[3-Deoxy-2-O,3-C-(methylene)-β-D-ribofuranosyl]-5-fluorouracil (1d)



The intermediate **101d** (0.100 g, 0.28 mmol) was cyclized to yield **1d** (0.011 g, 15%) as foam.

^1H NMR (400 MHz, CD_3OD) δ ppm 8.02 (d, $J = 6.8$ Hz, 1H), 5.82 (s, 1H), 5.49 (d, $J = 5.9$ Hz, 1H), 4.87-4.83 (m, 1H), 4.68-4.64 (m, 1H), 4.35 (dd, $J = 6.0, 3.9$ Hz, 1H), 3.69 (dd, $J = 11.8, 3.8$ Hz, 1H), 3.58 (dd, $J = 11.8, 5.8$ Hz, 1H), 3.42-3.36 (m, 1H)

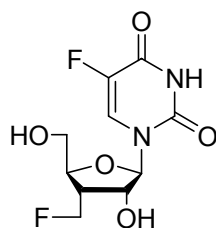
^{13}C NMR (100 MHz, CD_3OD) δ ppm 176.8, 151.1, 142.9, 140.7, 128.6, 128.1, 96.3, 92.3, 92.2, 76.4, 64.4, 42.5

HRMS (ESI): expected $\text{C}_{10}\text{H}_{12}\text{FN}_2\text{O}_5$ ($\text{M}+1$)⁺ 259.07221 found 259.07248

IR (neat) ν_{max} 2924, 1700, 1256 cm^{-1}

Anal. Calcd. for $\text{C}_{10}\text{H}_{11}\text{FN}_2\text{O}_5$ C, 46.52; H, 4.29; N, 10.85. Found: C, 46.27; H, 4.47; N, 10.74.

1-[3-Deoxy-3-C-(fluoromethyl)-β-D-ribofuranosyl]-5-fluorouracil (102)



The intermediate **101d** (0.100 g, 0.28 mmol) reacted with TBAF to provide **102** (0.023 g, 30%) as foam.

^1H NMR (400 MHz, CD_3OD) δ ppm 8.54-8.51 (m, 1H), 5.69 (s, 1H), 4.81-4.75 (m, 1H), 4.70-4.56 (m, 1H), 4.52-4.45 (m, 1H), 4.35 (d, $J = 5.4$ Hz, 1H), 4.21-4.15 (m, 1H), 3.97 (d, $J = 12.5$ Hz, 1H), 3.70-3.65 (m, 1H), 2.67-2.54 (m, 1H)

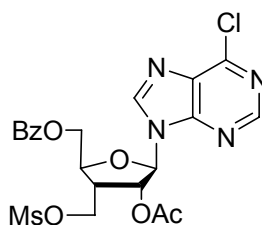
^{13}C NMR (100 MHz, CD_3OD) δ ppm 158.6, 158.3, 149.6, 141.5, 139.2, 125.4, 125.1, 108.8, 92.1, 83.5, 83.5, 81.4, 79.8, 75.9, 75.9, 60.9, 41.4, 41.2

HRMS (ESI): expected $\text{C}_{10}\text{H}_{13}\text{F}_2\text{N}_2\text{O}_5$ ($\text{M}+1$) $^+$ 279.07843 found 279.07870

IR (neat) ν_{max} 2924, 1700, 1256 cm^{-1}

Anal. Calcd. for $\text{C}_{10}\text{H}_{12}\text{F}_2\text{N}_2\text{O}_5$ C, 43.17; H, 4.35; F, 13.66; N, 10.07. Found: C, 43.27; H, 4.43; N, 9.94.

9-[2-O-Acetyl-5-O-benzoyl-3-deoxy-3-C-(mesyloxymethyl)- β -D-ribofuranosyl]-6-chloropurine (91e)



General procedure for nitrogen glycosylation reaction of purine bases in DCE

The 6-Cl-purine base (1.2eq) was refluxed in 10ml 1,1,1,3,3,3-hexamethyldisilazane (HMDS) in presence of trace amount of $(\text{NH}_4)_2\text{SO}_4$ for 6 hours. All solvent was evacuated under vacuum to yield 6-Cl-9-trimethylsilyl-purine.

To a solution of acetate **92** (0.600 g, 1.40mmol) and 6-Cl-9-trimethylsilylpurine in 20 ml of DCE, a portion of 1 M SnCl₄ solution (0.151 ml, 0.19 g, 1.2eq) was added slowly. The reaction mixture was stirred overnight and quenched by addition of saturated sodium dicarbonate solution. Layers were separated and the aqueous layer was extracted four times with dichloromethane. The combined organic layer was dried over anhydrous sodium sulfate. The solvent was evaporated and the residue was subjected to a column (1:1 Hexane/EtOAc) to give **91e** (0.459 g, 63%) as white solid.

M.P.: 120-121 °C

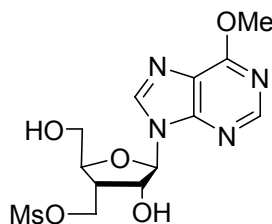
¹H NMR (600 MHz, CDCl₃) δ ppm 8.54 (s, 1H), 8.21 (s, 1H), 7.85-7.84 (m, 2H), 7.57-7.55 (m, 1H), 7.40-7.37 (m, 2H), 6.02 (d, J = 1.2 Hz, 1H), 5.99 (dd, J = 6.0, 1.2 Hz, 1H), 4.71 (dd, J = 12.6, 2.4 Hz, 1H), 4.63-4.58 (m, 2H), 4.56-4.53 (m, 1H), 4.45 (dd, J = 9.6, 6.0 Hz, 1H), 3.71-3.66 (m, 1H), 3.08 (s, 3H), 2.18 (s, 3H)

¹³C NMR (150 MHz, CD₃OD) δ ppm 170.2, 166.3, 152.2, 151.7, 150.8, 144.8, 133.8, 132.6, 129.7, 129.2, 128.7, 90.5, 81.1, 64.0, 62.6, 41.6, 37.9, 20.8

HRMS (ESI): expected C₂₁H₂₂ClN₄O₈S (M+1)⁺ 525.08469 found 525.08472

Anal. Calcd. for C₂₁H₂₁ClN₄O₈S C, 48.05; H, 4.03; N, 10.67. Found: C, 47.87; H, 4.05; N, 10.76.

9-[3-Deoxy-3-C-(mesyloxymethyl)-β-D-ribofuranosyl]-6-methoxypurine (**103**)



The intermediate **91e** (0.102 g, 0.19 mmol) was deprotected with 7 M methanolic ammonia to provide **103** (0.034 g, 46%) as foam.

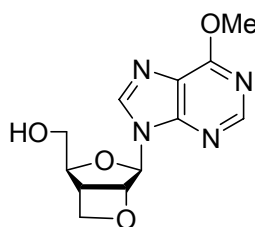
^1H NMR (4600 MHz, CD_3OD) δ ppm 8.71 (s, 1H), 8.68 (s, 1H), 6.08 (d, $J = 2.44$ Hz, 1H), 4.82-4.79 (m, 1H), 4.55-4.35 (m, 2H), 4.33-4.26 (m, 1H), 4.08 (s, 3H), , 3.96-3.87 (m, 1H), 3.08 (s, 3H), 3.01-2.92 (m, 1H)

^{13}C NMR (100 MHz, CD_3OD) δ ppm 153.2, 153.5, 153.3, 143.5, 93.6, 84.8, 76.9, 68.3, 63.4, 55.1, 42.7, 37.1

HRMS (ESI): expected $\text{C}_{13}\text{H}_{19}\text{N}_4\text{O}_7\text{S}$ ($\text{M}+1$)⁺ 375.09643 found 375.09632

Anal. Calcd. for $\text{C}_{13}\text{H}_{18}\text{N}_4\text{O}_7\text{S}$ C, 41.71; H, 4.85; N, 14.97. Found: C, 41.91; H, 5.00; N, 14.99.

9-[3-Deoxy-2-O,3-C-(methylene)- β -D-ribofuranosyl]-6-methoxypurine (**104**)



The intermediate **103** (0.034 g, 0.09 mmol) was cyclized to yield **104** (0.015 g, 69%) as white solid.

M.P.: 153-154 °C

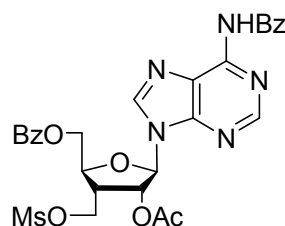
^1H NMR (400 MHz, CD_3OD) δ ppm 8.52 (s, 1H), 8.41 (s, 1H), 6.36 (s, 1H), 6.05 (d, $J = 5.6$ Hz, 1H), 4.97-4.93 (m, 1H), 4.72-4.69 (m, 1H), 4.49-4.46 (m, 1H), 4.15 (s, 3H), 3.66-3.62 (m, 1H), 3.47-3.435 (m, 1H), 3.43-3.37 (m, 1H)

^{13}C NMR (100 MHz, CD_3OD) δ ppm 161.0, 152.5, 151.2, 142.7, 104.7, 91.4, 90.3, 89.7, 75.4, 63.1, 53.6, 41.4

HRMS (ESI): expected $\text{C}_{13}\text{H}_{19}\text{N}_4\text{O}_7\text{S}$ ($\text{M}+1$)⁺ 279.10859 found 279.10869

Anal. Calcd. for $\text{C}_{12}\text{H}_{14}\text{N}_4\text{O}_4$ C, 51.80; H, 5.07; N, 20.13. Found: C, 51.78; H, 4.94; N, 20.29.

6-N-Benzoyl-9-[2,5-di-O-acetyl-3-deoxy-3-C-(mesyloxymethyl)- β -L-ribofuranosyl]adenine (91f)



The intermediate **92** (0.600 g, 1.4 mmol) was coupled to yield crude **91f** (0.510 g, 60%) as foam.

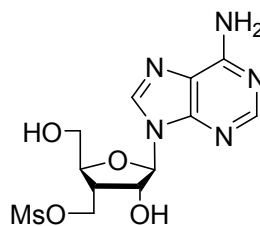
^1H NMR (400 MHz, CDCl_3) δ ppm 9.31-9.21 (b, 1H), 8.63 (s, 1H), 8.10-7.87 (m, 4H), 7.59-7.45 (m, 4H), 7.40-7.35 (m, 2H), 6.03-6.00 (m, 1H), 4.71 (dd, $J = 12.4$, 2.3 Hz, 1H), 4.61-4.56 (m, 2H), 4.55-4.51 (m, 1H), 4.44 (dd, $J = 10.2$, 6.3 Hz, 1H), 4.11-4.07 (m, 1H), 3.78-3.70 (m, 1H), 3.06 (s, 3H), 2.17 (s, 3H)

^{13}C NMR (100 MHz, CDCl_3) δ ppm 170.3, 166.4, 164.9, 152.9, 151.2, 150.0, 142.6, 133.7, 133.0, 129.8, 129.3, 129.0, 128.7, 128.1, 123.8, 90.4, 81.0, 77.2, 64.0, 60.62, 41.7, 37.8, 20.9

HRMS (ESI): expected $\text{C}_{28}\text{H}_{28}\text{N}_5\text{O}_9\text{S}$ ($\text{M}+1$)⁺ 610.16023 found 610.16136

Anal. Calcd. for $\text{C}_{28}\text{H}_{27}\text{N}_5\text{O}_9\text{S}$ C, 55.17; H, 4.46; N, 11.49. Found: C, 44.46; H, 4.58; N, 11.15.

9-[3-Deoxy-3-C-(mesyloxymethyl)-β-L-ribofuranosyl]adenine (101f)



The intermediate **91f** (0.500 g, 0.91 mmol) was deprotected with 7M methanolic ammonia to provide **101f** (0.246 g, 75%) as white solid.

M.P.: 172-174 °C

¹H NMR (400 MHz, CD₃OD) δ ppm 8.44 (s, 1H), 8.18 (s, 1H), 5.98 (d, *J* = 3.2 Hz, 1H), 4.75 (dd, *J* = 6.2, 3.0 Hz, 1H), 4.55 (dd, *J* = 9.9, 6.4 Hz, 1H), 4.43 (dd, *J* = 10.0, 6.2 Hz, 1H), 4.32-4.28 (m, 1H), 3.96 (dd, *J* = 12.6, 2.5 Hz, 1H), 3.71 (dd, *J* = 12.5, 2.9 Hz, 1H), 3.11 (s, 1H), 2.94-2.90 (m, 1H)

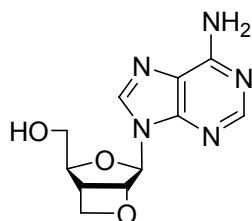
¹³C NMR (100 MHz, CD₃OD) δ ppm 157.6, 153.7, 149.9, 141.3, 120.8, 93.3, 84.5, 76.4, 68.3, 63.5, 42.5, 37.2

HRMS (ESI): expected C₁₂H₁₈N₅O₆S (M+1)⁺ 360.09723 found 360.09797

IR (neat) *V*_{max} 3342, 3190, 2935, 1650, 1346cm⁻¹

Anal. Calcd. for C₁₂H₁₇N₅O₆S C, 40.11; H, 4.77; N, 19.49. Found: C, 40.34; H, 4.73; N, 19.45.

9-[3-Deoxy-2-O,3-C-(methylene)-β-L-ribofuranosyl]adenine (1f)



The intermediate **101f** (0.246 g, 0.68 mmol) was cyclized to yield **1f** (0.086 g, 52%) as white solid.

M.P.: 211-213 °C

^1H NMR (400 MHz, CD_3OD) δ ppm 8.22 (s, 1H), 8.16 (s, 1H), 6.28 (s, 1H), 5.99 (d, $J = 5.7$ Hz, 1H), 4.93 (t, $J = 6.40$ Hz, 1H), 4.70-4.65 (m, 1H), 4.45 (dd, $J = 6.0$, 4.2 Hz, 1H), 3.67-3.60 (m, 1H), 3.50-3.39 (m, 2H)

HRMS (ESI): expected $\text{C}_{11}\text{H}_{14}\text{N}_5\text{O}_3$ ($\text{M}+1$)⁺ 264.10880 found 264.10912

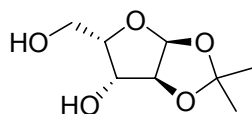
IR (neat) ν_{max} 3332, 1645, 1186 cm^{-1}

Anal. Calcd. for $\text{C}_{11}\text{H}_{13}\text{N}_5\text{O}_3$ C, 50.19; H, 4.98; N, 26.60. Found: C, 50.34; H, 5.17; N, 26.65.

2.3 Syntheses of L-3,6-dioxa-[3.2.0]bicyclonucleoside Analogs

2.3.1 Route Starting from L-xylose

1,2-O-Isopropylidene- α -L-xylofuranose (**112**)

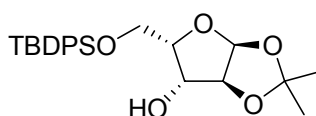


To a slurry of L-xylose **110** (25 g, 167 mmol) in 500ml acetone was added 20 ml concentrated sulfuric acid (about 0.66 M). The reaction mixture was stirred for 0.5 h until TLC (1:1 hexane/EtOAc) suggested that all starting material was consumed. The reaction mixture was neutralized by addition of concentrated

ammonium hydroxide solution. It was filtered and then concentrated. The residue was dissolved in DCM. A portion of sodium sulfate was added and the mixture was then filtered. The solvent was removed to provide a syrup as the mixture of mostly diisopropylidene protected L-xylose as well as some desired product. It was then dissolved in 400 ml 2:1 MeOH/0.1M HCl solution, and was stirred at room temperature for 4 h until TLC (1:1 hexane/EtOAc) suggest that all diisopropylidene protected sugar was consumed. The reaction mixture was neutralized by addition of solid sodium bicarbonate, and was filtered through silica gel funnel. The solvent was removed by evaporation and co-evaporation with toluene to provide the crude **112** (31 g, 98%) as colorless oil, which was directly used in next step.

^1H NMR (400 MHz, CDCl_3) δ ppm 5.99 (d, $J = 3.65$ Hz, 1H), 4.53 (d, $J = 3.66$ Hz, 1H), 4.34 (d, $J = 1.59$ Hz, 1H), 4.19-3.90 (m, 4H), 2.66 (s, 1H), 1.49 (s, 3H), 1.33 (s, 3H)

5-O-(tert-Butyldiphenylsilyl)-1,2-O-isopropylidene- α -L-xylofuranose (**113**)



To a solution of **112** (15.8 g, 83.1 mmol), triethyl amine (13.9 ml, 10.1 g, 1.2eq) and DMAP (2.0 g, 0.2eq) in DCM was added TBDPSCI (21.7ml, 23.3g, 83.1mmol, 1eq) slowly with stirring at 0 °C. The reaction was allowed to warm to r.t. and stirred for 10 h until TLC suggested that all starting material had been consumed. It was filtered and diluted with brine. Layers were separated, and the aqueous

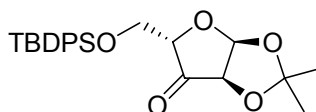
layer was extracted 3 times with DCM and dried over Na₂SO₄. All solvent was evaporated and the residue was subjected to a column to provide **113** (32.8 g, 92%) as white solid.

M.P.: 93-95 °C

¹H NMR (400 MHz, CDCl₃) δ ppm 7.74-7.65 (m, 4H), 7.46-7.37 (m, 6H), 6.01 (d, *J* = 3.7 Hz, 1H), 4.55 (d, *J* = 3.6 Hz, 1H), 4.37 (t, *J* = 2.7 Hz, 1H), 4.18-4.08 (m, 4H), 1.47 (s, 3H), 1.33 (s, 3H), 1.05 (s, 9H)

¹³C NMR (100 MHz, CDCl₃) δ ppm 135.9, 135.7, 132.0, 130.3, 128.2, 128.1, 111.7, 108.8, 105.2, 85.6, 78.5, 63.0, 26.9, 26.4, 19.3

5-O-(tert-Butyldiphenylsilyl)-1,2-O-isopropylidene- α -L-erythro-pentofuranos-3-ulose (114)

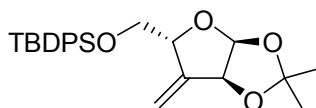


A solution of **113** (25.8g, 60 mmol) in minimal amount of DCM was added into a mixture of PDC (13.6 g, 0.6 eq) and Ac₂O (17 ml, 18.4 g, 3 eq) in DCM with stirring. The reaction mixture was then refluxed under argon for 12h. All solvent was removed and the residue was co-evaporated with toluene to remove most of acetic anhydride and acetic acid. The residue was diluted with ether. It was filtered through silica gel and dried over sodium sulfate. All solvent was evaporated to provide crude **114** (25.7 g, 100%) as pale yellow oil, which was used directly in next step.

^1H NMR (400 MHz, CDCl_3) δ ppm 7.70-7.58 (m, 4H), 7.47-7.36 (m, 6H), 6.26 (d, $J = 4.5$ Hz, 1H), 4.44-4.38 (m, 2H), 3.94-3.83 (m, 2H), 1.48 (s, 3H), 1.47 (s, 3H), 1.00 (s, 9H)

^{13}C NMR (100 MHz, CDCl_3) δ ppm 210.9, 135.7, 135.7, 130.2, 130.2, 128.1, 108.8, 104.0, 81.7, 77.4, 64.7, 27.9, 27.4, 26.9

3-Deoxy-5-O-(tert-butyldiphenylsilyl)-1,2-O-isopropylidene-3-methylene- α -L-erythro-pentofuranose (115)

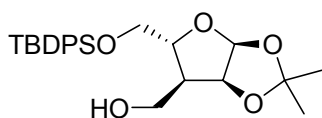


A portion of methyl triphenylphosphonium bromide (21.5 g, 1eq) was exposed to vacuum with slightly heating for 5 h to remove the moisture and then suspended in anhydrous THF. A portion of 2.5M BuLi hexane solution (24.1 ml, 1 eq) was then added dropwise at 0 °C and the mixture was stirred for another 1 h. Consequently, a solution of crude ketone **114** (25.7 g, 60.2 mmol) in dry THF was added slowly. Ice bath was replaced by heating mantle and the reaction mixture was refluxed for 6 h. After TLC indicates that the starting material was consumed, the reaction mixture was cooled down and filtered through a silica gel funnel to remove most of the triphenyl phosphine oxide and LiBr. All solvent was evaporated and the residue was dissolved in ether. The precipitate was filtered and the filtration was dried over anhydrous Na_2SO_4 . The solvent was removed and the residue was subjected to a column (3:1 to 1:1 hexane/EtOAc) to give **115** (21.2 g, 83%) as a syrup.

^1H NMR (400 MHz, CDCl_3) δ ppm 7.71-7.64 (m, 4H), 7.47-7.32 (m, 6H), 5.93 (d, $J = 4.1$ Hz, 1H), 5.47 (dd, $J = 2.1, 1.2$ Hz, 1H), 5.25 (t, $J = 1.7$ Hz, 1H), 4.99-4.95 (m, 1H), 4.85-4.81 (m, 1H), 3.82 (dd, $J = 10.7, 3.8$ Hz, 1H), 3.69 (dd, $J = 10.8, 3.5$ Hz, 1H), 1.51 (s, 3H), 1.41 (s, 3H), 1.04 (s, 9H)

^{13}C NMR (150 MHz, CDCl_3) δ ppm 147.7, 136.2, 135.5, 133.4, 128.3, 127.6, 112.8, 112.0, 101.8, 82.3, 81.3, 66.6, 27.2, 26.5, 19.4

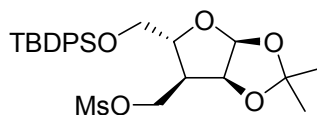
3-Deoxy-5-O-(tert-butyldiphenylsilyl)-3-(hydroxymethyl)-1,2-O-isopropylidene - α -L-ribofuranose (116)



To a solution of **115** (23.0 g, 54.2 mmol) in THF was added a solution of 2 M borane methyl sulfide complex (27.1 ml, 54.2 mmol, 1eq) dropwise under 0 °C with stirring. After the mixture was stirred for 3 h at room temperature, the reaction mixture was cooled down to 0 °C and oxidized with the pre-prepared mixture of 30% hydrogen peroxide (12.3 g, 2 eq) and 25ml 3M NaOH solution. After stirring for 14 h, potassium carbonate (38 g, 5 eq) was saturated in the reaction mixture and layers were separated. The aqueous layer was extracted four times with ether, and the combined organic layer was washed with distilled water. After dried over anhydrous Na_2SO_4 , the solvent was evaporated. The resulting oily crude **116** (24 g, 100%) was directly used in the next step.

^1H NMR (400 MHz, CDCl_3) δ ppm 7.73-7.64 (m, 4H), 7.46-7.35 (m, 6H), 5.81 (d, $J = 3.7$ Hz, 1H), 4.78 (dd, $J = 4.7, 4.0$ Hz, 1H), 4.18-4.12 (m, 1H), 3.92-3.79 (m, 2H), 3.77-3.72 (m, 2H), 1.87-1.83 (m, 1H), 1.52 (s, 3H), 1.33 (s, 3H), 1.05 (s, 9H)

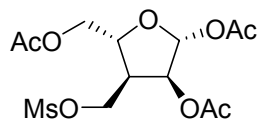
3-Deoxy-5-O-(tert-butyldiphenylsilyl)-1,2-O-isopropylidene-3-(mesyloxymethyl)- α -L-ribofuranose (117)



To a solution of **116** (24.0 g, 54.2 mmol) and triethyl amine (15.1 ml, 11.0 g, 2 eq) in DCM was added MsCl (6.3 ml, 1.5 eq) dropwise with stirring at 0 °C. The reaction mixture was stirred at 0 °C for 12h. After TLC suggested that all of the starting material was consumed, the reaction was quenched by water. Layers were separated. The aqueous layer was extracted 3 times with DCM. The combined organic layer was washed with brine and dried over Na_2SO_4 . After removal of all solvent, the residue was purified by a column (3:1 to 1:1 Hexane/EtOAc) to provide desired **117** (20.6 g, 73%) as white solid.

^1H NMR (400 MHz, CDCl_3) δ ppm 7.68-7.62 (m, 4H), 7.45-7.35 (m, 6H), 5.85 (d, $J = 3.7$ Hz, 1H), 4.77-4.73 (m, 2H), 4.44-4.33 (m, 1H), 3.74 (dd, $J = 11.2, 3.4$ Hz, 1H), 3.84 (dd, $J = 11.2, 4.2$ Hz, 1H), 3.94 (td, $J = 3.8, 9.8$ Hz, 1H), 2.96 (s, 3H), 2.69-2.60 (m, 1H), 1.49 (s, 3H), 1.33 (s, 3H), 1.04 (s, 9H)

^{13}C NMR (100 MHz, CDCl_3) δ ppm 135.8, 135.8, 133.1, 130.1, 130.0, 128.0, 128.0, 112.4, 105.3, 80.7, 79.6, 66.6, 63.9, 45.2, 37.3, 27.0, 26.6, 19.5

3-Deoxy-1,2,5-tri-O-acetyl-3-(mesyloxymethyl)- β -L-ribofuranose (118)

To a solution of **117** (9.7 g, 19 mmol) in 120ml 10:1 AcOH/Ac₂O was added 5 ml of concentrated sulfuric acid carefully with stirring at 0 °C. The reaction mixture was stirred overnight and was carefully poured into a mixture of 250 g ice and 800 ml saturated NaHCO₃ solution. The aqueous layer was extracted 5 times with DCM. The combined organic layer was washed with brine and dried over Na₂SO₄. After removal of all solvent, the residue was purified by a column (1:1 Hexane/EtOAc) to provide the desired **118** (6.0 g, 87%) as white solid.

M.P. 82-83°C

¹H NMR (400 MHz, CDCl₃) δ ppm 6.13 (s, 1H), 5.34 (d, J = 4.93 Hz, 1H), 4.46 (dd, J = 10.1, 8.4 Hz, 1H), 4.34-4.24 (m, 3H), 4.23-4.16 (m, 1H), 3.06 (s, 3H), 2.89-2.79 (m, 1H), 2.15 (s, 3H), 2.11 (s, 3H), 2.09 (s, 3H)

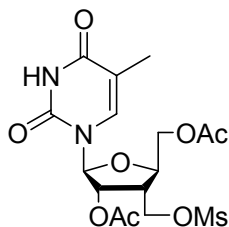
¹³C NMR (100 MHz, CDCl₃) δ ppm 170.8, 169.8, 169.1, 99.0, 80.2, 76.1, 65.7, 64.1, 42.1, 37.8, 21.3, 21.0, 20.9

HRMS (ESI): expected for found

IR (neat) V_{\max} 1744, 1358, 1221, 1176 cm⁻¹

Anal. Calcd. for C₁₃H₂₀O₁₀S C, 42.39; H, 5.47. Found: C, 42.51; H, 5.49.

1-[2,5-Di-O-acetyl-3-deoxy-3-C-(mesyloxymethyl)- β -L-ribofuranosyl]thymine (119a)



The intermediate **118** (0.300 g, 0.81 mmol) was coupled to yield **119a** (0.330 g, 93%) as white solid.

M.P.: 123-125 °C

^1H NMR (400 MHz, CDCl_3) δ ppm 9.46 (s, 1H), 7.15 (s, 1H), 5.60 (d, $J = 2.0$ Hz, 1H), 4.45-4.40 (m, 2H), 4.35-4.29 (m, 3H), 3.05 (s, 3H), 2.14 (s, 3H), 2.11 (s, 3H), 1.91 (s, 3H)

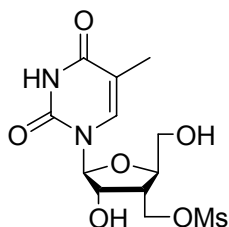
^{13}C NMR (100 MHz, CDCl_3) δ ppm 170.6, 170.1, 164.0, 150.3, 136.7, 111.4, 92.5, 79.97, 76.5, 64.2, 64.0, 41.3, 37.8, 21.0, 20.8, 12.7

HRMS (ESI): expected $\text{C}_{16}\text{H}_{23}\text{N}_2\text{O}_{10}\text{S}$ ($\text{M}+1$) $^+$ 435.10679 found 435.10677

IR (neat) ν_{max} 3195, 3029, 2935, 1744, 1693, 1225 cm^{-1}

Anal. Calcd. for $\text{C}_{16}\text{H}_{22}\text{N}_2\text{O}_{10}\text{S}$ C, 44.24; H, 5.10; N, 6.45. Found: C, 44.22; H, 5.21; N, 6.36.

1-[3-Deoxy-3-C-(mesyloxymethyl)- β -L-ribofuranosyl]thymine (**120a**)



The intermediate **119a** (0.330 g, 0.76 mmol) was deprotected with 7M methanolic ammonia to provide **120a** (0.220 g, 83%) as foam.

^1H NMR (400 MHz, CD_3OD) δ ppm 8.06 (s, 1H), 5.76 (d, $J = 1.8$ Hz, 1H), 4.51 (dd, $J = 9.9, 7.08$ Hz, 1H), 4.38-4.30 (m, 2H), 4.16 (td, $J = 2.4, 9.4$ Hz, 1H), 3.98 (dd, $J = 12.6, 2.3$ Hz, 1H), 3.73 (dd, $J = 12.6, 2.7$ Hz, 1H), 3.10 (s, 3H), 2.71-2.63 (m, 1H), 1.86 (s, 3H)

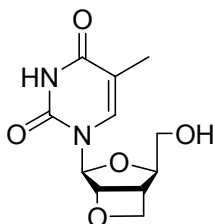
^{13}C NMR (100 MHz, CD_3OD) δ ppm 165.4, 151.2, 137.0, 109.5, 92.0, 83.0, 75.6, 66.7, 61.0, 40.6, 35.8, 11.2

HRMS (ESI): expected $\text{C}_{12}\text{H}_{19}\text{N}_2\text{O}_8\text{S}$ ($\text{M}+1$)⁺ 351.08566 found 351.08583

IR (neat) ν_{max} 3350, 1690, 1662, 1347, 1173 cm^{-1}

Anal. Calcd. for $\text{C}_{12}\text{H}_{18}\text{N}_2\text{O}_8\text{S}$ C, 41.14; H, 5.18; N, 8.00. Found: C, 40.97; H, 5.25; N, 7.76.

1-[3-Deoxy-2-O,3-C-(methylene)- β -L-ribofuranosyl]thymine (**2a**)



The intermediate **120a** (0.190 g, 0.54 mmol) was cyclized to yield **2a** (0.060 g, 44%) as white solid.

M.P.: 153-155 $^{\circ}\text{C}$

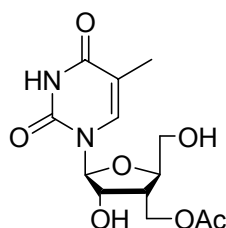
^1H NMR (400 MHz, CD_3OD) δ ppm 8.33 (s, 1H), 5.78 (s, 1H), 4.83-4.79 (m, 1H), 4.16-4.04 (m, 2H), 4.03-3.99 (m, 2H), 3.95-3.90 (m, 2H), 1.83 (s, 3H)

^{13}C NMR (100 MHz, CD_3OD) δ ppm 164.0, 151.7, 135.2, 108.5, 92.3, 83.4, 76.5, 59.5, 40.9, 35.0, 11.9

IR (neat) ν_{max} 3423, 1656, 1628 cm^{-1}

Anal. Calcd. for $C_{11}H_{14}N_2O_5$ C, 51.97; H, 5.55; N, 11.02. Found: C, 51.67; H, 5.48; N, 11.11.

1-[3-C-Acetoxymethyl-3-deoxy- β -L-ribofuranosyl]thymine



To a solution of **120a** (0.069 g, 0.20mmol) in acetonitrile was added TBAOAc (0.24g, 0.79mmol, 4eq) with stirring. The reaction was stirred at 70 °C for 10h. After removal of all solvent, the residue was first passed through an ion exchange resin (DOWEX marathon MSC cationic resin, water/ethanol) to remove the tetrabutylammonium salt. After concentration, the residue was purified by a column (9:1 DCM/MeOH) to provide product (0.048 g, 78%) as foam.

^1H NMR (400 MHz, CD_3OD) δ ppm 8.09 (s, 1H), 5.75 (d, $J = 1.5$ Hz, 1H), 4.37-4.29 (m, 2H), 4.16-4.09 (m, 2H), 3.99 (dd, $J = 12.5, 2.1$ Hz, 1H), 3.71 (dd, $J = 12.6, 2.8$ Hz, 1H), 2.58-2.50 (m, 1H), 2.03 (s, 3H), 1.85 (s, 3H)

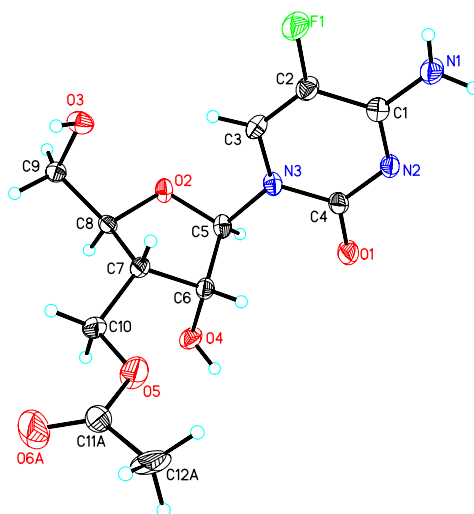
^{13}C NMR (100 MHz, CD_3OD) δ ppm 173.0, 152.5, 138.4, 110.7, 110.1, 93.3, 84.9, 77.4, 62.3, 62.2, 41.4, 20.9, 12.6

HRMS (ESI): expected $C_{13}H_{19}N_2O_7$ ($M+1$)⁺ 315.11923 found 315.11893

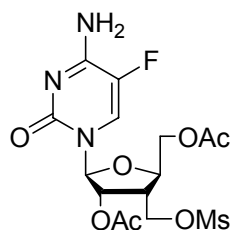
IR (neat) ν_{max} 3350, 1653, 1266 cm^{-1}

Anal. Calcd. for $C_{13}H_{18}N_2O_7$ C, 49.68; H, 5.77; N, 8.91. Found: C, 49.75; H, 5.88; N, 9.01.

The absolute stereochemistry was established by X-ray crystallographic analyses.



1-[2,5-Di-O-acetyl-3-deoxy-3-C-(mesyloxymethyl)- β -L-ribofuranosyl]-5-fluorocytosine (119b)



The intermediate **118** (0.100 g, 0.23 mmol) was coupled to yield **119b** (0.075 g, 93%) as white solid.

M.P.: 135-136 °C

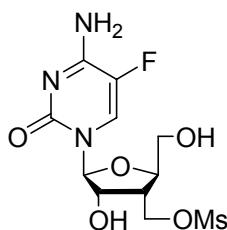
^1H NMR (400 MHz, CD_3CN) δ ppm 7.81 (d, $J = 7.0$ Hz, 1H), 6.89 (b, 1H), 5.63-5.62 (m, 1H), 5.52 (dd, $J = 6.2, 1.9$ Hz, 1H), 4.37 (dd, $J = 10.3, 6.8$ Hz, 1H), 4.34-4.27 (m, 3H), 4.24 (dd, $J = 10.3, 6.3$ Hz, 1H), 3.02 (s, 3H), 2.98-2.91 (m, 1H), 2.01 (s, 3H), 1.99 (s, 3H)

^{13}C NMR (100 MHz, CD_3CN) δ ppm 170.8, 170.1, 157.1, 154.0, 127.1, 126.8, 92.9, 80.8, 77.5, 66.3, 64.4, 41.8, 37.2, 20.8

HRMS (ESI): expected $C_{15}H_{21}FN_3O_9S$ ($M+1$)⁺ 438.09776 found 438.09771

IR (neat) V_{max} 3384, 1740, 1227 cm^{-1}

1-[3-Deoxy-3-C-(mesyloxymethyl)- β -L-ribofuranosyl]-5-fluorocytosine (120b)



The intermediate **119b** (0.101 g, 0.23mmol) was deprotected with 7M methanolic ammonia to provide **120b** (0.076 g, 93%) as foam.

1H NMR (400 MHz, CD_3OD) δ ppm 8.57 (d, $J = 7.1$ Hz, 1H), 5.70 (s, 1H), 4.55 (dd, $J = 9.9, 7.6$ Hz, 1H), 4.35-4.30 (m, 2H), 4.25-4.20 (m, 1H), 4.07 (dd, $J = 12.7, 2.0$ Hz, 1H), 3.77 (dd, $J = 12.6, 2.3$ Hz, 1H), 3.11 (s, 3H), 2.68-2.60 (m, 1H)

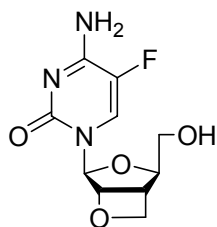
^{13}C NMR (100 MHz, CD_3CN) δ ppm 158.2, 154.2, 138.4, 126.0, 108.8, 94.6, 93.0, 83.5, 76.2, 66.4, 60.3, 39.7, 36.0

HRMS (ESI): expected $C_{11}H_{17}FN_3O_7S$ ($M+1$)⁺ 354.07651 found 354.07658

IR (neat) V_{max} 3342, 1683, 1339 cm^{-1}

Anal. Calcd. for $C_{11}H_{16}FN_3O_7S$ C, 37.39; H, 4.56; N, 11.89. Found: C, 37.79; H, 4.66; N, 11.85.

1-[3-Deoxy-2-O,3-C-(methylene)- β -L-ribofuranosyl]-5-fluorocytosine (2b)



The intermediate **120b** (0.144 g, 0.41 mmol) was cyclized to yield **2b** (0.046 g, 44%) as sticky white solid.

M.P.: 181-182 °C

^1H NMR (400 MHz, CD_3OD) δ ppm 8.00 (d, $J = 6.8$ Hz, 1H), 5.77 (s, 1H), 5.42 (d, $J = 5.9$ Hz, 1H), 4.83 (t, $J = 6.3$ Hz, 1H), 4.68-4.64 (m, 1H), 4.34 (dd, $J = 6.0, 4.0$ Hz, 1H), 3.70 (dd, $J = 11.9, 3.8$ Hz, 1H), 3.58 (dd, $J = 11.8, 5.7$ Hz, 1H), 3.40-3.34 (m, 1H)

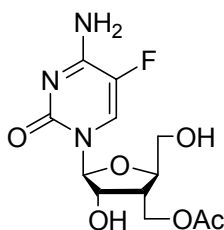
^{13}C NMR (150 MHz, CD_3CN) δ ppm 160.0, 156.7, 139.1, 137.5, 128.8, 128.5, 110.1, 97.0, 92.6, 92.0, 76.1, 64.5, 42.3

HRMS (ESI): expected $\text{C}_{10}\text{H}_{13}\text{N}_3\text{O}_4$ ($\text{M}+1$) $^+$ 258.08824 found 258.08846

IR (neat) ν_{max} 3333, 3197, 1683, 1608, 1508 cm^{-1}

Anal. Calcd. for $\text{C}_{10}\text{H}_{12}\text{FN}_3\text{O}_4$ C, 46.69; H, 4.70; N, 16.34. Found: C, 46.34; H, 4.71; N, 16.52.

1-[3-C-Acetoxymethyl-3-deoxy- β -L-ribofuranosyl]-5-fluorocytosine



The intermediate **120b** (0.172 g, 0.49 mmol) was reacted with TBAOAc to yield OAc substituted product (0.098 g, 63%) as foam.

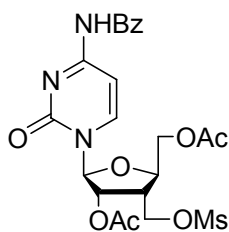
^1H NMR (600 MHz, CD_3OD) δ ppm 8.57 (d, $J = 5.4$ Hz, 1H), 5.66 (s, 1H), 4.34 (dd, $J = 10.8, 7.2$ Hz, 1H), 4.27 (d, $J = 4.2$ Hz, 1H), 4.17-4.13 (m, 1H), 4.12-4.09 (m, 1H), 4.03 (dd, $J = 12.6, 1.8$ Hz, 1H), 3.73 (dd, $J = 13.2, 2.4$ Hz, 1H), 2.51-2.46 (m, 1H), 2.02 (s, 3H)

^{13}C NMR (150 MHz, CD_3CN) δ ppm 172.9, 159.7, 156.7, 139.2, 137.6, 127.3, 127.1, 94.2, 85.3, 77.8, 61.9, 61.7, 40.6, 20.9

HRMS (ESI): expected $\text{C}_{12}\text{H}_{17}\text{FN}_3\text{O}_6$ ($\text{M}+1$) $^+$ 318.10959 found 318.10959

Anal. Calcd. for $\text{C}_{12}\text{H}_{16}\text{FN}_3\text{O}_6$ C, 45.43; H, 5.08; N, 13.24. Found: C, 45.54; H, 5.20; N, 13.50.

4-N-Benzoyl-1-[2,5-di-O-acetyl-3-deoxy-3-C-(mesyloxymethyl)- β -L-ribofuranosyl]cytosine (**119c**)



The intermediate **118** (0.300 g, 0.81 mmol) was coupled to yield **119c** (0.411 g, 96%) as white solid.

M.P. 168-170 $^{\circ}\text{C}$

^1H NMR (400 MHz, CD_3CN) δ ppm 9.15 (s, 1H), 8.14-7.95 (m, 2H), 7.68-7.51 (m, 3H), 5.79 (d, $J = 1.5$ Hz, 1H), 5.66 (dd, $J = 5.9, 1.3$ Hz, 1H), 4.45-4.34 (m, 4H),

4.27 (dd, $J = 10.3, 6.2$ Hz, 1H), 3.04 (s, 3H), 2.90-2.82 (m, 1H), 2.13 (s, 3H), 2.10 (s, 3H)

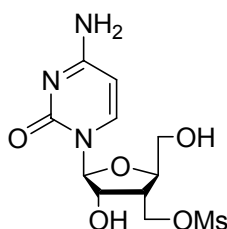
^{13}C NMR (150 MHz, CDCl_3) δ ppm 170.6, 169.8, 145.0, 133.6, 133.5, 129.9, 129.3, 127.8, 93.4, 81.0, 77.4, 63.9, 63.4, 41.0, 37.8, 21.0, 20.9

HRMS (ESI): expected $\text{C}_{22}\text{H}_{26}\text{N}_3\text{O}_{10}\text{S}$ ($\text{M}+1$)⁺ 524.13334 found 524.13349

IR (neat) ν_{max} 3325, 2938, 1743, 1663, 1485, 1355, 1233 cm^{-1}

Anal. Calcd. for $\text{C}_{22}\text{H}_{25}\text{N}_3\text{O}_{10}\text{S}$ C, 50.47; H, 4.81; N, 8.03. Found: C, 50.67; H, 4.98; N, 8.11.

1-[3-Deoxy-3-C-(mesyloxymethyl)- β -L-ribofuranosyl]cytosine (**120c**)



The intermediate **119c** (0.411 g, 0.79 mmol) was deprotected with 7M methanolic ammonia to provide **120c** (0.252 g, 96%) as foam.

^1H NMR (400 MHz, CD_3OD) δ ppm 8.25-8.20 (m, 1H), 5.98-5.77 (m, 1H), 5.73 (s, 1H), 4.51 (dd, $J = 9.7, 7.6$ Hz, 1H), 4.34-4.28 (m, 1H), 4.22-4.15 (m, 1H), 4.02-3.96 (m, 1H), 3.74 (dd, $J = 12.6, 2.6$ Hz, 1H), 3.33 (s, 1H), 3.09 (s, 3H), 2.62-2.53 (m, 1H)

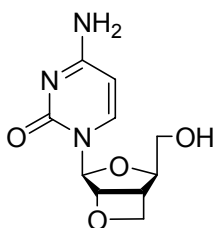
^{13}C NMR (100 MHz, CD_3OD) δ ppm 167.9, 158.4, 142.8, 95.5, 94.5, 84.6, 77.4, 67.9, 62.1, 41.7, 37.1

HRMS (ESI): expected $\text{C}_{11}\text{H}_{18}\text{N}_3\text{O}_7\text{S}$ ($\text{M}+1$)⁺ 336.08600 found 336.08602

IR (neat) ν_{max} 3338, 1635, 1608, 1491, 1348 cm^{-1}

Anal. Calcd. for $C_{11}H_{17}N_3O_7S$ C, 39.40; H, 5.11; N, 12.53. Found: C, 39.74; H, 5.05; N, 12.72.

1-[3-Deoxy-2-O,3-C-(methylene)- β -L-ribofuranosyl]cytosine (2c)



The intermediate **120c** (0.168 g, 0.48 mmol) was cyclized to yield **2c** (0.081 g, 66%) as sticky white solid.

M.P.: 201-203 °C

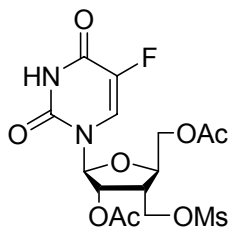
^1H NMR (400 MHz, CD_3OD) δ ppm 7.74 (d, $J = 7.4$ Hz, 1H), 5.83 (d, $J = 7.4$ Hz, 1H), 5.78 (s, 1H), 5.46 (d, $J = 5.9$ Hz, 1H), 4.85-4.81 (m, 1H), 4.68-4.63 (m, 1H), 4.36-4.32 (m, 1H), 3.68 (dd, $J = 11.8, 4.1$ Hz, 1H), 3.60 (dd, $J = 11.8, 6.0$ Hz, 1H), 3.41-3.35 (m, 1H), 3.26-3.19 (m, 1H)

^{13}C NMR (100 MHz, CD_3OD) δ ppm 166.8, 157.0, 143.5, 96.3, 94.3, 91.1, 90.6, 74.8, 63.4, 41.3

HRMS (ESI): expected $C_{10}H_{14}N_3O_4$ ($M+1$) $^+$ 240.09786 found 240.09788

Anal. Calcd. for $C_{10}H_{13}N_3O_4$ C, 50.21; H, 5.48; N, 17.56. Found: C, 50.58; H, 5.54; N, 17.82.

1-[2,5-Di-O-acetyl-3-deoxy-3-C-(mesyloxymethyl)- β -L-ribofuranosyl]-5-fluorouracil (119d)



The intermediate **118** (0.245 g, 0.67 mmol) was coupled to yield **119d** (0.260 g, 89%) as white solid.

M.P.: 175-177 °C

^1H NMR (400 MHz, CDCl_3) δ ppm 7.77-7.72 (m, 1H), 5.73 (s, 1H), 5.58 (d, $J = 5.5$ Hz, 1H), 4.49-4.33 (m, 3H), 4.29-4.18 (m, 2H), 3.04 (s, 3H), 2.90-2.80 (m, 1H), 2.14 (s, 6H)

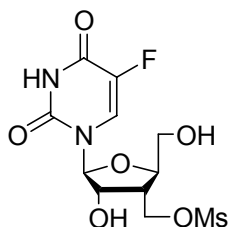
^{13}C NMR (100 MHz, CD_3OD) δ ppm 170.6, 169.8, 157.2, 148.8, 141.9, 139.5, 124.5, 124.2, 106.9, 91.0, 80.5, 76.4, 64.0, 63.2, 40.6, 37.7, 20.9, 20.8

HRMS (ESI): expected $\text{C}_{15}\text{H}_{20}\text{FN}_2\text{O}_{10}\text{S}$ ($\text{M}+1$) $^+$ 439.8172 found 439.8153

IR (neat) ν_{max} 3223, 2938, 1740, 1680, 1353, 1224 cm^{-1}

Anal. Calcd. for $\text{C}_{15}\text{H}_{19}\text{FN}_2\text{O}_{10}\text{S}$ C, 41.10; H, 4.37; N, 6.39. Found: C, 41.41; H, 4.54; N, 6.72.

1-[3-Deoxy-3-C-(mesyloxymethyl)- β -L-ribofuranosyl]-5-fluorouracil (**120d**)



The intermediate **119d** (0.150 g, 0.34 mmol) was deprotected with 7M methanolic ammonia to provide **120d** (0.095 g, 78%) as foam.

^1H NMR (400 MHz, CD_3CN) δ ppm 9.99-9.30 (b, 1H), 8.39-8.36 (m, 1H), 6.42-5.93 (b, 1H), 5.67 (s, 1H), 5.86-5.54 (b, 1H), 4.45 (dd, $J = 10.0, 7.7$ Hz, 1H), 4.41-4.36 (m, 1H), 4.27 (dd, $J = 10.0, 6.1$ Hz, 1H), 4.14 (td, $J = 2.1, 9.7$ Hz, 1H), 4.00-3.94 (m, 1H), 3.74-3.66 (m, 1H), 3.06 (s, 3H), 2.67-2.58 (m, 1H)

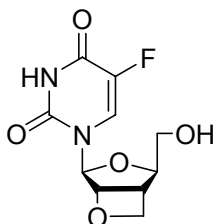
^{13}C NMR (100 MHz, CD_3CN) δ ppm 158.4, 158.1, 150.1, 142.5, 140.2, 125.9, 125.6, 92.8, 83.8, 76.5, 67.6, 61.5, 40.9, 37.4

HRMS (ESI): expected $\text{C}_{11}\text{H}_{16}\text{FN}_2\text{O}_8\text{S}$ ($\text{M}+1$)⁺ 355.6003 found 355.6059

IR (neat) ν_{max} 3359, 1699, 1653, 1339, 1170 cm^{-1}

Anal. Calcd. for $\text{C}_{11}\text{H}_{15}\text{FN}_2\text{O}_8\text{S}$ C, 37.29; H, 4.27; N, 7.91. Found: C, 36.99; H, 4.04; N, 7.72.

1-[3-Deoxy-2-O,3-C-(methylene)- β -L-ribofuranosyl]-5-fluorouracil (**2d**)



The intermediate **120d** (0.070 g, 0.20 mmol) was cyclized to yield **2d** (0.015 g, 29%) as foam.

^1H NMR (400 MHz, CD_3OD) δ ppm 8.04 (d, $J = 6.8$ Hz, 1H), 5.85 (s, 1H), 5.51 (d, $J = 5.9$ Hz, 1H), 4.89-4.86 (m, 1H), 4.71-4.67 (m, 1H), 4.38 (dd, $J = 6.1, 3.9$ Hz, 1H), 3.72 (dd, $J = 11.9, 3.9$ Hz, 1H), 3.61 (dd, $J = 11.8, 5.7$ Hz, 1H), 3.45-3.39 (m, 1H)

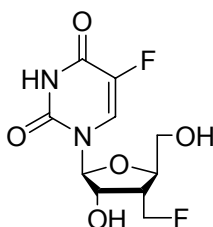
^{13}C NMR (100 MHz, CD_3OD) δ ppm 176.6, 150.9, 142.8, 140.4, 128.5, 128.1, 96.2, 92.2, 92.0, 76.3, 64.4, 42.4

HRMS (ESI): expected $C_{10}H_{10}FN_2O_5$ (M-1)⁻ 257.05789 found 257.05683

IR (neat) V_{max} 3350, 3187, 2924, 1699, 1652, 1253 cm^{-1}

Anal. Calcd. for $C_{10}H_{11}FN_2O_5$ C, 46.52; H, 4.29; N, 10.85. Found: C, 46.83; H, 4.44; N, 10.97.

1-[3-Deoxy-3-C-(fluoromethyl)-β-L-ribofuranosyl]-5-fluorouracil (**121**)



The intermediate **120d** (0.070 g, 0.20 mmol) reacted with TBAF to provide **121** (0.017 g, 31%) as foam.

¹H NMR (400 MHz, CD₃OD) δ ppm 8.54 (d, *J* = 7.2 Hz, 1H), 5.73 (d, *J* = 1.1 Hz, 1H), 4.86-4.79 (m, 1H), 4.72-4.62 (m, 1H), 4.40-4.37 (m, 1H), 4.25-4.19 (m, 1H), 4.00 (dd, *J* = 12.5, 2.1 Hz, 1H), 3.72 (dd, *J* = 12.6, 2.6 Hz, 1H), 2.70-2.58 (m, 1H)

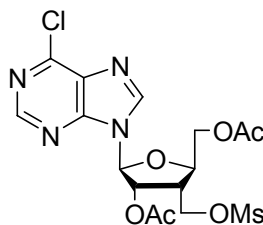
¹³C NMR (100 MHz, CD₃OD) δ ppm 158.5, 158.4, 149.8, 141.6, 139.2, 125.4, 125.0, 92.1, 83.5, 81.4, 75.9, 60.9, 41.4, 41.2

HRMS (ESI): expected $C_{10}H_{11}F_2N_2O_5$ (M-1)⁻ 277.06360 found 277.06421

IR (neat) V_{max} 3401, 1704, 1259 cm^{-1}

Anal. Calcd. for $C_{10}H_{12}F_2N_2O_5$ C, 43.17; H, 4.35; N, 10.07. Found: C, 42.95; H, 4.29; N, 9.98.

9-[2,5-Di-O-acetyl-3-deoxy-3-C-(mesyloxymethyl)-β-L-ribofuranosyl]-6-chloropurine (**119e**)



General procedure for nitrogen glycosylation reaction of purine bases in acetonitrile

The 6-Cl-purine base (1.2eq) was refluxed in 10ml 1,1,1,3,3,3-hexamethyldisilazane (HMDS) in presence of trace amount of $(\text{NH}_4)_2\text{SO}_4$ for 6 hours. The rest of HMDS was evacuated under vacuum to yield 6-Cl-9--trimethylsilyl-purine.

To a solution of acetate **118** (0.150 g, 0.41mmol) and 6-Cl-9--trimethylsilyl-purine in 7 ml of CH_3CN , a portion of 1 M SnCl_4 THF solution (0.151 ml, 0.19 g, 1.2 eq) was added slowly. The reaction mixture was stirred overnight and poured into saturated sodium dicarbonate solution. Layers were separated and the aqueous layer was extracted four times with dichloromethane. The combined organic layer was dried over anhydrous sodium sulfate. All solvent was evaporated and the residue was subjected to a column (1:1 Hexane/EtOAc) to give **119e** (0.115 g, 61%) as white solid.

M.P.: 121-123 °C

^1H NMR (600 MHz, CD_3OD) δ ppm 8.77 (s, 1H), 8.67 (s, 1H), 6.27 (s, 1H), 6.00 (d, $J = 6.1$ Hz, 1H), 4.58 (dd, $J = 10.3, 7.3$ Hz, 1H), 4.52-4.48 (m, 1H), 4.46-4.42 (m, 2H), 4.39 (dd, $J = 12.4, 4.6$ Hz, 1H), 3.52-3.47 (m, 1H), 3.15 (s, 3H), 2.18 (s, 3H), 1.98 (s, 3H)

^{13}C NMR (100 MHz, CD_3OD) δ ppm 171.0, 170.5, 152.0, 151.1, 150.5, 145.9,

131.8, 90.1, 80.7, 76.9, 65.2, 63.6, 41.5, 36.0, 19.4

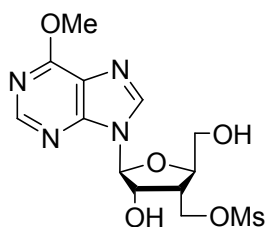
HRMS (ESI): expected $\text{C}_{10}\text{H}_{11}\text{F}_2\text{N}_2\text{O}_5$ ($\text{M}+1$)⁺ 463.06823 found 463.06849

IR (neat) V_{max} 2938, 1740, 1561, 1355, 1338, 1222 cm^{-1}

Anal. Calcd. for $\text{C}_{16}\text{H}_{19}\text{ClN}_4\text{O}_8\text{S}$ C, 41.52; H, 4.14; N, 12.10. Found: C, 41.87; H,

4.24; N, 12.29.

9-[3-Deoxy-3-C-(mesyloxymethyl)- β -L-ribofuranosyl]-6-methoxypurine (**122**)



The intermediate **119e** (0.062 g, 0.13 mmol) was deprotected with 7M methanolic ammonia to provide **122** (0.038 g, 76%) as foam.

^1H NMR (600 MHz, CD_3OD) δ ppm 8.63 (s, 1H), 8.48 (s, 1H), 6.07 (d, $J = 2.0$ Hz, 1H), 4.79-4.74 (m, 1H), 4.56-4.52 (m, 1H), 4.43-4.38 (m, 1H), 4.30-4.27 (m, 1H), 3.28-3.26 (m, 1H), 3.10 (s, 3H), 2.97-2.91 (m, 1H)

^{13}C NMR (100 MHz, CD_3OD) δ ppm 153.4, 153.3, 153.2, 143.4, 93.4, 84.8, 76.7, 68.38, 63.3, 55.0, 42.6, 37.2

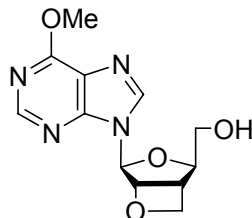
HRMS (ESI): expected $\text{C}_{13}\text{H}_{19}\text{N}_4\text{O}_7\text{S}$ ($\text{M}+1$)⁺ 375.09643 found 375.09690

IR (neat) V_{max} 3302, 1668, 1540, 1349, 1174 cm^{-1}

Anal. Calcd. for $\text{C}_{13}\text{H}_{18}\text{N}_4\text{O}_7\text{S}$ C, 41.71; H, 4.85; N, 14.97. Found: C, 41.87; H,

4.84; N, 14.89.

9-[3-Deoxy-2-O,3-C-(methylene)-β-L-ribofuranosyl]-6-methoxypurine (123)



The intermediate **122** (0.021 g, 0.056 mmol) was cyclized to yield **123** (0.011 g, 70%) as white solid.

M.P.: 152-154 °C

¹H NMR (600 MHz, CD₃OD) δ ppm 8.50 (s, 1H), 8.41 (s, 1H), 6.36 (s, 1H), 6.05 (d, *J* = 5.5 Hz, 1H), 4.97-4.94 (m, 1H), 4.72-4.69 (m, 1H), 4.49-4.46 (m, 1H), 4.15 (s, 3H), 3.67-3.63 (m, 1H), 3.48-3.45 (m, 1H), 3.43-3.39 (m, 1H)

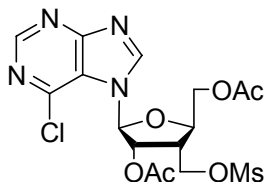
¹³C NMR (150 MHz, CD₃OD) δ ppm 161.0, 152.1, 151.2, 142.7, 104.9, 91.4, 90.3, 89.9, 75.5, 63.2, 53.6, 41.4

HRMS (ESI): expected C₁₃H₁₉N₄O₇S (M+1)⁺ 279.10859 found 279.10878

IR (neat) *V*_{max} 3303, 2944, 2389, 1600, 1578, 1313, 1211 cm⁻¹

Anal. Calcd. for C₁₂H₁₄N₄O₄ C, 51.80; H, 5.07; N, 20.13. Found: C, 51.72; H, 4.94; N, 19.98.

7-[2,5-Di-O-acetyl-3-deoxy-3-C-(mesyloxymethyl)-β-L-ribofuranosyl]-6-chloropurine (124)



The intermediate **118** (0.150 g, 0.41 mmol) was coupled to yield **124** (0.053 g, 28%) as minor product.

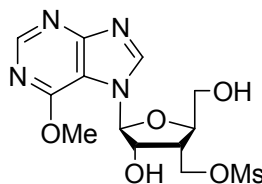
^1H NMR (600 MHz, CD_3OD) δ ppm 9.00 (s, 1H), 8.81 (s, 1H), 6.65 (s, 1H), 5.91 (dd, $J = 5.8, 1.0$ Hz, 1H), 4.60-4.56 (m, 1H), 4.53-4.46 (m, 2H), 4.43 (dd, $J = 12.8, 2.1$ Hz, 1H), 4.39-4.35 (m, 1H), 3.13-3.08 (m, 1H), 3.10 (s, 3H), 2.18 (s, 3H), 2.08 (s, 3H)

^{13}C NMR (150 MHz, CD_3OD) δ ppm 172.3, 171.4, 163.3, 153.6, 148.6, 144.8, 123.5, 92.0, 82.2, 78.7, 66.2, 64.4, 42.0, 37.3, 20.9, 20.7

HRMS (ESI): expected $\text{C}_{16}\text{H}_{20}\text{N}_4\text{O}_8\text{S}$ ($\text{M}+1$)⁺ 463.06823 found 463.06849

IR (neat) ν_{max} 2937, 1744, 1356, 1219, 1175 cm^{-1}

7-[3-Deoxy-3-C-(mesyloxymethyl)- β -L-ribofuranosyl]-6-methoxypurine (**125**)



The intermediate **124** (0.030 g, 0.065 mmol) was deprotected with 7M methanolic ammonia to provide **125** (0.023 g, 95%) as foam.

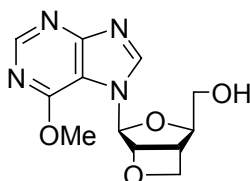
^1H NMR (400 MHz, CD_3OD) δ ppm 9.00 (s, 1H), 8.53 (s, 1H), 6.22 (s, 1H), 4.57-4.49 (m, 2H), 4.35 (dd, $J = 9.8, 6.3$ Hz, 1H), 4.30-4.25 (m, 1H), 4.19 (s, 1H), 4.03 (dd, $J = 12.5, 2.0$ Hz, 1H), 3.76 (dd, $J = 12.6, 2.7$ Hz, 1H), 3.07 (s, 3H), 2.83-2.74 (m, 1H)

^{13}C NMR (100 MHz, CD_3OD) δ ppm 162.4, 159.0, 153.4, 145.6, 110.1, 95.1, 85.0, 78.2, 67.8, 62.2, 55.3, 41.4, 37.1

HRMS (ESI): expected $C_{13}H_{19}N_4O_7S$ (M+1)⁺ 375.09656 found 375.09690

IR (neat) V_{max} 3257, 2934, 1611, 1345, 1172 cm^{-1}

9-[3-Deoxy-2-O,3-C-(methylene)- β -L-ribofuranosyl]-6-methoxypurine (126)



The intermediate **125** (0.023 g, 0.058 mmol) was cyclized to yield **126** (0.007 g, 41%) as white solid.

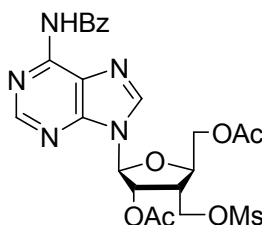
¹H NMR (600 MHz, CD₃OD) δ ppm 8.60 (s, 1H), 8.54 (s, 1H), 6.48 (s, 1H), 5.73 (d, J = 5.9 Hz, 1H), 4.94-4.91 (m, 1H), 4.77-4.74 (m, 1H), 4.50 (dd, J = 6.0, 4.2 Hz, 1H), 4.17 (s, 3H), 3.61-3.53 (m, 2H), 3.47 (dd, J = 11.9, 5.8 Hz, 1H)

¹³C NMR (100 MHz, CD₃OD) δ ppm 162.6, 159.1, 153.5, 145.7, 113.5, 95.2, 92.7, 91.7, 76.7, 64.5, 55.2, 42.2

HRMS (ESI): expected $C_{12}H_{14}N_4O_4$ (M+1)⁺ 279.10852 found 279.10878

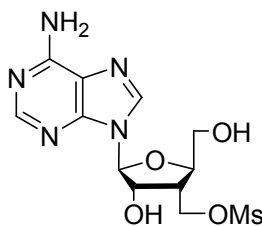
IR (neat) V_{max} 3307, 2950, 1665, 1610, 1560, 1393, 1117 cm^{-1}

6-N-Benzoyl-9-[2,5-di-O-acetyl-3-deoxy-3-C-(mesyloxymethyl)- β -L-ribofuranosyl]adenine (119f)



The intermediate **118** (0.200 g, 0.54 mmol) was coupled to yield crude **119f** (0.190 g, 64%) as white solid, which was difficult to purify and directly used in next step.

9-[3-Deoxy-3-C-(mesyloxymethyl)- β -L-ribofuranosyl]adenine (**120f**)



The intermediate **119f** (0.181 g, 0.33 mmol) was deprotected with 7M methanolic ammonia to provide **120f** (0.102 g, 86%) as foam.

^1H NMR (400 MHz, CD_3OD) δ ppm 8.43 (s, 1H), 8.17 (m, 1H), 5.97 (d, $J = 3.2$ Hz, 1H), 4.74 (dd, $J = 6.0, 4.2$ Hz, 1H), 4.54 (dd, $J = 9.6, 6.4$ Hz, 1H), 4.42 (dd, $J = 10.0, 4.0$ Hz, 1H), 4.30-4.27 (m, 1H), 3.95 (dd, $J = 12.4, 2.0$ Hz, 1H), 3.70 (dd, $J = 12.4, 2.8$ Hz, 1H), 3.10 (s, 2H), 2.94-2.88 (m, 1H)

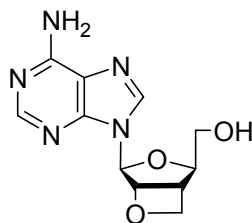
^{13}C NMR (100 MHz, CD_3OD) δ ppm 157.6, 153.7, 149.9, 141.3, 120.8, 93.3, 84.5, 76.4, 68.3, 63.5, 42.5, 37.2

HRMS (ESI): expected $\text{C}_{12}\text{H}_{18}\text{N}_5\text{O}_6\text{S}$ ($\text{M}+1$) $^+$ 360.09693 found 360.09723

IR (neat) ν_{max} 3337, 3187, 2927, 1647, 1336, 1173 cm^{-1}

Anal. Calcd. for $\text{C}_{12}\text{H}_{17}\text{N}_5\text{O}_6\text{S}$ C, 40.11; H, 4.77; N, 19.49. Found: C, 39.87; H, 4.78; N, 19.51.

9-[3-Deoxy-2-O,3-C-(methylene)- β -L-ribofuranosyl]adenine (**2f**)



The intermediate **120f** (0.140 g, 0.39 mmol) was cyclized to yield **2f** (0.059 g, 58%) as white solid.

M.P.: 211-213 °C

¹H NMR (400 MHz, CD₃OD) δ ppm 8.22 (s, 1H), 8.16 (s, 1H), 6.28 (s, 1H), 5.98 (d, *J* = 5.8 Hz, 1H), 4.95-4.91 (m, 1H), 4.69-4.65 (m, 1H), 4.47-4.43 (m, 1H), 3.67-3.59 (m, 1H), 3.49-3.39 (m, 2H)

¹³C NMR (100 MHz, CD₃OD) δ ppm 157.4, 153.9, 150.3, 141.9, 120.5, 92.6, 91.5, 91.3, 76.8, 64.6, 42.7

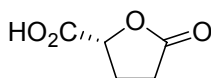
HRMS (ESI): expected C₁₁H₁₄N₅O₃ (M+1)⁺ 264.10880 found 264.10912

IR (neat) *V*_{max} 3332, 1645, 1186 cm⁻¹

Anal. Calcd. for C₁₁H₁₃N₅O₃ C, 50.19; H, 4.98; N, 26.60. Found: C, 50.10; H, 4.83; N, 26.57.

2.3.2 Route Starting from D-glutamic acid

(2R)-Tetrahydro-5-oxo-2-furancarboxylic acid (131)



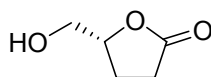
To the stirred suspension of D-glutamic acid **111** (25 g, 170 mmol) in water was added concentrated hydrochloric acid (35 ml, 2.5 eq). A solution of sodium nitrite (23 g, 2.0 eq) in 50ml water was then added during a period of 1 h at 0 °C. The

solution was warmed to room temperature and stirred overnight. All solvent was evaporated (temperature was kept under 40 °C to exclude racemization) and the residue was diluted with EtOAc. The precipitate was filtered, and the combined organic layer was dried over Na₂SO₄. All solvent was evaporated to give crude acid **131** (22 g, 100%) as pale yellow syrup.

$[\alpha]_D^{20}$ -14.4 (c 1.02, EtOH)

¹H NMR (400 MHz, CDCl₃) δ ppm 6.49 (b, 1H), 5.03-4.98 (m, 1H), 2.73-2.55 (m, 3H), 2.47-2.35 (m, 1H)

(5R)-5-(Hydroxymethyl)dihydro-2(3H)-furanone (**132**)

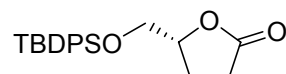


To a well stirred solution of carboxylic acid **131** (22 g, 170mmol) in anhydrous THF was slowly added a 2.0M solution of borane dimethylsulfide complex (152 ml, 1.8 eq) in THF during a period of 1 h at 0 °C. It was allowed to stir at room temperature overnight and was quenched by addition of methanol at 0 °C. After all solvent was removed, the residue was diluted with EtOAc and filtered through silica gel. The combined organic layer was dried over Na₂SO₄. All solvent was evaporated to give crude alcohol **132** (16 g, 81%), which was directly used in the next step.

$[\alpha]_D^{20}$ -33.3 (c 1.01, EtOH)

^1H NMR (400 MHz, CDCl_3) δ ppm 4.67-4.60 (m, 1H), 3.91 (ddd, $J = 12.5, 2.8, 1.2$ Hz, 1H), 3.65 (ddd, $J = 12.5, 4.7, 1.3$ Hz, 1H), 2.68-2.50 (m, 1H), 2.33-2.09 (m, 1H)

(5R)-5-[(tert-Butyldiphenylsilyloxy)methyl]dihydro-2(3H)-furanone (130)

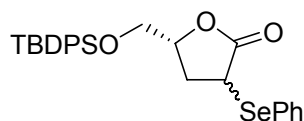


To a well stirred solution of alcohol **132** (21g, 178mmol) and imidazole (18 g, 1.5eq) in anhydrous DCM was added TBDPSCI in DCM. It was allowed to stir at room temperature over night. After all solvent was removed the residue was diluted with hexane and was allowed to stand in the freezer for 12 h. The precipitates was filtered and recrystalized to give pure product. The mother liquid was concentrated and the residue was subjected to a column (3:1 Hexane/EtOAc) to afford **130** (45 g, 71%) as white crystal.

M.P. 70-72 °C

^1H NMR (400 MHz, CDCl_3) δ ppm 7.68-7.64 (m, 4H), 7.45-7.37 (m, 6H), 4.64-4.58 (m, 1H), 3.88 (dd, $J = 11.4, 3.3$ Hz, 1H), 3.69 (dd, $J = 11.4, 3.3$ Hz, 1H), 2.68 (ddd, $J = 17.6, 10.1, 7.2$ Hz, 1H), 2.51 (ddd, $J = 17.7, 10.1, 6.6$ Hz, 1H), 2.35-2.17 (m, 2H), 1.05 (s, 9H)

(3RS, 5R)-5-[(tert-Butyldiphenylsilyloxy)methyl]-3-phenylseleno-dihydro-2(3H)-furanone (133)

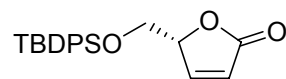


To a solution of LiHMDS (7.14 g, 1.0 eq) in THF was added a solution of starting material **130** (14.7 g, 41.4 mmol) in THF over a period of 1 h at -78 °C. After stirring for another 2 h at -78 °C, freshly distilled TMSCl (4.21 ml, 5.84 g, 1.3 eq) was added slowly and the reaction mixture was then stirred for 2 h at -78 °C and 1 h at room temperature. After being cooled down to -78 °C, a solution of PhSeBr (9.96 g, 1.0 eq) in THF was added. The reaction mixture was allowed to stir overnight. The reaction was quenched by addition of saturated NH₄Cl solution and the reaction mixture was diluted with ether. Layers were separated and the aqueous layer was extracted 3 times with ether. The combined organic layer was washed with 1M HCl and saturated NaHCO₃ solution consequently and dried over Na₂SO₄. It was then concentrated and the mixture of two diastereomers **133** (19.6 g total, 93%) was isolated by column (hexane to 3:1 hexane/EtOAc).

¹H NMR (600 MHz, CDCl₃) δ ppm 7.69-7.61 (m, 4H), 7.46-7.37 (m, 6H), 4.53-4.48 (m, 1H), 4.03 (t, *J* = 9.5 Hz, 1H), 3.67 (dd, *J* = 11.4, 4.4 Hz, 1H), 3.63 (dd, *J* = 11.4, 4.9 Hz, 1H), 2.65 (ddd, *J* = 13.6, 9.6, 7.1 Hz, 1H), 2.24 (ddd, *J* = 13.6, 9.2, 8.2 Hz, 1H), 1.04 (s, 9H)

¹H NMR (600 MHz, CDCl₃) δ ppm 7.69-7.59 (m, 4H), 7.46-7.30 (m, 6H), 4.38-4.33 (m, 1H), 4.09 (dd, *J* = 9.2, 5.4 Hz, 1H), 3.84 (dd, *J* = 11.6, 3.1 Hz, 1H), 3.61 (dd, *J* = 11.6, 3.1 Hz, 1H), 2.70 (ddd, *J* = 13.8, 9.2, 6.2 Hz, 1H), 2.29 (ddd, *J* = 13.6, 7.5, 5.4 Hz, 1H), 1.02 (s, 9H)

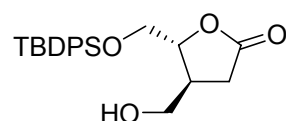
(5R)-5-[(tert-Butyldiphenylsilyloxy)methyl]-2(5H)-furanone (129)



To a solution of **133** (46.5 g, 91.3 mmol) in 600ml DCM was added to a vigorously stirred ice-cold 30% hydrogen peroxide (70.0 g, 617 mmol) dropwise with stirring over 1 h. The heterogeneous reaction mixture was stirred for 30 mins. Layers were separated. The combined organic layer was washed 3 times with water, 1 time with brine and dried over Na₂SO₄. After removal of all solvent, the residue was purified by a column (3:1 Hexane/EtOAc) to provide product **129** (30.0 g, 93%).

¹H NMR (600 MHz, CDCl₃) δ ppm 7.67-7.62 (m, 4H), 7.47-7.38 (m, 6H), 6.18 (dd, *J* = 5.7, 2.0 Hz, 1H), 5.09-5.06 (m, 1H), 3.93-3.85 (m, 2H), 1.03 (s, 9H)

(4S,5R)-5-[(tert-Butyldiphenylsilyloxy)methyl]-4-(hydroxymethyl)-dihydro-2(3H)-furanone (123)

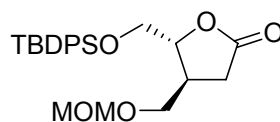


To a photochemical reactor with water-cooled, immersion-irradiation UV-visible lamp was added starting material **129** (12.0 g, 34.0mmol), benzophenone (6.20 g, 1.0eq) and 250ml methanol. Argon gas was bubbled in with stir for 1 h to remove oxygen dissolved in the solvent. It was irradiated using a 450 watt mercury vapor lamp for 20 h. ¹H NMR was taken to ensure the consumption of the starting material. After removal of all solvent, the residue was passed through a column (1:1 hexane/EtOAc to EtOAc) to provide the product **137** (11.5 g, 88%).

^1H NMR (400 MHz, CDCl_3) δ ppm 7.68-7.64 (m, 4H), 7.48-7.38 (m, 6H), 4.43 (dd, $J = 7.4, 3.4$ Hz, 1H), 3.90 (dd, $J = 11.4, 3.5$ Hz, 1H), 3.73 (dd, $J = 11.4, 3.0$ Hz, 1H), 3.71-3.62 (m, 2H), 2.81 (dd, $J = 17.4, 9.5$ Hz, 1H), 2.76-2.68 (m, 1H), 2.38 (dd, $J = 17.4, 5.0$ Hz, 1H), 1.05 (s, 9H)

^{13}C NMR (100 MHz, CDCl_3) δ ppm 176.9, 135.8, 135.7, 130.2, 128.1, 82.5, 65.4, 63.9, 39.3, 31.9, 26.9, 19.4

(4S,5R)-5-[(tert-Butyldiphenylsilyloxy)methyl]-4-[(methoxymethoxy)methyl]-dihydro-2(3H)-furanone (145)



To a solution of **137** (4.18 g, 10.9 mmol) in DIEPA (or mixture with DMF if not soluble) was added MOMCl (3.30 ml, 3.50 g, 4.0 eq) slowly with stirring at 0 °C. The mixture was allowed to stir at r.t. over night. The solvent was evaporated and the residue was diluted by distilled water. The aqueous solution was extracted 5 times with DCM and the combined organic layer was filter through silica gel and dried over Na_2SO_4 . The solvent was evaporated and the residue was subjected to a column to yield product **145** (3.28 g, 70%) as colorless oil.

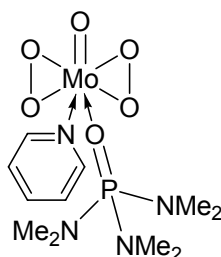
^1H NMR (600 MHz, CDCl_3) δ ppm 7.68-7.64 (m, 4H), 7.47-7.38 (m, 6H), 4.60 (s, 2H), 4.44-4.41 (m, 1H), 3.92 (dd, $J = 11.4, 3.1$ Hz, 1H), 3.71 (dd, $J = 11.4, 2.9$ Hz, 1H), 3.56-3.53 (m, 2H), 3.34 (s, 3H), 2.88-2.78 (m, 2H), 2.39 (dd, $J = 16.6, 3.8$ Hz, 1H), 1.05 (s, 9H)

^{13}C NMR (150 MHz, CDCl_3) δ ppm 176.8, 135.9, 132.6, 130.2, 128.1, 96.8, 82.7, 82.6, 68.8, 65.3, 55.8, 37.0, 32.4, 27.0, 19.4

HRMS (ESI): expected $\text{C}_{24}\text{H}_{33}\text{O}_5\text{Si}$ ($\text{M}+1$) $^+$ 429.20918 found 429.21028

IR (neat) ν_{max} 2929, 2856, 1776, 1427, 1110 cm^{-1}

**Oxidodiperoxymolybdenum pyridine (hexamethylphosphoric triamide)
(MoOPH) (142)**



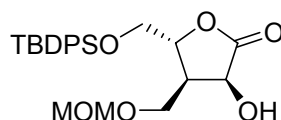
10 g Mo(VI) oxide was dissolved in 50ml of H_2O_2 . The mixture was gently heated to the temperature of 35 °C. The mildly exothermic reaction was controlled by water bath and heating mantle to maintain an internal temperature of 35 to 40 °C. After the initial exothermic period (approximately 30 mins), heating mantle was used to maintain the temperature and the reaction was stirred for 3.5 h at that temperature to form a yellow solution with a small amount of suspended white solid.

After being cooled down to 20 °C, the solution was filtered through celite. The yellow filtrate was cooled to 10 °C and HMPA was added dropwise over 5 mins to form a yellow crystalline precipitate. Stirring was continued for 15 mins, and the product was filtered through a funnel and pressed dry with a spatula. The filter cake is transferred to an Erlenmeyer. Minimum amount of methanol was added to dissolve the solid at 40 °C, and was cooled in the refrigerator to give needle

like crystals. It was collected by filtration and washed with cold methanol to give $\text{MoO}_5 \cdot \text{H}_2\text{O} \cdot \text{HMPA}$. The product crystal was dried over phosphorus oxide in a vacuum desiccator, shielded from the light for 24 h to give hygroscopic yellow solid $\text{MoO}_5 \cdot \text{HMPA}$.

$\text{MoO}_5 \cdot \text{HMPA}$ was dissolved in 50 ml of dry THF and the solution was filtered to remove the insoluble amorphous precipitate. The filtrate was stirred at r.t. while 1 eq (calculated from $\text{MoO}_5 \cdot \text{HMPA}$) of pyridine was added over 10 mins. The yellow crystalline product was collected by filtration, washed with dry THF and ether, and dried in a desiccator under reduced pressure to yield the final product $\text{MoO}_5 \cdot \text{Py} \cdot \text{HMPA}$ **128** (11 g, 36%) as light yellow crystal.

(3S,4R,5R)-5-[(tert-Butyldiphenylsilyloxy)methyl]-3-hydroxy-4-[(methoxymethoxy)methyl]-dihydro-2(3H)-furanone (146)



To a solution of **145** (3.3 g, 7.7 mmol) in THF was added the solution of KHMDS (2.9g, 1.8eq) in THF slowly at $-78\text{ }^\circ\text{C}$ and was stirred for more than 30 mins. MoOPH (3.7 g, 1.1 eq) was then added slowly. Reaction was stirred at $-78\text{ }^\circ\text{C}$ for 2 h (20 mins to 1 h according to literature) and was quenched by addition of a solution of sodium sulfite. Layers were separated and the aqueous layer was extracted 3 times with ether. The combined organic layer was washed with brine and dried over Na_2SO_4 . After removal of all solvent, the residue was purified by a

column (1:1 Hexane/EtOAc) to give two products **146**, **147** (1.13 g, 33%, 0.99 g, 29%).

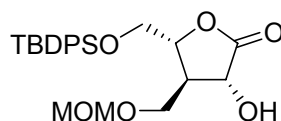
^1H NMR (600 MHz, CDCl_3) δ ppm 7.65-7.61 (m, 4H), 7.47-7.39 (m, 6H), 4.87 (dd, $J = 8.9, 6.4$ Hz, 1H), 4.61 (q, $J = 6.6$ Hz, 2H), 4.50 (dd, $J = 4.1, 2.2$ Hz, 1H), 3.93 (dd, $J = 11.6, 2.7$ Hz, 1H), 3.83 (dd, $J = 10.0, 5.7$ Hz, 1H), 3.75 (dd, $J = 10.0, 3.5$ Hz, 1H), 3.69 (dd, $J = 11.6, 2.3$ Hz, 1H), 3.35 (s, 3H), 2.88-2.84 (m, 2H), 1.05 (s, 9H)

^{13}C NMR (150 MHz, CDCl_3) δ ppm 177.4, 135.8, 135.7, 132.8, 132.3, 130.3, 128.1, 97.1, 81.5, 68.4, 65.8, 65.3, 56.0, 41.2, 27.0, 27.0, 19.4, 14.4

HRMS (ESI): expected $\text{C}_{24}\text{H}_{33}\text{O}_6\text{Si}$ ($\text{M}+1$) $^+$ 445.20409 found 429.20434

IR (neat) ν_{max} 3429, 2931, 2855, 1782, 1428, 1113 cm^{-1}

(3R,4R,5R)-5-[(tert-butyldiphenylsilyloxy)methyl]-3-hydroxy-4-[(methoxymethoxy)methyl]-dihydro-2(3H)-furanone (147)



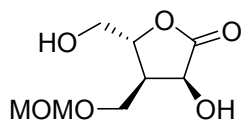
^1H NMR (600 MHz, CDCl_3) δ ppm 7.68-7.65 (m, 4H), 7.47-7.38 (m, 6H), 4.60 (s, 2H), 4.46 (d, $J = 9.7$ Hz, 1H), 4.40 (td, $J = 3.3, 8.9$ Hz, 1H), 3.98 (dd, $J = 11.9, 2.9$ Hz, 1H), 3.78 (dd, $J = 11.9, 3.7$ Hz, 1H), 3.73 (dd, $J = 10.2, 5.0$ Hz, 1H), 3.65 (dd, $J = 10.1, 4.1$ Hz, 1H), 3.32 (s, 1H), 2.79-2.73 (m, 1H), 1.05 (s, 9H)

^{13}C NMR (150 MHz, CDCl_3) δ ppm 176.3, 135.9, 135.8, 133.0, 132.7, 130.2, 128.1, 96.8, 79.3, 70.0, 64.7, 63.4, 55.7, 44.8, 26.9, 19.5, 14.4

HRMS (ESI): expected $\text{C}_{24}\text{H}_{33}\text{O}_6\text{Si}$ ($\text{M}+1$) $^+$ 445.20409 found 445.20489

IR (neat) V_{\max} 3422, 2932, 2858, 1783, 1428, 1113 cm^{-1}

(3S,4R,5R)-5-(Hydroxymethyl)-3-hydroxy-4-[(methoxymethoxy)methyl]-dihydro-2(3H)-furanone (148)

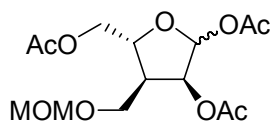


A portion of TBAF solution (4.3 mmol, 2.0 eq) was added to the solution of starting material **146** (0.96 g, 2.2 mmol) in 50 ml of THF. The reaction mixture was stirred at 0 °C for 15 min. After removal of all solvent, the residue was subject to a column (pure EtOAc) to give the product **148** (0.35 g, 78%).

^1H NMR (600 MHz, CDCl_3) δ ppm 4.76 (dd, $J = 8.7, 5.5$ Hz, 1H), 4.65-4.60 (m, 2H), 4.56-4.54 (m, 1H), 3.98-3.93 (m, 1H), 3.82-3.75 (m, 2H), 3.74-3.70 (m, 1H), 3.36 (s, 3H), 2.80-2.76 (m, 1H)

^{13}C NMR (150 MHz, CDCl_3) δ ppm 177.8, 97.1, 82.1, 68.2, 65.5, 64.0, 56.0, 41.1

3-Deoxy-1,2,5-tri-O-acetyl-3-[(methoxymethoxy)methyl]- β -L-ribofuranose (128)



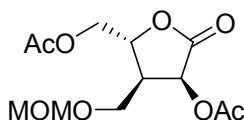
To a solution of **148** (0.057g, 0.28mmol) in DCM was added a portion of 1 M DIBAL-H (1.1 ml, 4.0 eq) slowly with stirring at -78 °C. The reaction was stirred at that temperature for about 1h until no starting material was present in TLC.

Pyridine (0.088 g, 4.0 eq), DMAP (0.068 g, 2.0 eq) and acetic anhydride (0.21ml,

0.23 g, 8.0 eq) were added respectively, and the reaction was then stirred at 0 °C. It was allowed to stir at room temperature overnight, and the reaction was quenched by Rochelle's salt. Layers were separated, and the aqueous layer was extracted 3 times with DCM. The combined organic layer was washed and dried over Na₂SO₄. After removal of all solvent, the residue was purified by a column (3:1 to 1:1 Hexane/EtOAc) to provide product **128** (0.030 g, 32%) as a syrup.

¹H NMR (400 MHz, CDCl₃) δ ppm 6.09 (s, 1H), 5.32 (dd, *J* = 8.9, 4.3 Hz, 1H), 5.28 (d, *J* = 4.8 Hz, 1H), 4.60-4.56 (m, 2H), 4.42-4.37 (m, 1H), 4.35-4.24 (m, 3H), 4.13-4.05 (m, 2H), 3.76-3.53 (m, 1H), 3.32 (s, 3H), 2.67-2.56 (m, 1H), 2.10-2.05 (m, 9H)

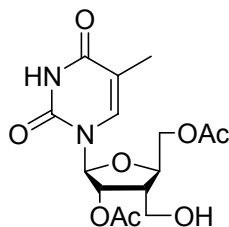
(3S,4R,5R)-5-(Acetoxymethyl)-3-acetoxy-4-[(methoxymethoxy)methyl]-dihydro-2(3H)-furanone



¹H NMR (400 MHz, CDCl₃) δ ppm 5.65 (d, *J* = 8.9 Hz, 1H), 4.74-4.71 (m, 1H), 4.56 (s, 1H), 4.33 (dd, *J* = 12.4, 2.8 Hz, 1H), 4.20 (dd, *J* = 12.4, 3.8 Hz, 1H), 3.54 (d, *J* = 5.0 Hz, 1H), 3.32 (s, 1H), 2.15 (s, 1H), 2.08 (s, 1H)

¹³C NMR (100 MHz, CDCl₃) δ ppm 171.9, 170.3, 169.8, 96.7, 78.2, 67.5, 65.1, 64.3, 55.7, 39.8, 20.9, 20.5

1-[2,5-Di-O-acetyl-3-deoxy-3-C-(mesyloxymethyl)-β-L-ribofuranosyl]thymine (127a)

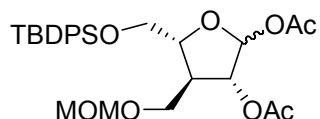


The thymine base (1.2eq) was refluxed in 10ml 1,1,1,3,3,3-hexamethyldisilazane (HMDS) in presence of trace amount of $(\text{NH}_4)_2\text{SO}_4$ for 6 hours. All solvent was evacuated under vacuum to yield 6-Cl-9-trimethylsilylthymine.

A portion of TMSOTf was injected slowly into the solution of silylated thymine in 5 ml of DCM. The mixture was stirred for 1 min and was injected into the solution of **128** (0.078 g, 0.22 mmol) in 10 ml of DCM. The reaction vessel was stirred at r.t. for 6 hr, and 1 more equivalent of TMSOTf was added at $-30\text{ }^\circ\text{C}$ to remove the MOM group. After stirring for 1 h, the reaction was quenched by addition of saturated sodium bicarbonate solution. Layers were separated, the aqueous layer was extracted 3 times with dichloromethane. The combined organic layer was washed with brine and dried over sodium sulfate. After removal of all the solvent, the residue was subject to a column (1:1 hexane/EtOAc) to give the product **127a** (0.051 g, 61%) as foam.

^1H NMR (400 MHz, CDCl_3) δ ppm 7.23 (s, 1H), 5.62 (d, $J = 2.1$ Hz, 1H), 4.45-4.40 (m, 2H), 4.35-4.29 (m, 3H), 2.13 (s, 3H), 2.11 (s, 3H), 1.93 (s, 3H)

(3R,4S,5R)-5-((tert-butyldiphenylsilyloxy)methyl)-4-((methoxymethoxy)methyl)-tetrahydrofuran-2,3-diyl diacetate (149)

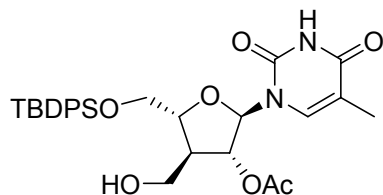


To a solution of **147** (0.088 g, 0.20 mmol) in DCM was added a portion of 1 M DIBAL-H (1.0 ml, 5.0 eq) slowly with stirring at $-78\text{ }^{\circ}\text{C}$. The reaction was stirred at that temperature for about 1 h until no starting material was present in TLC. Pyridine (0.064 ml, 4.0eq), DMAP (0.048 g, 2.0eq) and acetic anhydride (0.15 ml, 0.23 g, 8.0 eq) were added respectively, and the reaction was then stirred at $0\text{ }^{\circ}\text{C}$. It was allowed to stir at room temperature overnight, and the reaction was quenched by Rochelle's salt. Layers were separated, and the aqueous layer was extracted 3 times with DCM. The combined organic layer was washed and dried over Na_2SO_4 . After removal of all solvent, the residue was purified by a column (3:1 to 1:1 Hexane/EtOAc) to provide product **149** (0.067 g, 69%) as a syrup.

^1H NMR (400 MHz, CDCl_3) δ ppm 7.70-7.64 (m, 4H), 7.45-7.34 (m, 6H), 6.19 (s, 1H), 5.09 (d, $J = 2.6$ Hz, 1H), 4.60 (s, 2H), 4.16-4.10 (m, 1H), 3.83-3.77 (m, 1H), 3.73 (dd, $J = 9.6, 7.1$ Hz, 1H), 3.64 (dd, $J = 13.4, 5.9$ Hz, 1H), 3.34 (s, 3H), 2.67-2.59 (m, 1H), 2.07 (s, 3H), 2.02 (s, 3H), 1.06 (s, 9H)

^{13}C NMR (100 MHz, CDCl_3) δ ppm 170.4, 169.7, 135.9, 135.8, 129.9, 127.9, 100.7, 96.7, 83.8, 80.3, 67.0, 64.6, 55.5, 46.13, 27.0, 26.9, 21.4, 19.5

1-[(3R,4S,5R)-3-acetoxy-5-((tert-butylidiphenylsilyloxy)methyl)-4-(hydroxymethyl)-tetrahydrofuran-2-yl]thymine (151 β)



The thymine base (1.2eq) was refluxed in 10ml 1,1,1,3,3,3-hexamethyldisilazane (HMDS) in presence of trace amount of $(\text{NH}_4)_2\text{SO}_4$ for 6 hours. All solvent was evacuated under vacuum to yield 6-Cl-9-trimethylsilylthymine.

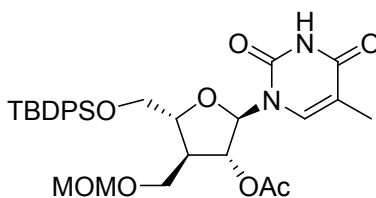
A portion of TMSOTf was injected slowly into the solution of silylated thymine in 5 ml of DCM. The mixture was stirred for 1 min and was injected into the solution of **149** (0.148 g, 0.28 mmol) in 10 ml of DCM. The reaction vessel was stirred at r.t. for 6 hr, and 1 more equivalent of TMSOTf was added at $-30\text{ }^\circ\text{C}$ to remove the MOM group. After stirring for 1 h, the reaction was quenched by addition of saturated sodium bicarbonate solution. Layers were separated, and the aqueous layer was extracted 3 times with dichloromethane. The combined organic layer was washed with brine and dried over sodium sulfate. After removal of all the solvent, the residue was subject to a column (1:1 hexane/EtOAc) to give the product **151 β** (0.051 g, 61%) as foam.

Deprotection of **150 β**

To the solution of **150 β** (0.035g, 58 μmol) was added 1 eq of TMSOTf at $-30\text{ }^\circ\text{C}$. The reaction was stirred for 2 h and quenched by saturated NaHCO_3 solution. Layers were separated and the combined organic layer was dried over anhydrous Na_2SO_4 . After removal of the solvent, the residue was subjected to a column to yield the desired **151 β** (0.021g, 72%) as a syrup.

^1H NMR (400 MHz, CDCl_3) δ ppm 8.65-8.43 (m, 1H), 7.70-7.65 (m, 4H), 7.49-7.37 (m, 6H), 7.12 (d, $J = 1.1$ Hz, 1H), 5.92 (d, $J = 5.1$ Hz, 1H), 5.40 (dd, $J = 6.9$, 5.3 Hz, 1H), 4.38-4.33 (m, 1H), 3.86 (dd, $J = 11.3$, 4.0 Hz, 1H), 3.81 (dd, $J = 11.3$, 5.1 Hz, 1H), 3.77-3.71 (m, 2H), 2.72-2.63 (m, 1H), 2.10 (s, 3H), 1.93 (s, 3H), 1.09 (s, 9H)

1-[(3R,4S,5R)-3-acetoxy-5-((tert-butyldiphenylsilyloxy)methyl)-4-(methoxymethoxymethyl)-tetrahydrofuran-2-yl]thymine (150 β)



^1H NMR (400 MHz, CDCl_3) δ ppm 8.14 (s, 1H), 7.69-7.64 (m, 2H), 7.46-7.35 (m, 31H), 7.22 (d, $J = 1.2$ Hz, 1H), 6.05 (d, $J = 4.96$ Hz, 1H), 5.36 (dd, $J = 6.6$, 5.0 Hz, 1H), 4.59 (s, 2H), 4.35 (td, $J = 7.2$, 3.54, 3.6 Hz, 1H), 3.87 (dd, $J = 11.2$, 3.6 Hz, 1H), 3.78-3.70 (m, 2H), 3.61 (dd, $J = 9.8$, 3.9 Hz, 1H), 3.31 (s, 3H), 2.07 (s, 3H), 1.93 (s, 3H), 1.08 (s, 9H)

2.4 Syntheses of Nucleoside Triphosphates

Nucleoside analog was dissolved in anhydrous pyridine and evaporated under vacuum twice to exclude moisture. Phosphoryl chloride (POCl_3) was distilled before use. Trimethyl phosphate (TMP) was dried over molecular sieve and freshly distilled from BaO. Tributyl amine and 2,4,6-collidine was distilled from CaH_2 .

HPLC Methods:

Analytical 1: 0.1 M TEAB solution (eluent A), Methanol (eluent B); 1 ml/min; 253.6 nm; 0 min: 90% A, 10% B; 5 min: 90% A, 10% B; 25 min: 30% A, 70% B; 30 min: 0% A, 100% B.

Analytical 2: 95% (20 mM KH₂PO₄, 5 mM NBu₄OH in water), 5% MeOH (eluent A), Methanol (eluent B); 1 ml/min; 253.6 nm; 0 min: 90% A, 10% B; 5 min: 90% A, 10% B; 25 min: 30% A, 70% B; 30 min: 0% A, 100% B.

Preparative: 0.1 M TEAB solution (eluent A), Methanol (eluent B); 253.6 nm; 20 ml/min; 0 min: 95% A, 5% B; 5 min: 95% A, 5% B; 50 min: 50% A, 50% B; 60 min: 0% A, 100% B.

Typical procedure: To a solution of nucleoside analog (0.036g 5-fluorocytidine analog, 0.03mmol) in 1ml of TMP and 1ml of 2,4,6-collidine was stirred at 0 °C for 10 mins. A solution of POCl₃ (1 M in TMP, 0.3 ml, 2.5eq) was added, and the reaction mixture was stirred for 4 h at 0 °C. A solution of (tributylammonium) pyrophosphate (0.5 M in anhydrous DMF, 1.4 ml, 5eq) and 0.6 ml of tributyl amine was added. After the reaction mixture was stirred at room temperature for 30 min, 2 ml of 1M TEAB solution was added and the resulting mixture was stirred for 1 h. After filtration, the reaction mixture was purified by preparative RP-HPLC. The peak at retention time of 10 mins was collected and lyophilized.

3 ABBREVIATIONS AND DEFINITIONS

AIDS	Acquired Immune Deficiency Syndrome
CDC	Center of Disease Control and Prevention
DBU	1,8-Diazabicyclo[5.4.0]undec-7-ene
DCE	1,2-Dichloroethane
DCM	Dichloromethane
DIBAL-H	Diisobutylaluminum hydride
DMAP	4-Dimethylaminopyrimine
DNA	Deoxyribonucleic acid
ESLD	End-stage liver disease
FDA	Food and Drug Administration
FDOC	2',3'-Dideoxy-5-fluoro-oxacytidine
HAART	Highly active anti retroviral therapy
HBV	Hepatitis B virus
HCV	Hepatitis C virus
HIV	Human immunodeficiency virus
HMDS	Hexamethyldisilazane
HMPA	Hexamethylphosphoric triamide
HOMO	Highest occupied molecular orbital
IFN	Interferon
IRES	Internal ribosome entry site
ISC	Intersystem crossing

KHMDS	Potassium hexamethyldisilazane
LUMO	Low unoccupied molecular orbital
m-CPBA	3-Chloroperoxybenzoic acid
Min	Minutes
MOM	Methoxymethyl
MoOPH	Oxidiperoxymolybdenum (pyridine) (hexamethylphosphoric triamide)
Ms	Methanesulfonyl
NANB	Non A-non B
NIH	National Institutes of Health
NOE	Nuclear Overhauser effect
NRTI	Nucleoside reverse transcriptase inhibitors
NS	Nonstructural
ON	Oligonucleotides
ORF	Open reading frame
PDC	Pyridinium dichromate
PEG	Polyethylene glycol
Py	Pyridine
RdRp	RNA dependent RNA polymerase
RNA	Ribonucleic acid
rNTP	Ribonucleoside triphosphates
RP-HPLC	Reverse phase high pressure liquid chromatography

S_N2	Nucleophilic substitution type 2
TBAF	Tetra-n-butylammonium fluoride
TBAOAc	Tetra-n-butylammonium acetate
TBDPS	tert-Butyldiphenylsilyl
THF	Tetrahydrofuran
TMP	Trimethyl phosphate
TMS	Trimethylsilyl
TMSOTf	Trimethylsilyl trifluoromethanesulfonate
Ts	p-Toluenesulfonyl
WHO	World health organization

4 REFERENCES

1. Choo, Q. L.; Kuo, G.; Weiner, A. J.; Overby, L. R.; Bradley, D. W.; Houghton, M., *Science* **1989**, 244, (4902), 359-362.
2. Shepard, C. W.; Finelli, L.; Alter, M. J., *Lancet Infect Dis* **2005**, 5, (9), 558-67.
3. Davis, G. L.; Wong, J. B.; McHutchison, J. G.; Manns, M. P.; Harvey, J.; Albrecht, J., *Hepatology* **2003**, 38, (3), 645-52.
4. Moussalli, J.; Opolon, P.; Poynard, T., *J. Viral Hepat.* **1998**, 5, (2), 73-82.
5. Feinstone, S. M.; Kapikian, A. Z.; Purcell, R. H.; Alter, H. J.; Holland, P. V., *New Eng. J. Med.* **1975**, 292, (15), 767-770.
6. Kuo, G.; Choo, Q. L.; Alter, H. J.; Gitnick, G. L.; Redeker, A. G.; Purcell, R. H.; Miyamura, T.; Dienstag, J. L.; Alter, M. J.; Stevens, C. E.; Tegtmeier, G. E.; Bonino, F.; Colombo, M.; Lee, W. S.; Kuo, C.; Berger, K.; Shuster, J. R.; Overby, L. R.; Bradley, D. W.; Houghton, M., *Science* **1989**, 244, (4902), 362-364.
7. CDC, Hepatitis C fact sheet. **2005**,
<http://www.cdc.gov/ncidod/diseases/hepatitis/c/fact.htm>.
8. Frank, C.; Mohamed, M. K.; Strickland, G. T.; Lavanchy, D.; Arthur, R. R.; Magder, L. S.; El Khoby, T.; Abdel-Wahab, Y.; Ohn, E. A.; Anwar, W.; Sallam, I., *Lancet* **2000**, 355, (9207), 887-891.
9. Simmonds, P., *Journal of Hepatology* **1999**, 31, 54-60.
10. Hoofnagle, J. H.; Mullen, K. D.; Jones, D. B.; Rustgi, V.; Dibisceglie, A.; Peters, M.; Waggoner, J. G.; Park, Y.; Jones, E. A., *New Eng. J. Med.* **1986**, 315, (25), 1575-1578.

11. Hadziyannis, S. J.; Sette, H.; Morgan, T. R.; Balan, V.; Diago, M.; Marcellin, P.; Ramadori, G.; Bodenheimer, H.; Bernstein, D.; Rizzetto, M.; Zeuzem, S.; Pockros, P. J.; Lin, A.; Ackrill, A. M.; Grp, P. I. S., *Ann. Intern. Med.* **2004**, 140, (5), 346-355.
12. Falck-Ytter, Y.; Kale, H.; Mullen, K. D.; Sarbah, S. A.; Sorescu, L.; McCullough, A. J., *Ann. Intern. Med.* **2002**, 136, (4), 288-292.
13. Walker, B. D.; Lauer, G. M., *New Eng. J. Med.* **2001**, 345, (19), 1427-1428.
14. Robertson, B.; Myers, G.; Howard, C.; Brettin, T.; Bukh, J.; Gaschen, B.; Gojobori, T.; Maertens, G.; Mizokami, M.; Nainan, O.; Netesov, S.; Nishioka, K.; Shin-i, T.; Simmonds, P.; Smith, D.; Stuyver, L.; Weiner, A., *Arch. Virol.* **1998**, 143, (12), 2493-2503.
15. Major, M. E.; Feinstone, S. M., *Hepatology* **1997**, 25, (6), 1527-1538.
16. Bartenschlager, R.; Lohmann, V., *J. Gen. Virol.* **2000**, 81, 1631-1648.
17. Ahlquist, P.; Noueir, A. O.; Lee, W. M.; Kushner, D. B.; Dye, B. T., *J. Virol.* **2003**, 77, (15), 8181-8186.
18. Swan, T.; Raymond, D., TAG, Hepatitis C Virus (HCV) and HIV/HCV Coinfection: A Critical Review of Research and Treatment. **2004**, <http://www.aidsinfonyc.org/tag/coinf/hcv2004/index.html>.
19. Op de Beeck, A.; Cocquerel, L.; Dubuisson, J., *J. Gen. Virol.* **2001**, 82, 2589-2595.
20. Schneider-Schaulies, J., *J. Gen. Virol.* **2000**, 81, 1413-1429.

21. Bartosch, B.; Vitelli, A.; Granier, C.; Goujon, C.; Dubuisson, J.; Pascale, S.; Scarselli, E.; Cortese, R.; Nicosia, A.; Cosset, F. L., *J. Bio. Chem.* **2003**, 278, (43), 41624-41630.
22. Tsukiyamakohara, K.; Iizuka, N.; Kohara, M.; Nomoto, A., *J. Virol.* **1992**, 66, (3), 1476-1483.
23. Wang, C. Y.; Sarnow, P.; Siddiqui, A., *J. Virol.* **1993**, 67, (6), 3338-3344.
24. Bartenschlager, R., *J. Viral Hepat.* **1999**, 6, (3), 165-181.
25. Hijikata, M.; Kato, N.; Ootsuyama, Y.; Nakagawa, M.; Shimotohno, K., *Proceedings of the National Academy of Sciences of the United States of America* **1991**, 88, (13), 5547-5551.
26. Grakoui, A.; Wychowski, C.; Lin, C.; Feinstone, S. M.; Rice, C. M., *J. Virol.* **1993**, 67, (3), 1385-1395.
27. Lin, C.; Lindenbach, B. D.; Pragai, B. M.; Mccourt, D. W.; Rice, C. M., *J. Virol.* **1994**, 68, (8), 5063-5073.
28. Grakoui, A.; Mccourt, D. W.; Wychowski, C.; Feinstone, S. M.; Rice, C. M., *Proceedings of the National Academy of Sciences of the United States of America* **1993**, 90, (22), 10583-10587.
29. Hijikata, M.; Mizushima, H.; Akagi, T.; Mori, S.; Kakiuchi, N.; Kato, N.; Tanaka, T.; Kimura, K.; Shimotohno, K., *J. Virol.* **1993**, 67, (8), 4665-4675.
30. Grakoui, A.; Mccourt, D. W.; Wychowski, C.; Feinstone, S. M.; Rice, C. M., *J. Virol.* **1993**, 67, (5), 2832-2843.
31. Bartenschlager, R.; Ahlbornlaake, L.; Mous, J.; Jacobsen, H., *J. Virol.* **1994**, 68, (8), 5045-5055.

32. Failla, C.; Tomei, L.; Defrancesco, R., *J. Virol.* **1994**, 68, (6), 3753-3760.
33. Failla, C.; Tomei, L.; Defrancesco, R., *J. Virol.* **1995**, 69, (3), 1769-1777.
34. Lin, C.; Pragai, B. M.; Grakoui, A.; Xu, J.; Rice, C. M., *J. Virol.* **1994**, 68, (12), 8147-8157.
35. New York Medical College Chironian, **2003**,
<http://www.nymc.edu/pubs/Chironian/Spring2003/hepCvirus.asp>.
36. Carrere-Kremer, S.; Montpellier-Pala, C.; Cocquerel, L.; Wychowski, C.; Penin, F.; Dubuisson, J., *J. Virol.* **2002**, 76, (8), 3720-3730.
37. Lau, J. Y.; Tam, R. C.; Liang, T. J.; Hong, Z., *Hepatology* **2002**, 35, (5), 1002-1009.
38. Tanabe, Y.; Sakamoto, N.; Enomoto, N.; Kurosaki, M.; Ueda, E.; Maekawa, S.; Yamashiro, T.; Nakagawa, M.; Chen, C. H.; Kanazawa, N.; Kakinuma, S.; Watanabe, M., *Journal of Infectious Diseases* **2004**, 189, (7), 1129-1139.
39. Tan, S. L.; Pause, A.; Shi, Y. U.; Sonenberg, N., *Nature Reviews Drug Discovery* **2002**, 1, (11), 867-881.
40. HCVadvocate.org, Hepatitis C Drugs in Development. **2007**,
<http://www.hcvadvocate.org/hepatitis/hepC/HCVDrugs.html>.
41. Pani, A.; Loi, A. G.; Mura, M.; Marceddu, T.; La Colla, P.; Marongiu, M. E., *Current Drug Targets - Infectious Disorders* **2003**, 2, 17-32.
42. Gallo, R. C.; Sarin, P. S.; Gelmann, E. P.; Robertguroff, M.; Richardson, E.; Kalyanaraman, V. S.; Mann, D.; Sidhu, G. D.; Stahl, R. E.; Zollapazner, S.; Leibowitch, J.; Popovic, M., *Science* **1983**, 220, (4599), 865-867.

43. Barresinoussi, F.; Chermann, J. C.; Rey, F.; Nugeyre, M. T.; Chamaret, S.; Gruest, J.; Dauguet, C.; Axlerblin, C.; Vezinetbrun, F.; Rouzioux, C.; Rozenbaum, W.; Montagnier, L., *Science* **1983**, 220, (4599), 868-871.
44. Sherman, K. E.; Rouster, S. D.; Chung, R. T.; Rajjicic, N., *Clinical Infectious Diseases* **2002**, 34, (6), 831-837.
45. Tedaldi, E. M.; Hullsiek, K. H.; Malvestutto, C. D.; Arduino, R. C.; Fisher, E. J.; Gaglio, P. J.; Jenny-Avital, E. R.; McGowan, J. P.; Perez, G., *Clinical Infectious Diseases* **2003**, 36, (10), 1313-1317.
46. Thomas, D. L., *Hepatology* **2002**, 36, (5), S201-S209.
47. Bica, I.; McGovern, B.; Dhar, R.; Stone, D.; McGowan, K.; Scheib, R.; Snyderman, D. R., *Clinical Infectious Diseases* **2001**, 32, (3), 492-497.
48. Martin-Carbonero, L.; Soriano, V.; Valencia, E.; Garcia-Samaniego, J.; Lopez, M.; Gonzalez-Lahoz, J., *Aids Research and Human Retroviruses* **2001**, 17, (16), 1467-1471.
49. Monga, H. K.; Rodriguez-Barradas, M. C.; Breaux, K.; Khattak, K.; Troisi, C. L.; Velez, M.; Yoffe, B., *Clinical Infectious Diseases* **2001**, 33, (2), 240-247.
50. Rosenthal, E.; Poiree, M.; Pradier, C.; Perronne, C.; Salmon-Ceron, D.; Geffray, L.; Myers, R. P.; Morlat, P.; Pialoux, G.; Pol, S.; Cacoub, P.; Grp, G. J. S. o., *Aids* **2003**, 17, (12), 1803-1809.
51. Mitsuya, H.; Yarchoan, R.; Broder, S., *Science* **1990**, 249, (4976), 1533-1544.
52. Maag, D.; Castro, C.; Hong, Z.; Cameron, C. E., *J. Bio. Chem.* **2001**, 276, (49), 46094-46098.

53. Wu, J. Z.; Hong, Z., *Current Drug Targets - Infections Disorders* **2003**, 3, 207-219.
54. Ismaili, H. M. A.; Cheng, Y.-X.; Lavallee, J.-F.; Siddiqui, A.; Storer, R. **2001**, WO 2001060315.
55. Wu, J. Z.; Walker, H.; Lau, J. Y. N.; Hong, Z., *Antimicrob. Agents Chemother.* **2003**, 47, (1), 426-431.
56. Sommadossi, J.-P.; Lacolla, P. **2001**, WO 2001090121.
57. Carroll, S. S.; Maccoss, M.; Olsen, D. B.; Bhat, B.; Bhat, N.; Cook, P. D.; Eldrup, A. B.; Prakash, T. P.; Prhavc, M.; Song, Q. **2002**, WO 2002057287.
58. Devos, R.; Dymock, B. W.; Hobbs, C. J.; Jiang, W.-r.; Martin, J. A.; Merrett, J. H.; Najera, I.; Shimma, N.; Tsukuda, T. **2002**, WO 2002018404.
59. Schinazi, R. F.; Liotta, D. C.; Chu, C. K.; McAtee, J. J.; Shi, J.; Choi, Y.; Lee, K.; Hong, J. H. **1999**, WO 9943691.
60. Devos, R. R.; Hobbs, C. J.; Jiang, W.-r.; Martin, J. A.; Merrett, J. H.; Najera, I. **2002**, WO 2002094289.
61. Storer, R. **2001**, WO 2001032153.
62. Stuyver, L. J.; Whitaker, T.; McBrayer, T. R.; Hernandez-Santiago, B. I.; Lostia, S.; Tharnish, P. M.; Ramesh, M.; Chu, C. K.; Jordan, R.; Shi, J. X.; Rachakonda, S.; Watanabe, K. A.; Otto, M. J.; Schinazi, R. F., *Antimicrob. Agents Chemother.* **2003**, 47, (1), 244-254.
63. Carroll, S. S.; Tomassini, J. E.; Bosserman, M.; Getty, K.; Stahlhut, M. W.; Eldrup, A. B.; Bhat, B.; Hall, D.; Simcoe, A. L.; LaFemina, R.; Rutkowski, C. A.;

- Wolanski, B.; Yang, Z. C.; Migliaccio, G.; De Francesco, R.; Kuo, L. C.; MacCoss, M.; Olsen, D. B., *J. Bio. Chem.* **2003**, 278, (14), 11979-11984.
64. Fischer, E.; Helferich, B., *Ber.* **1914**, 47, 210-235.
65. Hilbert, G. E.; Johnson, T. B., *J. Am. Chem. Soc.* **1930**, 52, 4489-4494.
66. Vorbruggen, H.; Ruh-Pohlenz, C., *Organic Reactions* **2000**, 55, 1-630.
67. Vorbruggen, H.; Krolikiewicz, K.; Bennua, B., *Chem. Ber.* **1981**, 114, (4), 1234-1255.
68. Vorbruggen, H.; Bennua, B., *Chem. Ber.* **1981**, 114, (4), 1279-1286.
69. Niedball, U.; Vorbrugg, H., *J. Org. Chem.* **1974**, 39, (25), 3660-3663.
70. Vorbruggen, H.; Krolikiewicz, K., *Angew. Chem.-Int. Ed.* **1975**, 14, (6), 421-422.
71. Niedballa, U.; Vorbruggen, H., *J. Org. Chem.* **1976**, 41, (12), 2084-2086.
72. Choi, W. B.; Wilson, L. J.; Yeola, S.; Liotta, D. C.; Schinazi, R. F., *J. Am. Chem. Soc.* **1991**, 113, (24), 9377-9379.
73. Vorbruggen, H.; Hofle, G., *Chem. Ber.* **1981**, 114, (4), 1256-1268.
74. Chu, C. K.; Babu, J. R.; Beach, J. W.; Ahn, S. K.; Huang, H. Q.; Jeong, L. S.; Lee, S. J., *J. Org. Chem.* **1990**, 55, (5), 1418-1420.
75. Paterno, E.; Chieffi, G., *Gazz. Chim. Ital.* **1909**, 39, (1), 341.
76. Buchi, G.; Inman, C. G.; Lipinsky, E. S., *J. Am. Chem. Soc.* **1954**, 76, (17), 4327-4331.
77. Mattay, J.; Gersdorf, J.; Leismann, H.; Steenken, S., *Angew. Chem.-Int. Ed.* **1984**, 23, (3), 249-250.

78. Gersdorf, J.; Mattay, J.; Gerner, H., *J. Am. Chem. Soc.* **1987**, 109, (4), 1203-1209.
79. Hambalek, R.; Just, G., *Tetrahedron Lett.* **1990**, 31, (38), 5445-5448.
80. Nishiyama, S.; Yamamura, S.; Kato, K.; Takita, T., *Tetrahedron Lett.* **1988**, 29, (37), 4743-4746.
81. Thopate, S. R.; Kulkarni, M. G.; Puranik, V. G., *Angew. Chem.-Int. Ed.* **1998**, 37, (8), 1110-1112.
82. Norbeck, D. W.; Kramer, J. B., *J. Am. Chem. Soc.* **1988**, 110, (21), 7217-7218.
83. Wilson, F. X.; Fleet, G. W. J.; Vogt, K.; Wang, Y.; Witty, D. R.; Choi, S.; Storer, R.; Myers, P. L.; Wallis, C. J., *Tetrahedron Lett.* **1990**, 31, (47), 6931-6934.
84. Nicolaou, K. C.; Ueno, H.; Liu, J. J.; Nantermet, P. G.; Yang, Z.; Renaud, J.; Paulvannan, K.; Chadha, R., *J. Am. Chem. Soc.* **1995**, 117, (2), 653-659.
85. Magee, T. V.; Bornmann, W. G.; Isaacs, R. C. A.; Danishefsky, S. J., *J. Org. Chem.* **1992**, 57, (12), 3274-3276.
86. Ettouati, L.; Ahond, A.; Poupat, C.; Potier, P., *Tetrahedron* **1991**, 47, (47), 9823-9838.
87. Zhang, M.; Yin, D. L.; Guo, J. Y.; Liang, X. T., *Tetrahedron* **2005**, 61, (23), 5519-5527.
88. Meldgaard, M.; Wengel, J., *J. Chem. Soc. Perkin I* **2000**, (21), 3539-3554.
89. Ichikawa, E.; Kato, K., *Curr. Med. Chem.* **2001**, 8, (4), 385-423.

90. Mikhailopulo, I. A.; Poopeiko, N. E.; Tsvetkova, T. M.; Marochkin, A. P.; Balzarini, J.; DeClercq, E., *Carbohydrate Research* **1996**, 285, 17-28.
91. Christensen, N. K.; Petersen, M.; Nielsen, P.; Jacobsen, J. P.; Olsen, C. E.; Wengel, J., *J. Am. Chem. Soc.* **1998**, 120, (22), 5458-5463.
92. Sorensen, M. H.; Nielsen, C.; Nielsen, P., *J. Org. Chem.* **2001**, 66, (14), 4878-4886.
93. Christensen, N. K.; Andersen, A. K. L.; Schultz, T. R.; Nielsen, P., *Org. Biomol. Chem.* **2003**, 1, (21), 3738-3748.
94. Sharma, P. K.; Petersen, M.; Nielsen, P., *J. Org. Chem.* **2005**, 70, (13), 4918-4928.
95. Oyang, C.; Kurz, W.; Eugui, E. M.; Mcroberts, M. J.; Verheyden, J. P. H.; Kurz, L. J.; Walker, K. A. M., *Tetrahedron Lett.* **1992**, 33, (1), 41-44.
96. Bogucka, M.; Naus, P.; Pathmasiri, W.; Barman, J.; Chattopadhyaya, J., *Org. Biomol. Chem.* **2005**, 3, (24), 4362-4372.
97. Ludwig, J., *Acta Biochimica et Biophysica Academiae Scientiarum Hungaricae* **1981**, 16, (3-4), 131-3.
98. Moffatt, J. G.; Khorana, H. G., *J. Am. Chem. Soc.* **1961**, 83, (3), 649-&.
99. Ludwig, J.; Eckstein, F., *J. Org. Chem.* **1989**, 54, (3), 631-635.
100. Plavec, J.; Thibaudeau, C.; Chattopadhyaya, J., *J. Am. Chem. Soc.* **1994**, 116, (15), 6558-6560.
101. Birnbaum, G. I.; Cygler, M.; Watanabe, K. A.; Fox, J. J., *J. Am. Chem. Soc.* **1982**, 104, (26), 7626-7630.

102. Alibes, R.; Alvarez-Larena, A.; de March, P.; Figueredo, M.; Font, J.; Parella, T.; Rustullet, A., *Org. Lett.* **2006**, 8, (3), 491-494.
103. Baker, D. C.; Tindall, C. G.; Horton, D., *Carbohydrate Research* **1972**, 24, (1), 192-&.
104. Kjellberg, J.; Johansson, N. G., *Tetrahedron* **1986**, 42, (23), 6541-6544.
105. Mathe, C.; Gosselin, G., *Antiviral Research* **2006**, 71, (2-3), 276-281.
106. Taniguchi, M.; Koga, K.; Yamada, S., *Tetrahedron* **1974**, 30, (19), 3547-3552.
107. Sugisaki, C. H.; Ruland, Y.; Baltas, M., *European Journal of Organic Chemistry* **2003**, (4), 672-688.
108. Ortuno, R. M.; Bigorra, J.; Font, J., *Tetrahedron* **1987**, 43, (9), 2199-2202.
109. Alguacil, R.; Farina, F.; Martin, M. V., *Tetrahedron* **1996**, 52, (10), 3457-3472.
110. Mann, J.; Weymouth-Wilson, A. C., *Organic Syntheses* **1998**, 75, 139.
111. Chen, B.-C.; Zhou, P.; Davis, F. A.; Ciganek, E., *Organic Reactions* **2003**, 62, 1-356.
112. Davis, F. A.; Sheppard, A. C., *Tetrahedron* **1989**, 45, (18), 5703-5742.
113. Hara, O.; Takizawa, J.; Yamatake, T.; Makino, K.; Hamada, Y., *Tetrahedron Lett.* **1999**, 40, (44), 7787-7790.
114. Moritani, Y.; Fukushima, C.; Ogiku, T.; Ukita, T.; Miyagishima, T.; Iwasaki, T., *Tetrahedron Lett.* **1993**, 34, (17), 2787-2790.